SEDIMENTOLOGY OF THE KATBERG SANDSTONE IN THE EASTERN CAPE PROVINCE

by

Nicholas Stavrakis B.Sc. (Natal), B.Sc. Hons. (U.P.E.)

Thesis presented for the degree of Master of Science in the Department of Geology, Rhodes University, Grahamstown.

Frontispiece : View of the Katberg Mountains taken from the top of the Elandsberg, looking west over the Nico Malan Pass.

DECLARATION

All work in this thesis is the original work of the author except where specific acknowledgement is made to work of others.

SIGNED : M Stavrakis

Department of Geology
University of Fort Hare
ALICE
5700

DATE : 1979-01-15

ACKNOWLEDGEMENTS

The Anglo American Corporation, which sponsored the thesis, and Mr John Strathern, who arranged the sponsorship, are both gratefully acknowledged.

Dr N Hiller who was my supervisor, is thanked for the interest he showed in the study, and the helpful suggestions he offered.

Prof. H V Eales and Mr D Gouws are thanked for their patience and willingness to help with the laboratory research.

My former colleagues, Prof. J C Theron and Dr C S Kingsley, and present colleague Mr C J Gunter, are thanked for their discussions related to the study.

Dr W E L Minter is thanked for the instruction he gave at the Sedimentological Winter School at Welkom, which was attended by the author.

Thanks go also to those persons who assisted in one way or another namely, Mr A J Reynolds, Dr R E Jacob and Prof. R Mason.

Mrs R Hayward of Fort Beaufort is thanked for typing the manuscript.

Special thanks go to my wife Brenda, who wrote the FORTRAN program, typed the draft and helped in so many ways.

The University of Fort Hare provided financial assistance and granted sabbatical leave during which the study was concluded.

ABSTRACT

The Katberg Sandstone is an arenaceous formation occuring stratigraphically three quarters of the way up in the Beaufort Group in the south-eastern part of the main Karoo basin.

A sedimentological study was carried out on the Katberg Sandstone and adjacent formations, in a 2 000 km^2 area south of Queenstown.

Stratigraphic sections were measured and lithofacies based on the style of Miall (1977) were established for the Katberg Sandstone, Balfour and Burgersdorp Formations. Stratigraphic relationships show that the Burgersdorp Formation in the study area, is the lateral (distal) equivalent of the Katberg Sandstone. The changeover from sandstone to predominantly shale lithology occurs roughly east-west between Cathcart and Whittlesea.

Stream hydraulic theory is discussed and the sedimentary structures of the various lithofacies are explained in terms of this theory. An analysis was done of thirty-four palaeochannels, and their various ancient flow characteristics were derived via multiple regression equations and a FORTRAN computer program. A statistical analysis of bedform structures, showed that flat-bedding of the upper flow regime is the dominant sedimentary structure of the Katberg Sandstone. Trough cross-bedding originating in aqueous dunes and planar cross-bedding of transverse bars, are fairly well represented while ripples are virtually absent. The opposite applies to the Balfour Formation where lower flow regime structures, viz., ripple cross-lamination and trough cross-bedding predominate. There is an even spread of (upper) flat-bedding, trough cross-bedding and ripple cross-lamination in the Burgersdorp Formation.

Detailed measurement of typical short sequences from sections of the three formations, and transition matrix analyses, showed the facies assemblages to be of three stream types :

(i) Katberg type : similar to Platte type of Miall (1977). Sediments were deposited by swiftly flowing, low sinuosity, braided, ephemeral streams with a predominantly sand bedload. Each flow started with preconsolidated silt and mud (flakes), and movement of exogenetic pebble lags. Channel avulsion and deposition of mud

drapes in higher topographic levels of the stream were common phenomena.

(ii) Balfour type : characterised by lateral accretion point bar type sequences of high sinuosity streams, and vertical accretion floodplain deposits. Lower flow regime dune and ripple bedform structures overlying (upper) flat-beds indicate a loss of stream power with channel migration.

(iii) Burgersdorp type : similar to Katberg type for sandstone units, also crevasse-splays onto thick subaerially exposed floodplain aggradation reddish shales.

Conventional microscopy and SEM studies showed tremendous diagenetic effects mostly in the form of secondary quartz growth in the sandstones of the three formations. Electron microprobe analyses were done on titanomagnetite grains from heavy mineral layers of the Katberg Sandstone, so that thermometric predictions could be made on provenance rocks.

Palaeocurrents of the Katberg Sandstone are mostly Rank 4 and 5 types (Miall, 1974), i.e., they were generated within bars with not much change in stream orientation. Burgersdorp and Balfour formation palaeocurrents are Rank 1 - 3 types. In the case of the former this is owing to directional changes in channels as a result of frequent crevasse-splays, and in the case of the latter owing to differences in orientation between entire tracts of highly sinuous palaeostreams.

Palaeocurrent directions in the Katberg Sandstone indicate a south-easterly provenance which accords with the findings of other Beaufort Group workers. Bed relief index calculations (Smith, 1970), made on Katberg rocks, considered together with the abundance of planar cross-bedding (of transverse bars) and apparent absence of longitudinal bars, testify to the deposition of the Katberg Sandstone in the distal parts of the braided stream environment.

The Beaufort sediments of the study area have the sedimentological characteristics of a molasse sequence, but a different implied tectonogenesis.

During Balfour sedimentation the equilibrium base was being raised very slowly at the source and complete fluvial sequences were deposited under a humid temperate climate, on a slowly subsiding plain. During Katberg/Burgersdorp times, source area tectonism was pronounced but interrupted and incomplete sequences were deposited under an arid climate.

Provenance rocks for the formations studied included biotite mesoperthitic granite, granulite, charnockite, granite porphyry, granophyre, metaquartzite, greenschist and possibly diorite, epidosite and alkaline volcanic rocks.

CONTENTS

I. INTRODUCTION

A. PHILOSOPHY OF APPROACH

A sedimentological study was carried out in the area indicated (Fig. 1), which includes the type locality for the Katberg Sandstone. Although previous work along the lines of stratigraphy and sedimentology has been done in this south-eastern part of the country, our knowledge of the stratigraphy and understanding of the sedimentology is still fairly limited. This being the state of affairs, and considering the recent prolific growth of relevant literature, a re-look at select sequences throughout the Karoo and other strata was inevitable. The Katberg Sandstone is but one of these. Compared to the surrounding Beaufort Group mudstones, siltstones and minor sandstones, this 580 m thick sandstone sequence is outwardly impressive in many ways and therefore a logical attraction and starting place. Although its surface outcrop area is approximately 1% of the Beaufort Group (Theron, 1973, p. 62), its significance in terms of our understanding of the sedimentation, tectonism and source material for the overall Beaufort Group is indeed many times greater.

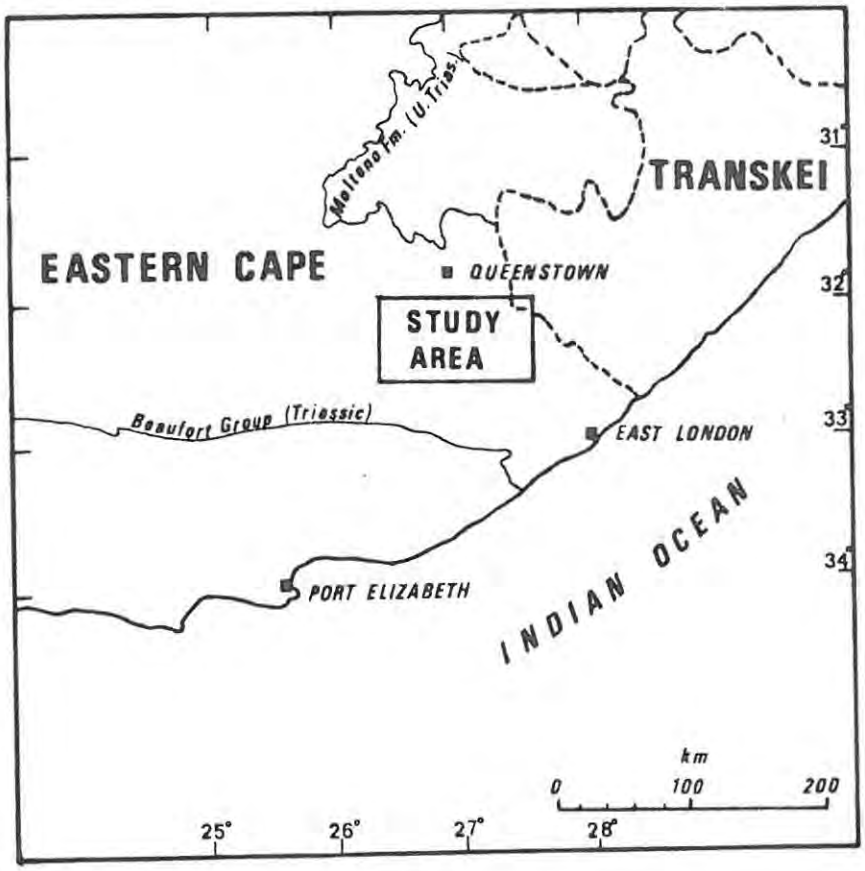

Fig. 1 Locality map

In the main, standard field and laboratory methods were followed, however, in parts, the special techniques of a number of individuals have been applied and in certain cases integrated for overall better understanding. Criticism has been leveled against statistical manipulation of data, mainly because infallible rules for choice of parameters and organisation of data do not exist. In any simulation model the secret is to include only those attributes having an influence on the efficiency of the system (OPE 202, 1978, p. 4). Invariably criticism will be forthcoming at any attempt to analyse stratigraphic sequences in terms of empirical and theoretical considerations. However, this type of analysis can only help in our understanding of the sedimentary processes and in the interpretation of the sedimentary environment.

With any mathematical manipulation process or simulation model there are complexities, and invariably assumptions have to be made. How good is the reasoning then, we might ask? Grobbelaar (OPE 202, 1978, p. 10) reflecting the views of other model researchers puts it this way. "It is impossible for man, with his limited abilities, to be able to simultaneously consider and evaluate in perspective all the interactions and interdependencies within a system. Because of this limitation, he experiments to see what inputs would give him the best answer."

The approach adopted in this thesis, one of substantiating physical observation of sedimentary processes as embodied in the rocks and their structures, with theoretical considerations, satisfies the norm for what a good simulation model should be. In this case it is a sedimentary model of a sandy fluviatile system.

B. HISTORICAL REVIEW

The Katberg Sandstone Formation is part of a thick succession of sediments belonging to the Beaufort Group of the Karoo Supergroup. According to Winter and Venter (1970, p. 397), the Beaufort Group exceeds 3 000 m in thickness in this south-eastern part of the country. Johnson and Keyser (1976) give a figure of 5 300 m. The present surface area of the main Beaufort basin is approximately

200 000 km^2 (Theron, 1973, p. 61), and thus covers about 20% of the total surface area of South Africa.

The sediments of this group comprise a monotonous arrangement of shales and mudstones with interbedded siltstones and lenticular sandstones (Truswell, 1977, p. 143). In the past, six reptilian assemblage zones were recognised, and based on these a biostratigraphic correlation was attempted (Mountain, 1968, p. 69). Strata that were previously regarded as part of the Endothiodon zone have now been assigned to the Cistecephalus zone. The other zone which has been dropped is the old Procolophon zone which is now included in the Lystrosaurus zone. A new zone, Daptocephalus, has been established and was introduced for the upper horizons of the old Cistecephalus zone (Kitching, 1977, p. 3). The zonal reduction and vertical distribution of the currently used five zones is shown below (after Kitching, 1977, p. 3).

CYNOGNATHUS	Upper	EARLY TRIASSIC
LYSTROSAURUS	Middle	
DAPTOCEPHALUS		LATE PERMIAN
CISTECEPHALUS	Lower	
TAPINOCEPHALUS		MIDDLE PERMIAN

Except for the Tapinocephalus zone which is restricted to the south-western parts, the remaining four zones form a somewhat orderly concentric distribution pattern within the main Karoo basin (Truswell, 1977, Fig. 63).

The Beaufort Group is subdivided on loose lithostratigraphic grounds into a lower Adelaide Subgroup and upper Tarkastad Subgroup. These are further subdivided into the Koonap, Middleton, and Balfour Formations in the case of the former, and Katberg Sandstone and Burgersdorp Formations in the case of the latter (Johnson, 1966, p. 49; 1976, p. 241). This is also the official Geological Survey (1976) version.

The Katberg Sandstone, according to Johnson and Keyser (1976), outcrops over most of the study area (Fig. 1), and extends laterally, east and west, from it. Two downfaulted fragments of this same formation have avoided denudation and are preserved along the coastal belt between the Kiwane and Gxulu rivers south of East London and around the Kwelera estuary north of the city (Mountain et al., 1975).

GENERALIZED GEOLOGICAL SECTIONS OF SOUTHERN BEAUFORT FORMATIONS

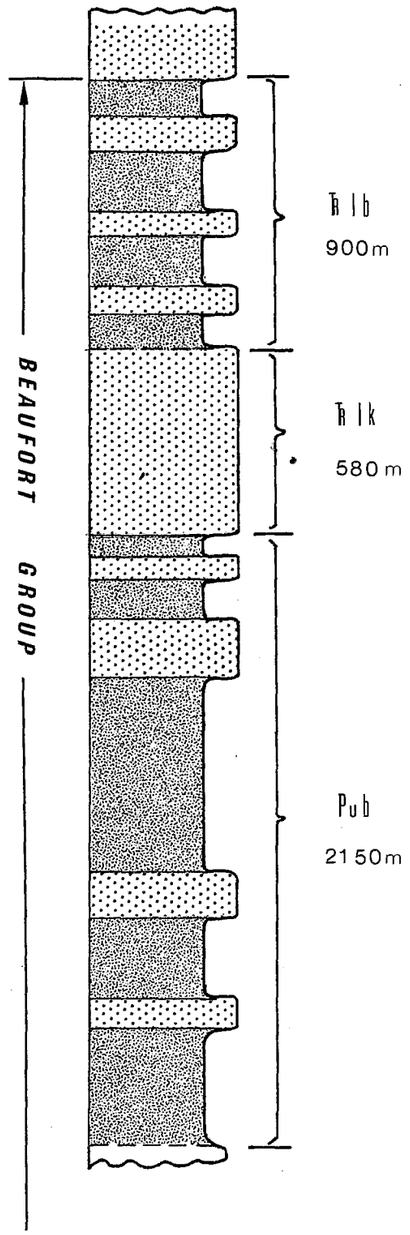

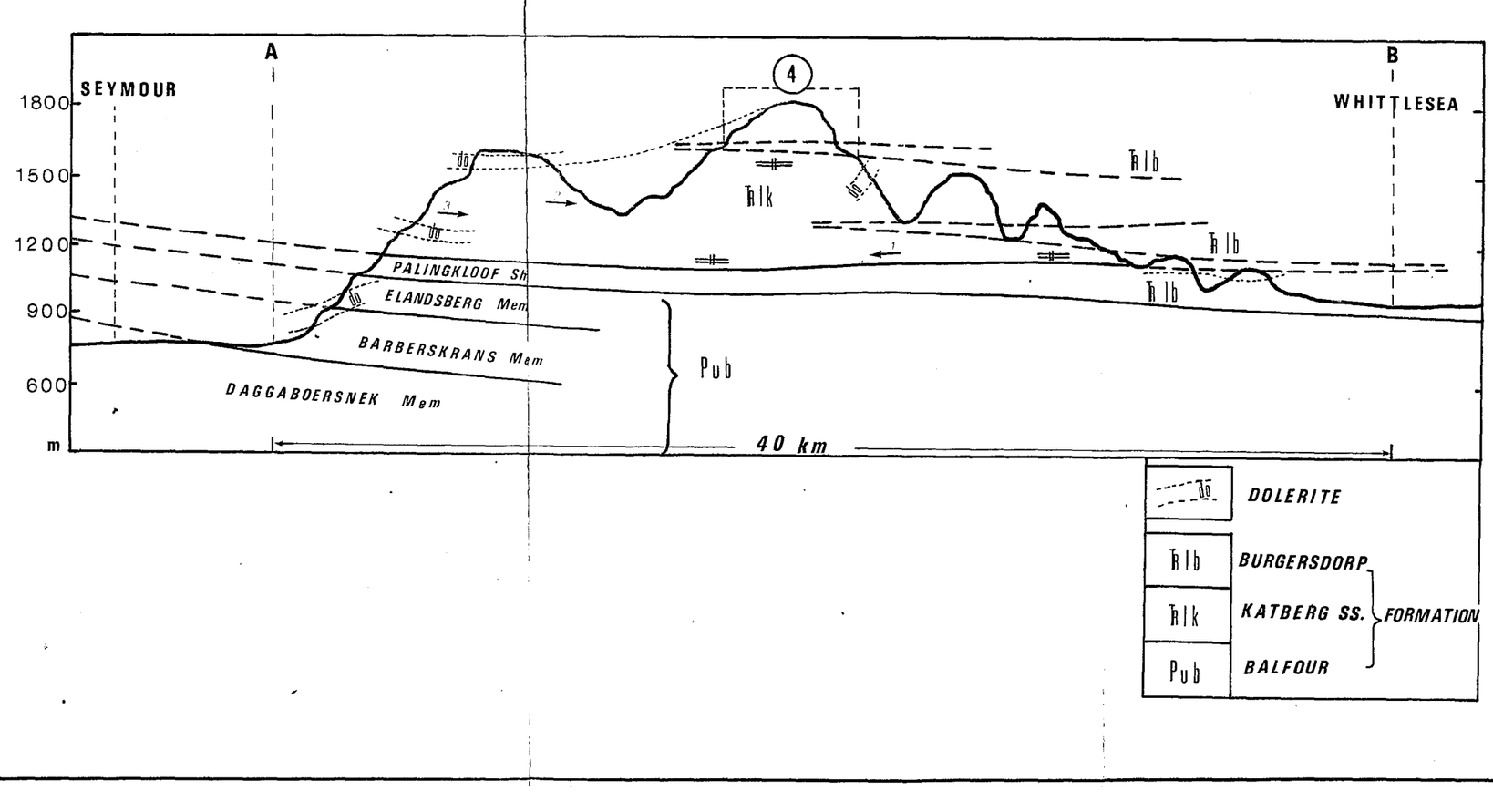

Fig. 2 Vertical column time-stratigraphy after Geological Survey. Cross-section : results of present study.

The Katberg Sandstone occurs stratigraphically about three-quarters of the way up in the Beaufort Group (Fig. 2), and the following thicknesses according to Johnson and Keyser (1976) refer :

Kwelera coastal area	920 m	(± 50 m)
Central study area	800 m	(± 50 m)
East of study area	600 m	(± 100 m)
West of study area	600 m	(± 100 m)

The same workers regard the base of the formation as that stratigraphic horizon above which the sand/shale ratio > 1. Similarly the top of the Katberg Sandstone is an arbitrarily selected line, "below which sandstone is more abundant than mudstone." They admit that the contact, in view of its transitional nature, is not easily located in practice. This aspect will be elaborated on in the next chapter.

C. PHYSICAL GEOGRAPHY AND CLIMATE

The area is bounded on the south by the eastern edge of an arcuate spur detached from the highveld plateau of South Africa. This projecting outlier hinges on the main escarpment along the 2 500 m high Sneeuberg range and gradually loses height eastwards through the Tandjesberg, Bankberg, Winterberge and Amatole ranges (Agnew, 1958, p. 1). The whole area therefore is particularly vulnerable to erosional attack, since the Queenstown Basin formed by the Great Kei River offers a local base level on the northern side (northern half of map), while the Indian Ocean on the south side of the mountains is a mere 150 km away. The ensuing discussion is partly after D Kopke (pers. comm., 1978). Erosional surface terminology is that of King (1963).

The inselberg of Gaika's Kop (Hogsback area) and the crest of the Elandsberg and Katberge (Winterberg range) are sections of the mono= clinally warped Gondwana (Cretaceous) surface. These ranges are all approximately 2 000 m in height. Ramifying juvenile streams and subsequent well established drainage networks have given rise to two large depressions, namely the Great Kei or Queenstown Basin and the Great Fish Basin. The former drains to the east and the latter to the south as classic superimposed drainage systems, (not adjusted to

structure), with deeply incised meanders commonplace along their entire lengths. These intervening basins represent King's 1st Post-African (P.A. I. Miocene) cyclic erosion surfaces. Remnant hilltops jutting out from the P.A. I surface in the Great Fish Basin are the residual fragments of a truly dissected former African (early Tertiary) erosion surface. These can be seen in the left-hand rear distance on the frontispiece plate. The smoothly bevelled African surface is clearly evident in the middle of the right-hand side of the photograph.

De Swardt and Bennet (1974, p. 309) have questioned King's idea of the presence of recognisable Cretaceous and Tertiary cyclic erosion surfaces over the whole of Natal. They furthermore challenge King's dating of the erosion surfaces, stating that it rests on insecure grounds. The writers state that with the break-up of Gondwanaland during the Jurassic a major graben developed roughly parallel to the coast. The ancestral fault-line scarps of the graben were driven back by erosion and now form the very irregular great escarpment of Southern Africa. They also disagree with the long held view that the Jurassic coastal flexure of south-east Africa is a monocline structure, and have furnished proof that the dominant structure of central and southern Natal is an arch and not a monocline. It is possible that this argument applies to the case of the present study area (see crossection Fig. 2, and discussion p. 94).

De Swardt and Bennet (1974, p. 309) describe the post-Gondwanaland development of Natal in terms of four physiographic features. They are the Drakensberg escarpment, the Pietermaritzburg step, the Natal hingeline and the straight coastline. Sometime after the Jurassic graben formation accelerated uplift along the Natal arch in the Palaeocene, led to the development of a scarp or 'treppe' (Pietermaritzburg step) on the older polycyclic erosion surface. In De Swardt and Bennet's (1974) terminology the east-west mountain ranges of the present study area would represent the retreating ancestral Southern African fault scarp. The local base level of the Queenstown Basin may correspond to their Pietermaritzburg step. South of the mountains the land surface is polycyclic, the tops of incised meanders representing older surfaces while the river valleys represent presently active surfaces.

Scenery in the mountainous areas especially along the southern escarpment is breathtaking. Slope profiles are convex in the outcrop area of the Katberg Sandstone but concave in the Cathcart-Queenstown-Whittlesea region, due to the predominantly shaly lithologies of the Burgersdorp Formation in these areas. Normally these hills have a dolerite or thin sandstone cap for their waxing slopes.

Climate is invigorating and usually that of temperate highlands for the southern half of the area, grading into true continental type in the Queenstown-Whittlesea areas, where mean annual ranges can be considerable. The Great Fish and Queenstown Basins receive 465 - 600 mm of rain on average every year, while along the south-facing mountain slopes precipitation is considerably higher, ranging between 1 000 and 2 000 mm annually. Snowfalls are common on higher ground during the winter months, and changes about freezing point can be a daily event. Where moisture is involved, such as melting snow, mist and light rain, mechanical weathering is considerable and large volumes of rock have been stripped and dumped into thick piedmont type talus slopes. The entire southern mountain range is wooded with dense indigenous forests and other plantations. Yellow wood, blackwood, oak, red pear, wattle, bluegum, wild lemon and white stinkwood are among the main types present. Two north-south tarred roads and many gravel and other roads transect the area. Some magnificent road cuttings can be seen along the new tarred road between Seymour and Whittlesea. The road and some of its cuttings are clearly visible on the frontispiece.

II. STRATIGRAPHY AND FIELDWORK

A. BACKGROUND AND FIELD METHODS

Prior to December 1977, when the field study was begun in earnest, the area was visited on a number of occasions. In the earlier part of that year the area was thoroughly reconnoitered for the purpose of selecting suitable locations for stratigraphic measurements. It soon became apparent that the task of sorting out the stratigraphy was immense, if not impossible. Very few potential sections transgressed the base of the Sandstone and those that did were usually located in dense indigenous forest with deep soil cover on the south-facing slopes of the Winterberg and Amatole mountain ranges. Even in the best road cuttings correlation across the width of a road was seldom possible. Ubiquitous dolerite intrusions further complicate the puzzle.

The stratigraphic 'top' of the Katberg Sandstone proved to be elusive and often where it was located, according to the geological map (King-williamstown Sheet, 1976), horizontally bedded Katberg Sandstone was seen overlying 'younger' Burgersdorp rocks with no evident overturning of strata. No fossils were found although many likely localities were investigated. In spite of the fact that the Beaufort Group is rich in reptilian fossils in general, none have hitherto been reported from the Katberg Sandstone of the study area. The Lystrosaurus locality at Hobb's Hill (see geological map), according to this study, belongs to a wedge shaped red-shale lithosome of the Burgersdorp Formation.

No lithostratigraphic marker beds were noticed, and although, in general, exposures are good, individual sandstone units and minor sequences were noticed to be interfered with by numerous irregular erosional surfaces followed by similarly ravaged sedimentation units. At this stage one thing was obvious, that a conventional 'layer cake' subdivision of the Katberg Sandstone was well-nigh impossible. During the intervening period of reflection, the words of Blatt et al. (1972), p. 7) were recalled, "A geologist's ability to describe an outcrop is closely related to his understanding of the observable phenomena." Consequently at various stages thereafter, assistance and advice were sought in order to partially realise this objective.

During December 1977 three weeks were spent in the area for the purpose of measuring selected stratigraphic sections. Twelve sections were measured (see geological map), the descriptions of which appear in the next section, and over 300 rock samples were collected for laboratory work. Stratigraphic measurement was either done using a Jacob Staff with Abney hand level (Fig. 3) in well exposed outcrops, or with a metricated Paulin altimeter. The latter method was especially useful in less accessible mountainous country. Changes in atmospheric pressure affected readings where the latter method was used. However, since the greatest fluctuations were noticed to occur usually between 09 h 00 and 11 h 00, stratigraphic measurement was avoided during these times. Instead, palaeocurrent data collecting and other activities were carried out during those unstable hours. Nevertheless, the data from the raw method still had to be amended. Procedures were as follows :

1. Altimeter Method

The complete distance of the section was covered very quickly, by motor car if possible, and elevation readings were recorded at top and bottom. Where sections extended over long distances, e.g., at Devil's Bellows Nek (section 2), a number of such quick traverses were done. Immediately following this, detailed measurement of the section concerned was begun, at the same previous starting or finishing point, whichever proved to be the most convenient. Altimeter readings were carried out at the base (corresponding with observer eye level) of every sedimentation unit as recorded on the sections. When the predetermined length of the section had been covered, the discrepancy was proportionately split over the whole section. Measurement normally started at approximately 06 h 00. Where it was not possible to perform a quick traverse, e.g., up mountain slopes, actual starting and finishing elevations were obtained from 1 : 50 000 topo cadastral sheets. However, in most cases a rough check could still be made using the altimeter since the descent from such high places usually took only from thirty to forty-five minutes. Only in the case of the 2 000 m high Elandsberg traverse (section 3) was the time of descent over two hours, owing to hazardous scree slopes. In some cases corrections were made to stratigraphic thickness where dips of 2^{o} or more were present. Generally though, correction

was unnecessary because strata were found to be essentially horizontal.

2. Jacob Staff Method

All the sections were retraced at a later stage for the purpose of statistical analyses of bedforms (Chapter III) and in the case of sections 1, 6 and 8 the entire column was revised. In the latter two cases alternate thickness measuring techniques were deliberately applied. In both cases the discrepancy arising from using Jacob Staff methods was ± 1% of the total stratigraphic thickness, as obtained from quick altimeter traverse. Kottlowski (1965, p. 61 - 75) outlines the various Jacob Staff methods. For this study an Abney hand level was used in conjunction with the staff (Fig. 3).

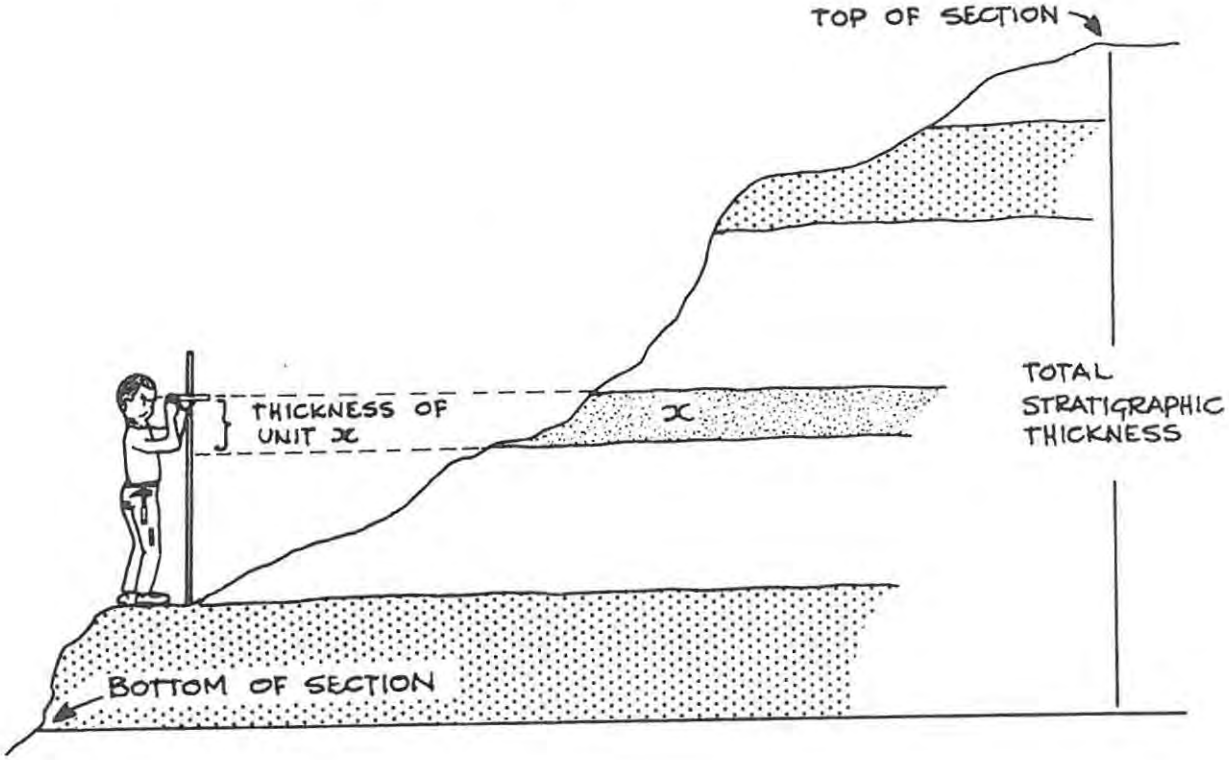

Fig. 3 Stratigraphic measurement by Jacob Staff (after Kottlowski).

B. GEOLOGICAL MAPPING AND STRATIGRAPHIC NOMENCLATURE

The outcrop area of the Katberg Formation (Johnson, 1976, p. 245) is shown on the 1 : 250 000 Geological Series, Kingwilliamstown Sheet. Explanatory notes for the sheet are by Johnson and Keyser (1976). There appears to be some confusion as regards this lower formation of the Tarkastad Subgroup. In the explanatory notes the name Katberg Sandstone Formation is used and, as mentioned in the previous chapter, has been delineated as that area in which sand/shale > 1. However, Johnson (1976, p. 245) states, "For the northern areas the name Katberg Sandstone is no longer valid, and the designation Katberg Formation will have to be employed." This has been done presumably because lithologic continuity is lost from the predominantly sandstone rocks of the south (i.e., south and central parts of the geological map for this study) to mostly shales and mudstones in the north. The above writer goes on (p. 243), "North of 32° S, however, sandstone is not necessarily always predominant in the Katberg Formation and it will have to be distinguished purely on the grounds of its more arenaceous character relative to the Burgersdorp Formation. North of 31° S the distinction between these two formations is no longer obvious ..."

The following emerge from the above discussion. Two formations, viz. Katberg Sandstone and Katberg Formation (Katberg Sandstone Formation of Johnson and Keyser is a hybrid of the two) have been proposed, the word Katberg being the confusing ingredient. The word has been retained in both cases presumably because of the appearance of 'typical Katberg sandstone' in both formations. If this is so, the case is invalid because, by definition, a formation is "A body of rock characterised by lithologic homogeneity." (A.C.S.N., Art. 6). This homogeneity is lost in a northerly direction, therefore two formations without similar connotation should be set up, or two members should be designated to one, say Katberg Formation, thus obviating the need for two of these units. According to the code of stratigraphic nomenclature (A.C.S.N. Art. 7b), "Even though all members of a formation are locally mappable, it does not follow that they should be raised to formational rank, because multiplicity of formation names may obscure rather than clarify relations with other areas." It is true that according to the same code, unit names may be duplicated but this is undesirable and should be avoided.

Since, in the specific case of the Katberg Sandstone, continuity is lost along strike in a northerly direction, the two formations of Johnson (1976) are laterally equivalent, and it might be proposed that they be considered as two members of the same Katberg Formation, i.e., a southern sandstone member and a northern shale member. All along, a facies change from south to north has been implied. This indeed appears to be the case, and interdigitation of sandstone of Johnson's (1976) Katberg Sandstone, and shale from his Katberg Formation, are present and visible at places along the entire northern contact of the Katberg Sandstone Formation for this study (see geological map) hereafter called Katberg Sandstone.

The sandstone unit, corresponding to Johnson's (1976) Katberg Sandstone was concentrated on in this study and although the present writer is in agreement with the delineation of the lower contact of the sandstone (Geological Series, Kingwilliamstown Sheet) the horizon of changeover from sandstone to shale, usually sudden but interfingering, has been completely revised between the East London-Queenstown national road in the east and the Whittlesea-Katberg Pass road in the west. Between these boundaries the limit of revision in a northerly direction is roughly 32° 10' S. Some of the more important dolerites are shown, mostly redrawn from the Kingwilliamstown Sheet, however, in a number of cases where dolerite was indicated it could not be located or was mistaken for sandstone by the compilers of that map. The criteria used by the present writer to distinguish between the three formations indicated on the geological map for this study namely Balfour, Katberg Sandstone and Burgersdorp Formations, are outlined in chapters III and V, and are based on the following :

(i) petrology of the sandstones
(ii) primary sedimentary structures
(iii) palaeohydraulic analysis
(iv) rank of palaeocurrent variance and its palaeoenvironmental significance
(v) statistical analysis of bedforms
(vi) facies relationship (matrix) analysis.

In some cases the differences between Katberg Sandstone and Burgersdorp Formations is not cut and dried, and subjective reasoning was used.

Since fossil evidence and other time indicators are generally lacking, no subdivision implying time has been attempted. As mentioned earlier, the strata in this area are essentially horizontal. Only three reported fossil localities, all from the Lystrosaurus Zone (Zonal Locality Map, Kitching, 1977), appear in the area and all are from virtually identical red shales of the Balfour Formation 'below', and the Burgersdorp Formation 'above'. Both immediately underlie the Katberg Sandstone of this study. Therefore the notion that the red shales (Palingkloof Member) immediately below the Katberg Sandstone in the south and those interfingering with it in the north (Burgersdorp Formation of this study = Johnson's northern Katberg Formation) are stratigraphically different and of different ages is quite possibly incorrect. What is in fact being suggested by the present writer is that the red shales at the top of the Balfour Formation or 'Palingkloof Member' (Johnson , 1976, p. 241) may be part of the same mudstone lithosome enveloping the predominantly arenaceous Katberg Sandstone (Fig. 4). The distal end of the sandstone wedge would represent the changeover point in time from progradation of Katberg Sandstone to aggradation of Burgersdorp Formation shales.

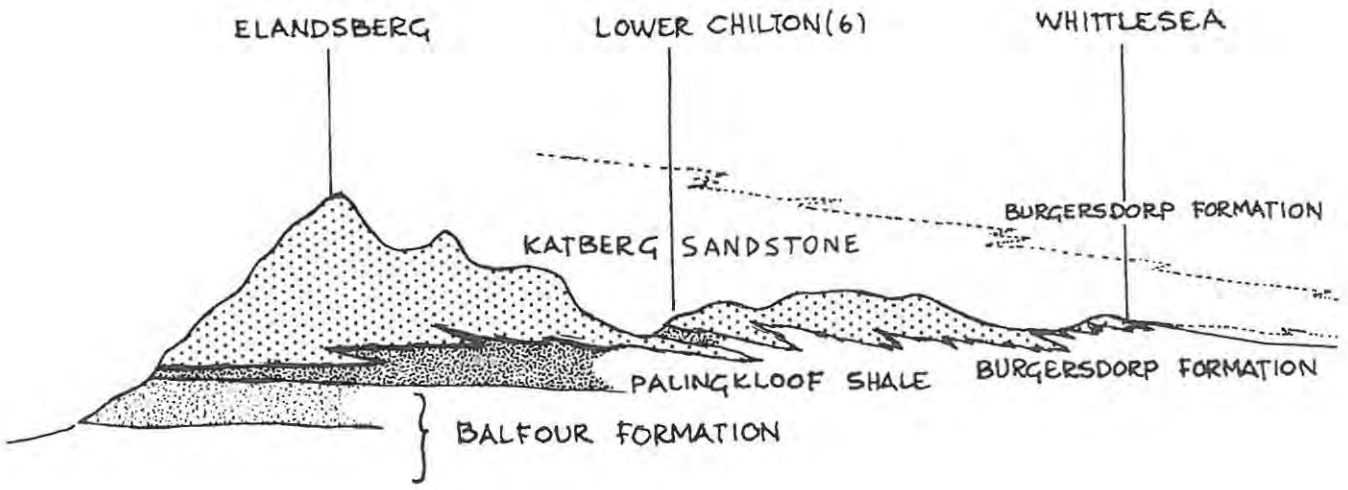

Fig. 4 Idealized cross-section showing progradation of Katberg Sandstone wedge.

C. DESCRIPTION OF SECTIONS

The scheme used to describe measured sections in the field and illustrated sections later is based on the nomenclature and style of Selley (1970, Fig. 0.1), and terminology of Jackson (1976, Fig. 5, based on de Raaf and Boersma, 1971) and Miall (1977, p. 20).

Section 6 - Lower Chilton, Topo. 3226 BD, Date: 14/12/77, Jacob Staff Elevation of base (1156 m)

Thick m	Basal Type	Colour	Grain	ss/sh %	c.p.s	Miall Facies	Comments
2,95	~~~	5GY 6/1	f	80/20	22	Sp Sh	Planar cosets, Epsil. at base, some Shale flakes, horiz. bedd. (UFB) in between. ≈ lamin. and ripples at top. Sample no. 77/016/4 and photo.
1,75	- - - -	5YR 4/1	v.f.	5/95	31	Fm Fl	Palingkloof type red shale with thin silt layers. Concretions 2-25 cms diam. Garnetized? nodules.

Fig. 5 Specimen of field stratigraphic log.

No predictable sequence of bedforms was noted although some semblance of fining upward cycles was recorded at Hobb's Hill (10) and parts of Lower Chilton (6), Fairford (8) and Nico Malan Pass (3). Six lithofacies have been isolated and are classified mainly according to their primary sedimentary structures. They are described as follows :

1. Intraformational conglomerates

These are mainly of the mud ball or shale flake type. No true conglomerates have been seen in the study area, although in places lag material up to cobble size (- 6ϕ) and consisting mainly of quartzite was found. These shale pellet conglomerates are similar to those described by Clark (1962, p. 423) in his classification of redbeds. Individual clasts vary in size from small flecks through

pebble and cobble sized balls to large (0,5 m) blocks. Pebble sized predominate, however. The clasts are mostly reddish brown (5R 4/2) in the Katberg Sandstone. Virtually every sandstone lithosome and minor sequence overlies such an intraformational conglomerate unit, usually 5 - 50 cm thick, lying on top of an irregular scour surface. The mud clasts are usually matrix supported by pinkish medium sandstone. Trough crossbedding with heterogeneous foresets is sometimes present. Other primary structures include orientated flakes, mud balls and flute casts. The packing density of the clasts appears to be closely related to the immediately underlying rocks. Where these take the form of extensive mudstone beds (facies 5, below) densities of 90 - 100% are common and clast size is often large. The opposite is also true proving that the material is locally derived.

2. Horizontally-bedded sandstone and siltstone facies

A distinction is made here between two types; (a) with pronounced parting lineation and grain orientation, and (b) with no grain movement and usually restricted to the finer grain sizes (4ϕ - 6ϕ). The former originates in the upper flow regime while the latter characterises standing water conditions of the lower flow regime where current velocities are virtually nil (see Chapter III). The writer has learnt to distinguish between these two types of horizontal lamination in the field.

(i) Upper flat bed (UFB) type (Southard, 1975)

This subfacies corresponds roughly to Miall's (1977, p. 28) Sh-facies. Sorting of sand grains is very good and the Wentworth class size is that of fine sand (2,5ϕ). Horizontal bedding (UFB) is the dominant bedform structure of the Katberg Sandstone. Parting lineation is ubiquitous in this subfacies. UFB laminated sets can vary in thickness from a few centimetres to a few metres. Sets are commonly less than 1 metre thick especially where they overlie different bedforms such as planar or trough cross bedded units, but cosets can reach 5 metres in thickness where continuous channel fill has taken place, e.g., upper part of Elandsberg section (3). Colour is variable but commonly greenish grey (5 GY 6/2) when fresh. Discreet heavy mineral laminae are frequently found comprising some of the sets or parts of them (Fig. 6).

(ii) Lower flat bed (LFB) type

This type is restricted to the finest silt sizes and fine graded bedding is usually evident. Mottling, although common, is not characteristic of this subfacies. This LFB type shows no grain orientation, can occur in considerably thick, 5 - 15 metre deep layers, and breaks with an uneven fracture. Its higher energy counterpart shows pronounced parting lineation and grain orientation (pseudoschistosity) and has a very good 'cleavage' parallel to the bed. Colour is also fairly diagnostic and experience shows that darker shades, e.g., 5Y 3/2, 5 GY 4/1, 5G 2/1 predominate in fresh exposures, oxidizing to beige and yellowish hues (5Y 6/4). This subfacies is especially common in the siltstones and very fine sandstones of the Balfour Formation.

3. Cross-bedded sandstone facies

(i) Trough cross-bedded sandstone

This subfacies corresponds to Miall's (1977, p. 20) St-facies, the characteristics of which are well described by that writer and which are outlined below. Trough cross-bedding as observed in the Katberg Sandstone and adjoining formations is highly variable. Terminology used to describe the types is from Allen (1963). Solitary 5 m wide zeta sets (Fig. 7) were seen at Hobb's Hill (10), Katberg Pass (1 and 2), Deep River (4) and Nico Malan Pass/Elandsberg (3). This type, however, was generally rare. Using the definitions of Allen (1963), ambiguity often arises and many of the considered zeta type scoops may in fact be theta and iota units. Examples pointed out to the writer at a recent sedimentological Winter School run by Dr W E L Minter at Welkom, showed that three dimensional exposures of dunes mostly had discordant lower bounding surfaces of the theta and pi types. Transverse and longitudinal sections of large solitary sets displaying apparently concordant lower surfaces were also noticed. In both cases the units occur in Upper Witwatersrand Group quartzites corresponding to Miall's (1977, p. 20) St-facies. It is based on this experience that the selection of type was made. The significance of these zeta troughs is discussed in Chapter III.

By far the most abundant trough cross-stratification in the Katberg

Sandstone and Burgersdorp formations within the limits of the study area is the festoon type pi, followed by nu and to a very limited extent kappa. Xi - cross-bedding by its very nature was found to be the most difficult to recognise because it resembles chaotically stacked pi - cosets, as is the case at Katberg Pass (1 and 2) where the upper parts of both sections display this latter type to the total exclusion of other trough units. The host sandstones here are generally pinkish-grey (5 YR 7/2) when fresh, and a light speckled creamy colour (10 YR 8/2) when bleached. This is the rock that has been generally regarded as 'typical' Katberg sandstone by workers in the past and on which many assumptions have been made. The pink colour owes its origin to flecks and tiny specks of reddish mudstone particles interspersed throughout the rock. Grain size is variable, with the clay flakes reaching pebble size and tough, Witteberg-type quartzitic pebbles being commonly around - 4,5ϕ in diametre. Other pebbly material includes porphyritic-granite, opalized-wood, agate, jasper and pre-consolidated sandstone, but these are generally smaller in size (- 3,73ϕ). The sand sized bulk of the rock is usually reasonably well sorted and in the medium-sand range (1,5ϕ).

(ii) Planar cross-bedded sandstone

The characteristics of this group are generally similar to the Sp-facies of Miall (1977, p. 26). The host sandstones vary from the feldspathic graywackes of Katberg Pass (1 and 2), to the finer grained arkoses of Lower Chilton (6). [Sandstone terminology is after Pettijohn (1975, p. 211).] Planar units of the Katberg Sandstone are usually 0,15 - 0,8 m thick and occur in the following configurations. They rest on either an irregular erosional base (Figs. 7 and 8) or horizontal non-erosional surfaces, or are superimposed on one another or alternate with cosets of UFB lamination of equal thickness (Fig. 8). Using the terminology of Allen (1963) they are of the alpha, beta, gamma and epsilon types. All these combinations can be seen in Figs. 7 and 8. The bar types containing this planar cross-bedding are laterally continuous for up to 30 m in some places. In rare, well preserved cases, ripple lamination is seen discordantly overlying topsets, as with the classic example just above the base of the Katberg Sandstone at 1 193 m (a.s.l.) in the Nico Malan Pass (Fig. 9). The planar units described under this subfacies are therefore of the restricted-thickness Platte River-type (Smith, 1970, p. 2995;

Fig. 6 Heavy mineral laminae in UFB-Katberg-sandstone.

Fig. 7 Planar cross-bedded sandstone overlying zeta-type trough cross-bedded sandstone. Hobb's Hill (10), Katberg Sandstone.

Fig. 8 Heavy mineral laminae in UFB-Katberg-sandstone separating planar alpha sets at top from planar epsilon sets below. Loc., Lower Chilton (6).

Fig. 9 Longitudinal section of former transverse bar with ripples and silt drape superimposed. Loc., Nico Malan Pass (3), Katberg Sandstone.

Fig. 10 Large scale planar foresets of former sand wave. Loc., Nico Malan Pass (3), Balfour Formation.

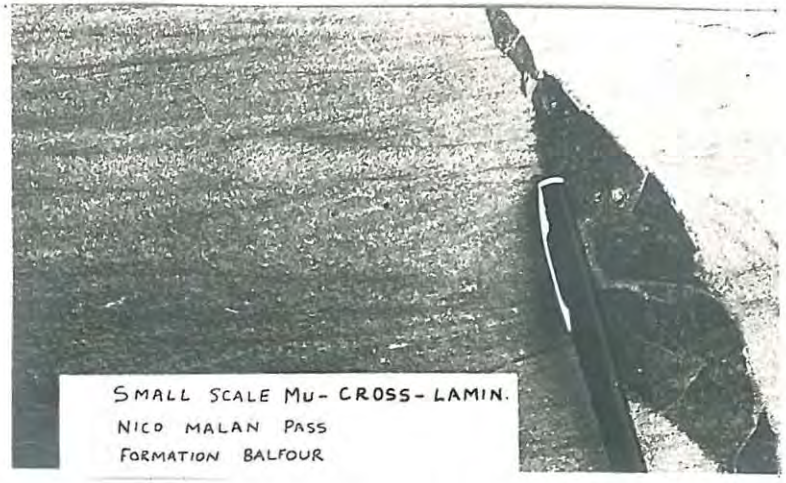

Fig. 11 Mu-cross-stratification. Loc., Nico Malan Pass (3), Balfour Formation.

Fig. 12 Sinuous assymetrical current ripples on mud drape layer. Loc., Lower Chilton (6), Katberg Sandstone.

Fig. 13 Cornstone from Katberg Sandstone (4).

1972, p. 625), the laboratory deltas of Jopling (1965, pp. 53 - 65), Boothroyd and Ashley's (1975, p. 214) linguoid bar planar-cross-stratification, and those designated planar A-type by Turner (1977, p. 243). The latter writer has in turn likened them to the avalanche front cross-stratification of Picard and High (1973).

Larger planar-B units (Turner, 1977, p. 244) were not observed in the Katberg Sandstone, although large scale, laterally extensive planar units with low angle foreset bedding (Fig. 10) were seen in fine-medium (grain) sized sandstones of the Balfour Formation, albeit in restricted sections. The extrapolated size of the bedforms containing this type gave wave heights of up to 7 m which would put them almost in the sand-wave class of Coleman (1969, p. 190), who worked on modern day bedforms of the enormous Brahmaputra river.

4. Ripple cross-bedded facies

This facies corresponds to Facies Sr and partly to Facies Fl of Miall (1977, p. 20). Terminology used for this facies is from McKee (1965, p. 66) and Allen (1963). The whole spectrum of ripple types is present in Balfour, Katberg and Burgersdorp rocks. Ripples are mostly assymetrical, low amplitude (2 - 5 cms) and most commonly seen as ripple drift lamination and superimposed ripple sets without drift. These two latter types are very common and could be said to form the dominant internal structure of Balfour Formation siltstones and very fine sandstones. Grain size, however, does not seem to be a criterion for ripple formation insofar as sandstone grain size rarely exceeds 0,65 mm in the Katberg Sandstone yet ripples are virtually absent from this formation. Nearly every Balfour sandstone investigated was found to be ripple laminated. The following modes of occurrence were recorded :

(i) superimposed kappa cross-lamination with or without drift in longitudinal sections and wavy in cross sections;
(ii) pseudo flat-bedded lamda cross-stratification as evidenced in thick sandstone lithosomes south of Seymour (just off map);
(iii) small mu-cosets (Fig. 11), with foreset azimuths normal to palaeo-stream thalweg.

All of these occur mostly in silt and fine to medium sandstones. There is no obvious preferential development. On close observation, kappa and lamda micro cross-lamination can be seen in dark mudstones of the same formation. In plan view rib and furrow structures are ever present.

Ripples are virtually absent in the sandstones of the Katberg Sandstone and Burgersdorp Formations. This surprising revelation became apparent during close scrutiny of selected sections for the purpose of comparing the statistical abundance of the most common bedforms (see Chapter III). Where seen they occur as solitary, one-layer sets on thin mudstone-veneer surfaces (Fig. 12).

5. Silt and Mudstone facies

This includes the Fl and Fm facies of Miall (1977, p. 30). In the Balfour Formation mudstones and shales are mostly medium bluish-grey, dark greenish-grey to greenish-black in colour. Mudstones may either be locally massive, show internal bedding of the LFB type, or contain small scale ripple lamination as described above. They are usually of variable grain size, but generally within the range 4,5 - 7,0ϕ . Frequently mudstones are interbedded with thin layers of siltstone and very fine sandstones.

Immediately underlying the Katberg Sandstone are ± 50 m of greyish-red (5R 4/2) mudstones with dark greenish-grey (5 GY 4/1) blotches and similarly coloured, tough siliceous nodules of all shapes and up to 0,5 m in size. The overall lithology and stratigraphic position of these mudstones with respect to the Katberg Sandstone appears to be consistent. There are usually two or three of these reddish layers individually up to 10 m in thickness and separated by lighter coloured trough cross-bedded sandstones and massive to bedded greenish-grey mudstone.

This facies is represented by similar greyish-red (5R 4/2) mudstones in the Burgersdorp Formation. It is, however, usually found interbedded with thin siltstone layers within any given thick mudstone lithosome, and it is also the dominant rock type of the lower part of the Burgers-dorp Formation. Unlike the very nodular mudstones of the southern outcrop

area, those of the Burgersdorp Formation contain far fewer concretions. Reddish mudstones identical to those of the Burgersdorp Formation but thinner, occur at places within the Katberg Sandstone. These are indicated by the letter R within facies designated Fm on the sections.

North of Cathcart in the Hobb's Hill area, there is a zone of indeterminancy between Katberg and Burgersdorp Formations where the degree of mixing between sandstone and mudstone is very high (c.f. high entropy value, Krumbein and Sloss, p. 465).

These greyish-red mudstones often contain sand-wedge polygons and actual mud-cracked surfaces. Vertical tube-like sand and mud filled structures have been noticed within a couple of these mudstone outcrops of the Katberg Sandstone and Burgersdorp Formations.

Thin lenticular mudstone lithosomes, usually of the dark greenish black variety occur as veneers over thicker sandstone units and generally take up depressions in the bed relief of the numerous channels and bars of the Katberg Sandstone. These have been described as mud drapes by Minter (pers. comm., 1978). See also Smith (1970, p. 3010) and Miall (1977, p. 36).

6. Massive sandstone facies

Seemingly structureless sandstones have been designated as Facies-Sm in accordance with Miall terminology, but it is possible that such units may prove to be actually stratified. Hamblin (1971, p. 252) has shown how similar rocks do in fact possess a variety of inherent structures.

Vague symmetrical cross-bedding patterns have been observed in sandstones of this facies in the eastern part of the study area. The inferred significance of this is discussed in Chapter III.

Cornstone

This term was introduced by Allen (1960, p. 43) to describe concretionary material in the Old Red Sandstone. Intense development

of iron- and manganese-rich calcareous concretions in usually pinkish-grey (5 YR 7/2) fine to medium sandstone occurs in association with reddish mudstones of the previous facies. Concretionary development is either perfectly spherical or so irregular and diffused throughout the sandstone host that it sometimes becomes difficult to distinguish the concretions from the host sandstone. Cornstones of the Katberg Sandstone and Burgersdorp Formations are of the calcareous concretionary types of Allen (1960, p. 43) and not the siliceous and conglomeratic correlatives. Their abundance and stratigraphic positions are indicated on the sections. The characteristic 'cat's brain' texture (porous fluted appearance) often associated with such rocks (Hatch et al., 1965, p. 211) appeared to be absent. Some vague fluting was noticed, which is evidently related to the above structure, but this was unconvincing. Leisgang bands (discordant reddish streaks) are common. Incipient weathering along these ferruginous layers may be responsible for the suggested fluting.

III. SEDIMENTOLOGY AND SEDIMENTARY PROCESSES

PREAMBLE

This chapter deals with the processing and interpretation of all the accumulated field data. The likely origins of observed sedimentary structures are discussed in terms of hydrodynamic theory. The background and continuation of this endeavour, the comparison between flume experiments and field observations is also discussed. Equations based on empirical considerations and reasonable assumption have been condensed and integrated into a logical computer program. Typical minor sequences, based on detailed field observations, and facies relationship models for the Balfour, Katberg Sandstone and Burgersdorp Formations have been established, and finally a technique by which palaeostream bedforms can be predicted (and indeed later checked in the field) has been presented in simplified model form.

A. HYDRODYNAMIC THEORY

The following section is an up to date summary of the relevant literature and is based on the writing of Simons (1969, p. 124), Jopling (1965, p. 53), McKee (1965, p. 5), Allen (1968), Schumm (1972, p. 98), Smith (1972, p. 624), Southard (1975, p. 5), Walker (1975, p. 63), Boothroyd and Ashley (1975, p. 193), Miall (1977) and Selley (1976) to name the main sources. A list of symbols and definitions appear at the end of this chapter.

1. Flow in open channels

There are basically two types of open channel flow;

(a) laminar flow
(b) turbulent flow.

In laminar flow the layers of flow in the fluid stream evenly and with uniform velocity throughout the mass and parallel to the bedform configuration. There is no diffusion between stream lines and thus no turbulence. With laminar flow the shear stress τ_o being transmitted through each layer of depth varies uniformly from zero at the surface to a maximum at the stream bed, while the velocity curve is parabolic in shape with maximum velocity roughly three-quarters of the way up from

the bed (Figs. 1 and 2, in Briggs and Middleton, 1965, pp. 6,7). In natural streams, disturbances are present in such magnitude that laminar flow is rarely found. Hence turbulent flow is the dominant type in nature.

In turbulent flow there is a continuous interference of streamlines and infinite degrees of mixing in the stream. As a result energy loss is high in this type of flow and eddies and vorticies are characteristic. The velocity distribution from water surface to bed is more uniform in turbulent than in laminar flow.

Values of Reynolds' number $Re = \frac{VR\rho}{\mu} = \frac{VR}{\nu}$

which is the ratio of Inertia force/Viscous force, can be used to predict whether flow will be laminar or turbulent. For natural channels the critical Reynolds' number separating laminar from turbulent flow should be near 500 (Simons, 1969, p. 125).

A second important coefficient of fluid dynamics is the Froude number which is the ratio between the force required to stop a particle and the force of gravity. For open channel flow the Froude number is expressed as follows :

$$Fr = \frac{V}{\sqrt{gD}}$$

This dimensionless number is the criterion used to distinguish between three conditions of flow, namely tranquil, critical and rapid. When $Fr < 1$, flow is tranquil; when $Fr = 1$, flow is said to be critical; when $Fr > 1$, flow is rapid. Based on the calculated Froude number and consequent condition of flow, Simons and Richardson (1961, p. IV) introduced the concept of flow regime. Sections of natural rivers are said to belong to either the lower or upper flow regime. Flow regime is defined as follows : "A range of flows with similar bedforms, resistance to flow and mode of sediment transport has been called a flow regime." (Middleton, 1965, p. 249).

The sequence of bedforms characterising the various regimes of flow

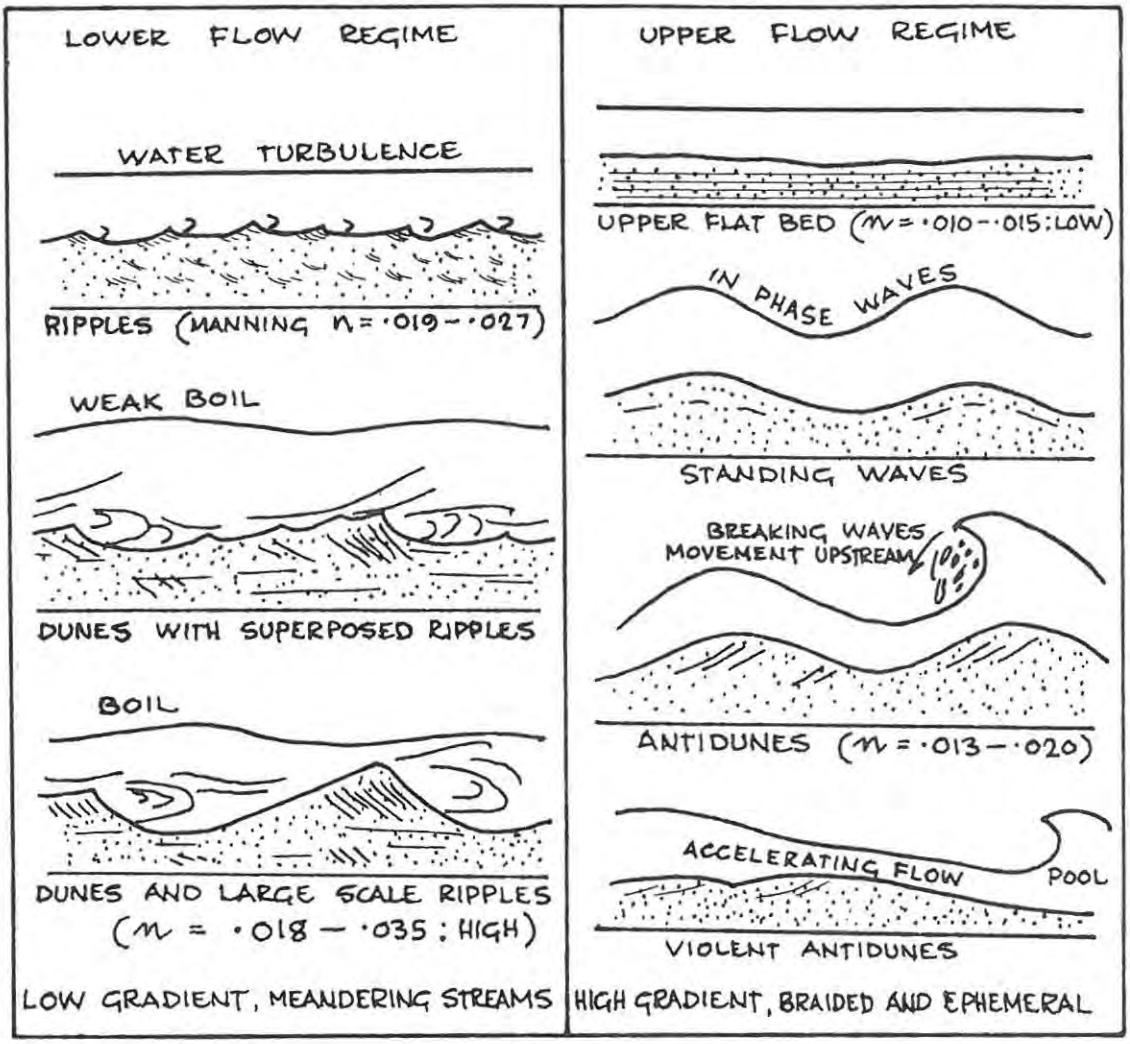

Fig. 14 Types of flow and corresponding bedforms found in alluvial channels (modified after Simons and Richardson, 1961).

is shown in Fig. 14. It can be seen from Fig. 15 that a Froude number equal to one separates tranquil from rapid flow, and thus the lower from the upper flow regime. (Simons, 1969, p. 136). A transition zone where Fr = 0,8 - 1,0 has also been established. Simons (1969, p. 128) has suggested that slope more than anything else determines whether flow is tranquil, critical or rapid. The following factors affect the bed configuration; bed roughness and resistance to flow in alluvial channels with a sand bed; slope, depth, particle size and roughness, and median fall diameter, which in turn depends on fluid viscosity and density, and mass density of bed material.

The typical bedforms and associated sedimentary structures found in the lower and upper flow regimes (Figs. 14 and 15) in increasing hierarchial order are as follows :

Lower flow regime :

Bedform	Structures	Miall facies
Ripples (fall diam. 0,65 mm)	Ripple cross-lamination, kappa, lamda, and mu sets and cosets.	Sr Fl
Lower flat bed (fall diam. 0,65 mm)	Flat bed lamination, some graded bedding and blocky uneven rock fracture.	Gm *Sm Fm[1]
Large ripples (amplitude 0,25 - 0,5 m)	Mu, nu and omikron cross stratification.	Sr St
Sand waves Transverse bars	Planar cross-stratification Mostly alpha and epsilon types.	Sp
Dunes, megaripples	Trough cross-stratification. Pi and zeta to iota scoops.	St

Upper flow regime :

Bedform	Structures	Miall facies
Upper flat bed	Flat bed lamination, parting lineation with grain orientation. 'Cleavage' parallel to bed.	Sh
Standing waves	Symmetrical cross-bedding, also massive.	*Sm_2
Antidunes	Cross-stratification, dips upstream, also massive but with trochoidal cross section.	*Sm_3

* indicates facies introduced by present writer since no Miall facies defined.

Yet another important consideration regarding bedforms of open channels is the Manning coefficient of boundary roughness which has been designated Manning n. The Manning equation is as follows :

$$\bar{U} = \frac{1,49}{n} R^{\frac{2}{3}} S^{\frac{1}{2}}$$

This formula only applies to turbulent flow. 1,49 is constant for ft/sec units. (Middleton, 1965, p. 250). In Figure 14 a range of Manning n values is given for the characteristic bedform surfaces of the various flow regimes. Data is from Harms and Fahnestock (1965, p Plate 1) and applies only to channels with a sand bed. The Manning n 'curve' has a high profile owing to boundary roughness imparted by the various ripple bedforms in the lower flow regime. A peak is reached at n = 0,035 with dunes, and thereafter drops to very low values with upper flat bed. Empirical data derived by Simons (1969, p. 139) showed that in the transition zone a well defined relationship between n and boundary shear does not exist, and that for this zone n varied from the largest value for the lower flow regime to the smallest of the upper flow regime. Manning n is large for bedforms of the lower flow regime because here the water surface is out of phase with bedform topography

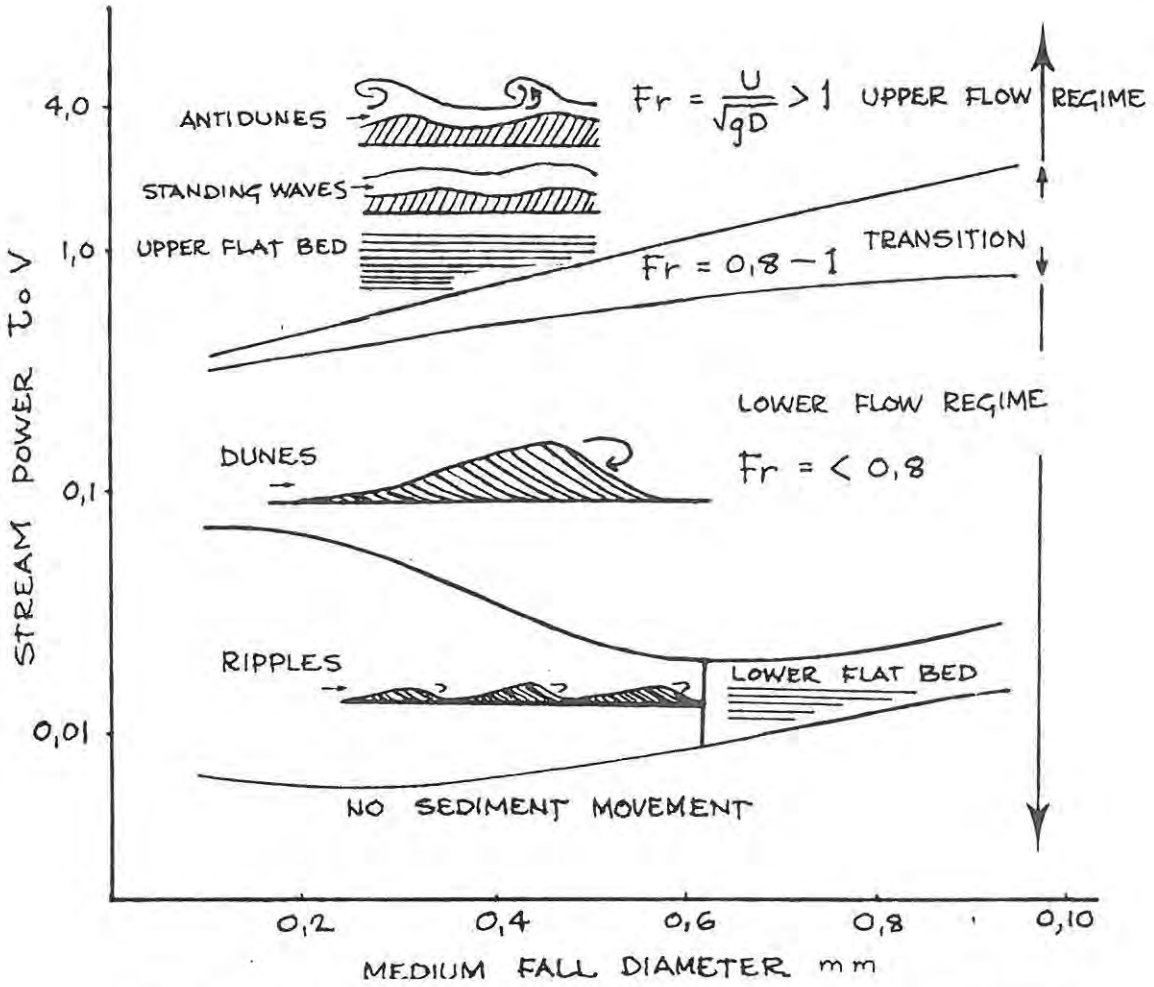

Fig. 15 Relationship between particle size and stream power (modified after Allen, 1968).

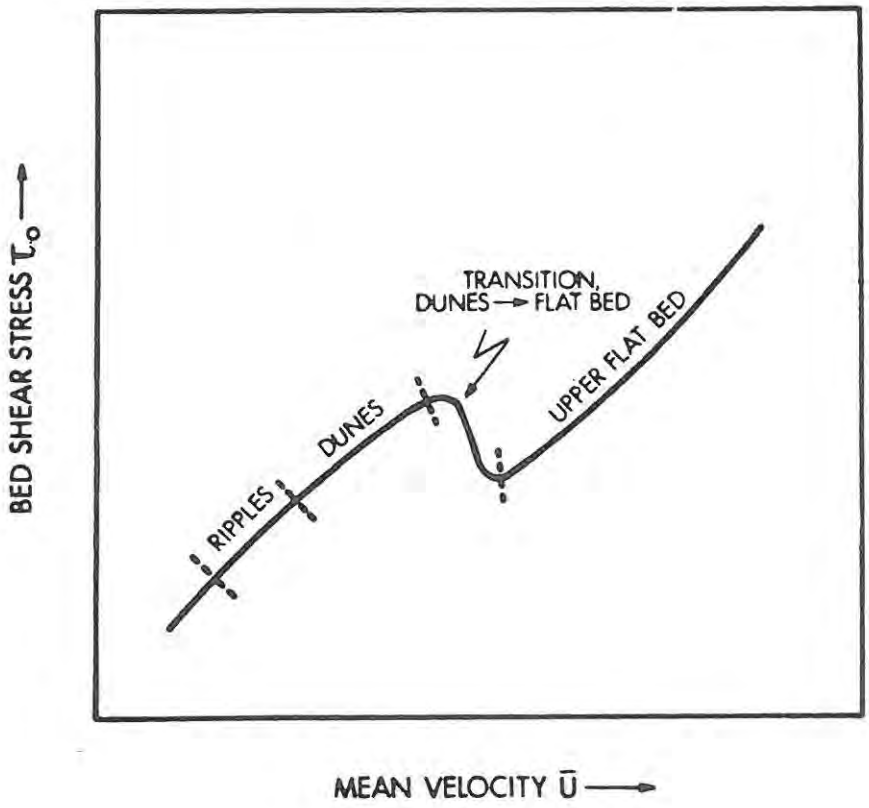

Fig. 16 After Harms et al., (1975).

(Fig. 14), which increases resistance because separation of the flow from the boundary layer generates large scale turbulence that dissipates considerable energy (Simons, 1969, p. 139). The opposite generally applies for the upper flow regime. Before closing this discussion on bed roughness, it should be mentioned that n is a measure of only the boundary layer roughness and not of the grains themselves. The Von Karman constant k is the measure of the magnitude of all the roughness elements combined, i.e., of particles and bedform surface. k may be derived from a curve relating stream velocity and the log of height above the bed. Such functions, using data from measured profiles in the Rio Grande, are illustrated in Blatt et al. (1972, p. 89). The value k was found there to be greater than 0,4 for dunes and less than this for flat bed.

Having discussed types of flow and the elements resisting this flow, the two can be combined to give an idea of "the rate at which a stream does work on a unit area of its bed," (Blatt et al., 1972, p. 122). Allen (1967, p. 429) states that sedimentary texture and structure of bedforms are dependant on the power of the fluid flow (stream power), which is the product of the boundary shear stress and flow velocity, $\tau_o V$, and which was defined in the preceeding sentence. Figure 15 shows how stream power is related to flow regime, bedforms and their internal structures. Southard (1975, p. 12) contests the notion that stream power is a better basis for thinking about dynamics of sediment transport and bed configurations, than the other kinds of flow variables, namely width/depth ratios and mean flow velocity. The main objection is that bottom shear stress is involved since more than one bed phase can be associated with the same value of τ_o. The same writer argues that velocity is sedimentologically more significant than bottom shear stress. Figure 16 shows the relationship between mean velocity and bed shear stress.

2. Comparison between flume and field observation

Conditions in flumes are more ideal than in natural streams. Flow is two dimensional and a very limited range of depth and discharge can be effected. Slope and velocity, on the other hand, can be varied within a wide range. River gradients (slope) are generally constant

in the field, but much larger ranges of depth and discharge are common here. Large Froude numbers can be derived from flume experiments than will apply in most natural channels since river banks cannot withstand prolonged high-velocity flow without eroding. The erosion of natural banks increases the cross-sectional area, which has the effect of reducing the flow velocity and hence the Froude number. Fr based on velocity and depth is rarely found to be greater than 1 for any length of time in natural streams with erodible banks. This is in fact true for Fr > 0,25 (Simons, 1969, p. 140). Perhaps it is of greatest value to use the flume variables that can be best simulated with field phenomena. Two of these are velocity and grain size (Fig. 17).

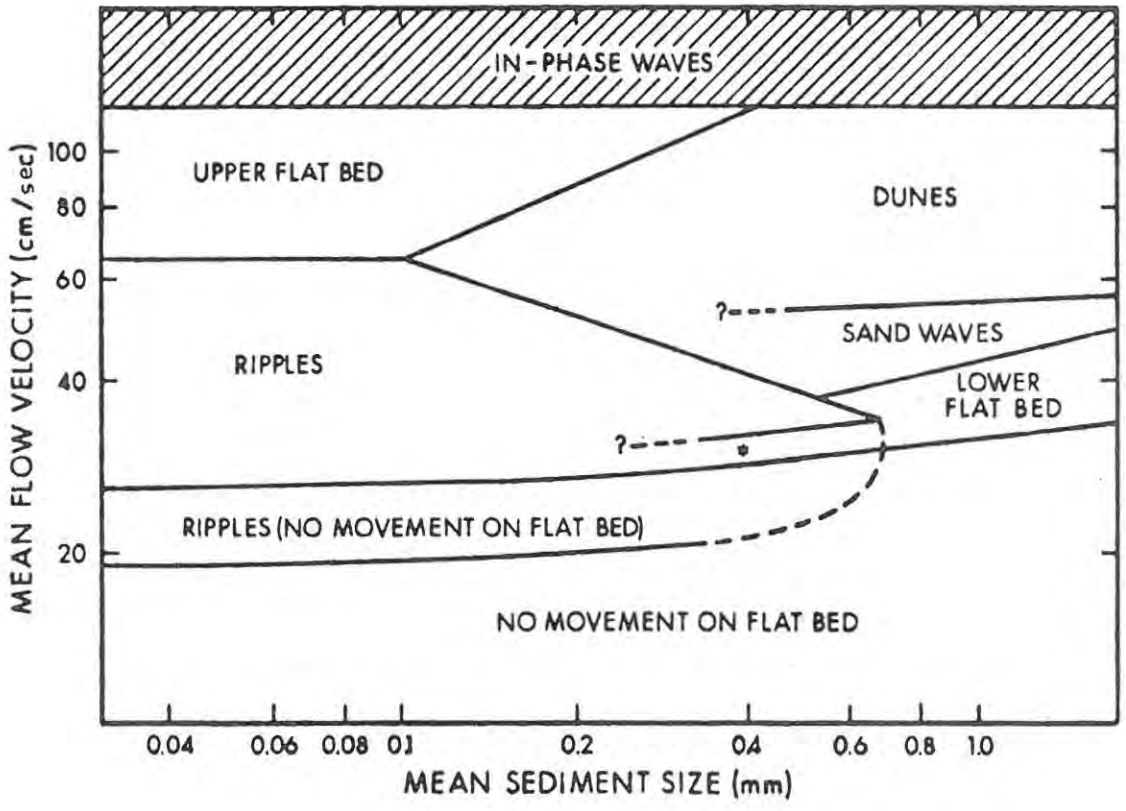

Fig. 17 After Harms et al., (1975).

Some bedforms behave in the same way in flumes and in nature. Recently flume studies correlated with field data have begun to make a contribution to understanding the differences between sand waves and dunes (Southard, 1975, p. 36). Sandwaves here refer to the very large (WH = 8 - 16 metres) bedforms of Coleman (1969, p. 199) and those considered by Harms et al. (1975).

Before concluding this section it is perhaps appropriate to regard Figure 17 and mention that recent workers (Harms et al., 1975, p. 18) no longer emphasise the distinction between lower and upper flow regime. They suggest that it might be more natural to think in terms of the distinction between the sequence of bed phases from ripples through dunes to upper flat bed on the one hand, and in-phase waves on the other hand (standing waves, antidunes). The distinction between lower and upper flow regimes, based on calculated Froude number, is important when regarding resistance to flow, and not with respect to basic dynamics. The main problem in this whole matter is that rivers and their bedforms are not accessible at times of flood or waning stages, and that the two-variable data obtained from flumes cannot represent the resultant bedforms of a large enough range of depth and velocity (Harms et al., 1975, pp. 15 and 19).

B. ORIGIN OF SEDIMENTARY STRUCTURES

1. Intraformational shale-pellet conglomerates

These are formed along scour surfaces and as lag material in the bottom of channels. They are especially common in the Katberg Sandstone and have been described in detail in Chapter II. They are interpreted here as having originated from the highest current velocities achieved by the palaeostreams, since in many instances the presence of large angular to subrounded mud clasts were noticed, 0,5 m across in some places. The most likely sources for this reddish and greenish shale material are the immediately underlying mudstone strata, which probably represent the thin mud drapes, abandoned channel fills and vertical accretion flood plain deposits (probably rare) of the palaeoriver systems. Although clast material was most probably locally derived, what is important is that it would represent cohesive semi-consolidated mud and silt. Because these fine grain sized particles have a low value of

Manning n = 0,012, higher than normal velocities are required to effect bottom shear and thus move the material. The well known Hjulstrom graph, shown in Figure 18 below, gives an idea of the critical velocities required to erode, transport and deposit sediments of various grades (Selley, 1976, p. 172).

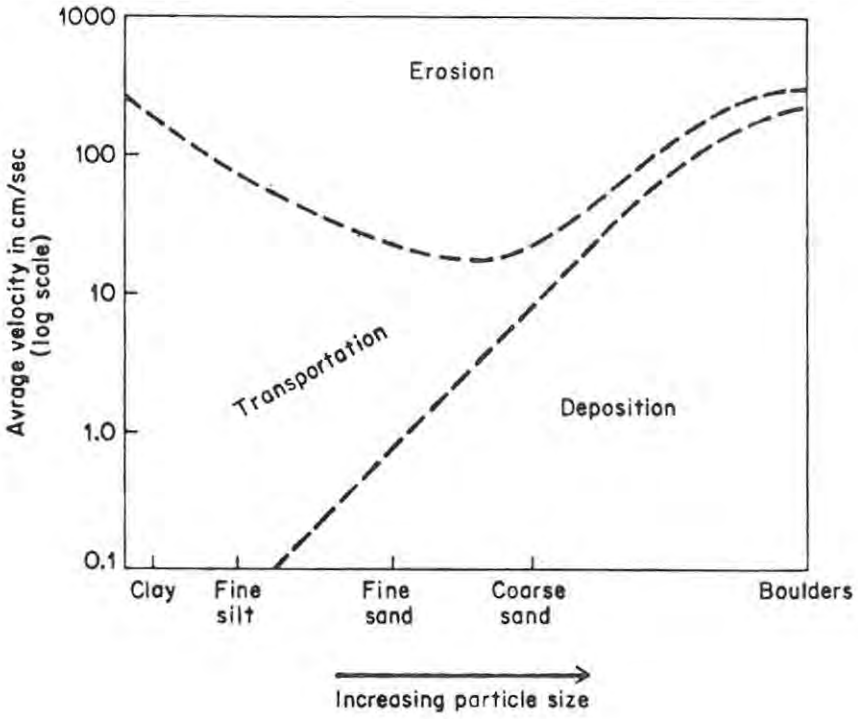

Fig. 18 Relationship between erosion, transportation and deposition of various particle sizes and corresponding flow velocity of water (after Hjulstrom, 1939).

2. Horizontally-bedded sandstone

(i) Upper flat bed type (UFB)

Upper flat bed stratification is the dominant sedimentary structure of the Katberg Sandstone. In over 5 000 symmetrically recorded bedform structures from 10 different sections, it was found that more than 60% of these represented UFB lamination.

Allen (1968, p. 29) states that parting (syn. with UFB) lineation is one structure on which hydraulic engineers have not worked extensively. This still seems to be the case today. An attempt was made during this study to find evidence of palaeochannel cross-sections filled with UFB

laminated sandstone, in order to ascertain what fluid dynamics apply to this structure. The results, although inconclusive, to a certain extent conform to data from open channels (see palaeochannel analysis). Allen (1968, p. 33) has likened the parting lineation of fluvial environments to that created on sandy beaches by wave backwash. In this latter case, where the lineation was being produced, the sediment charged lower levels of flow were divided up into dense turbulent clouds separated laterally from each other by narrow zones of clearer fluid. Figure 19 below illustrates this idea. Where streamlines of adjacent vorticies converge and flow is slowing down, those grains which are more difficult to move accumulate in slight ribs.

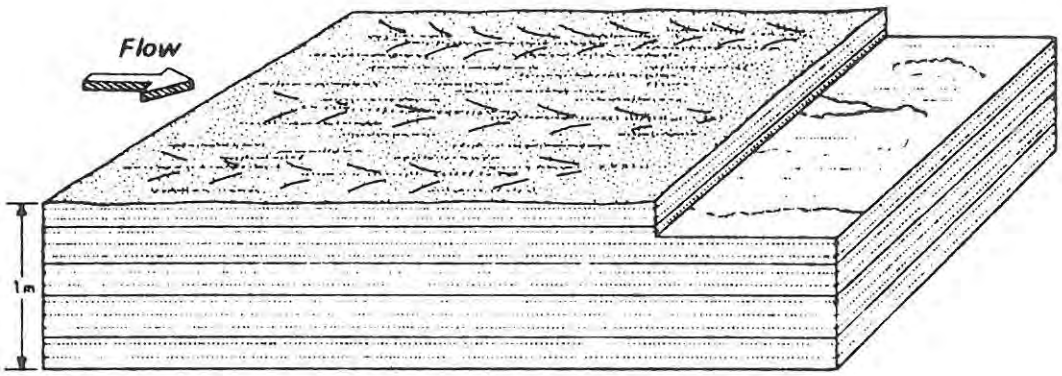

Fig. 19 Stylized diagram of UFB-laminated sets in sandstone. Note convergence of streamlines to form ribs, and parting lineation surfaces between sets (modified after Harms et al., 1975).

Jopling (1967), cited by Reineck and Singh (1975, p. 10), evidently demonstrated that the striations were in some cases coarser, and in other cases finer grained than the average material. The last two mentioned workers speculate that random superposition might provide the size contrast necessary to create the characteristic parting lineation. Harms et al. (1975, pp. 50 and 88) regard UFB lamination as being hydrodynamically equivalent to their hummocky cross-stratification. They attribute hummocky cross-stratification to surges of greater displacement and velocity than that required to form ripples.

UFB lamination has been shown from flume and field experiment to be the bedform structure replacing dunes (trough cross-bedding) as slope,

and thus velocity is increased and Froude numbers become greater than 1 (Simons, 1969, p. 139).

In the Katberg Sandstone UFB lamination is commonly seen overlying planar cross-bedded units and indeed running laterally into them. All the indications are that this phenomenon represents an increase in palaeostream velocity. Relatively hard to move, heavy mineral traction particles (Stavrakis, in prep.) form 20 mm thick layers within UFB strata. In addition, pronounced grain orientation is characteristic of Katberg Sandstone UFB lamination. In the Balfour Formation where this structure is present, it often appears in bottom-set sandstone lithosomes of fining upward sequences showing a compatible series of bedform structures characteristic of the Sp, St, Sr and Fl facies of Miall (1977, p. 20). This UFB sandstone in typical Balfour sequences is interpreted (here) as upper flow regime channel fill sand deposited in the highest velocity part of the stream. In the Katberg Sandstone where UFB lamination is present overlying planar or trough cross-bedded sandstone, as in Figures 7 and 8, this is interpreted as an increased velocity response to decreased cross-sectional area of the channel by upward building dune and other sandbar bedforms. As this happens, the Froude number would increase to become > 1 and Manning n would decrease as the bed became flat. Shooting flow (Selley, 1976, p. 175) of the upper flow regime would dominate and create this flat bed lamination. In his study of the Platte River depositional environment Smith (1970, p. 3000) observed that in some of the swifter flowing anarbranches, sand was moved as plane beds. Miall (1977, p. 50), in his review of the four classic braided river models, refers to parting lineation as an upper flow regime structure.

(ii) Lower flat bed type (LFB)

The criteria used to distinguish this type of stratification from that of UFB were described earlier. Harms et al. (1975, p. 50) write that a lower flat bed exists at low velocities (and low stream power) for sand coarser than 0,6 mm (Fig. 15). Apparently ripples form at similar values of stream power but different grain diameters. Allen (1968, p. 143) uses a grain diameter of 0,7 mm to separate ripples from plane beds with movement. Harms et al. (1975, p. 50) are of the opinion that because transport rates (stream power) are low in the LFB phase, resultant

deposits will be very limited in vertical and horizontal extent. The sediments referred to as lower flat bed in this study correspond rather to the Fl and Fm facies of Miall (1977, p. 20) than to his Sh group which is here reserved for flat bed stratification of the upper flow regime.

LFB-lamination which is common and widespread in the greenish-grey siltstones of the Balfour Formation, less so in the Burgersdorp, but rare and limited in the Katberg Sandstone, is interpreted here as a particle settling phenomenon, giving rise to differentiated, sometimes graded beds. It also refers to a less common (absent in the Katberg Sandstone) horizontal structure arising from transverse sections of superimposed composite ripple trains. Close scrutiny of the section will reveal which of the two mechanisms is involved. Fortunately, this is possible in most cases because outcrops are blocky. It is important to distinguish between the two for purposes of hydrodynamic interpretation, because the one involves traction and the other a lack of it. In terms of fluid dynamics LFB-strata of this study form in the whole field below the curve separating dunes from ripples but excluding the latter (Fig. 15). Nowhere in the sections studied was the LFB phase of Harms et al. (1975, p. 50) seen, i.e., flat-bed lower phase with sediment diameter > 0,65 mm.

3. Cross-bedding

Included under this heading, the following sedimentary structures will be discussed :

(i) Trough cross-bedding

Trough cross-bedding is one of the commonest sedimentary structures known and yet there is much controversy still about its origin. Allen (1968, p. 130) gives a comprehensive review of the earlier ideas on dunes, citing the work of people like Gilbert, Bagnold and Kennedy, to name a few. However, with the advent of flumes and the intense research by this method since the early sixties, the hydrodynamic interpretation of trough cross-bedding appears to have been standardised. Harms and Fahnestock (1965, p. 84) report from their studies of the Rio Grande that trough cross-bedding is formed by the process of dune migration in the upper part of the lower flow regime

where water depths exceed 30 cms. Except for a lack of agreement on water depth this appears to be the accepted norm today. The range of hydraulic variables within which dunes, also referred to as megaripples by some workers, occur is shown in Figs. 14 - 17. Workers such as Visher (1972, p. 86) and J C Theron (pers. comm., 1978) are not convinced of this. Visher cites work done by McKee who found trough cross-bedding to be rare in dunes. Theron on the other hand, drawing on his extensive sampling of directional sedimentary structures of the Beaufort Group, is of the opinion that trough cross-bedding is indicative of a higher energy environment than primary current lineation. He also does not reconcile the structure with dunes. While these views should be respected, the intense and quantitative research on flumes and natural channels cannot be ignored.

In the Katberg and adjacent formations a full range of trough cross-bedding types exist as outlined in Chapter II. Solitary scoops such as the *zeta* types seen at Hobb's Hill are, according to Pettijohn *et al.* (1972, p. 135), rare. This was also found to be the case with the present study. They are interpreted as representing positions where a pool is located in the stream channel. At such points, due to increased depth and bed roughness, stream power declines and deposition of bedload material as curved sets fills the hollow. It was initially suspected that these *zeta* troughs, because of their apparent concordant lower bounding surfaces, represented interdune-hollow fills. However, their solitary nature would tend to preclude this idea.

The more frequently observed *nu*-cosets, especially common at Deep River and Nico Malan Pass, are interpreted as belonging to the threshold of stream power between ripples and dunes. This is based on the accordance of the structure with the well documented and described three dimensional bedforms of Williams (1971, pp. 8 and 25) viz. caternary large-scale ripples. In terms of size, Katberg cosets are commonly 30 - 40 cms thick, and where preserved, wave heights of 10 - 15 cms are indicated. The problem here is that only xy or yz sections were visible at any one time, and that individual sets had their tops eroded before the next set was deposited, thus obliterating evidence of ripple top morphology. Nevertheless, large scale (WH = 30 - 40 cms) caternary or lunate rather than sinuous ripples of the lower flow regime are indicated. The size class of this

type of cross-bedding is not that obvious and it is likely that large scale ripples often graded into dunes. It is suggested here that this smaller scale trough cross-bedding originated in shallow streams as was found by Williams (1971, p. 38) for the streams he investigated. In that case stream depths ranged from 0,8 - 2,5 m. This also seems to be the case for the Katberg Sandstone as a whole (see Table 1). Selley (1976, p. 218) writes that water depth cannot have been less than the preserved set height in aqueous flows. Harms et al. (1975, p. 47) regard water depths over dunes as being somewhat unreliable, stating that trough sets suggest a minimum flow depth equal to twice the set height, but that dunes also exist under very deep flows.

The ubiquitous pi-cross-bedding observed in all three formations is evidently not very easy to explain. It is generally accepted to be the internal structure of dunes which hydrodynamically belong to the upper part of the lower flow regime (Figs. 14 and 15). Individual sets are large in scale, commonly 1 - 2 metres thick. Bluck (1971, p. 135) reports that on point bars the bedforms of many of the accreting deposits appear to be out of phase with most of the flow conditions. This is consistent with the lower flow regime water-surface/bed relationship. However, apparently standard shaped dunes, called megaripples by Bluck, have forms that contradict their internal structure. The same worker discovered that two main currents operate over a point bar, one over the bar head and the other through the pool (convex bank) and partly over the bar supra-platform (Bluck, 1971, Fig. 24). The significance of this is that the bar-head current dominates when it flows and generates dunes on the bed which mould themselves over other structures. This could be the reason why some workers do not associate trough cross-bedding with dunes. Even during the present study it was found that predominantly pi-cosets often contained other structures such as planar sets and sometimes ripples. Allen's (1963) classification is highly idealised and is best used for descriptive purposes. The mixed cosets described above are seen as an interaction of a range of bedforms.

The predominantly large scale festoon cosets of Katberg Pass (1 and 2), Woodburn (5) and Elandsberg (3) are interpreted as in-channel dunefields. Palaeocurrent vector magnitude of trough axes is high at these places, indicating unidirectional flow. Very large scale (WH = 5 - 15 m) structures corresponding to the sand waves of Coleman (1969, p. 199)

Fig. 20 Dissected former transverse bar (above assistant). Note reactivation surfaces (lined in) and subsequent occupation by mud drape. Loc., 7 km north of (3), Katberg Sandstone.

appear to be absent in the Katberg Sandstone and Burgersdorp Formations. However, there is evidence that structures larger than dunes were present during Balfour sedimentation. In parts of the central study area where mud drape lenses are common, trough cross-bedded sets of fine sand, silt and even mudstone were seen as minor channel fills (Fig. 20). These sites would represent relatively elevated areas along the channel profile, corresponding to topographic level 3 (little water movement, only at flood stages) of Williams' and Rust's (1969, p. 650) Donjek study. They found that only at times of bankfull discharge was there overbank flooding when suspended fine material was transferred into abandoned channels and other slack water areas. Normally the type of trough cross-bedding resulting from this abandoned channel fill forms in the lower flow regime, but reactivation surfaces, (Boothroyd, 1976, pp. I - 21) which are rare in the Katberg Sandstone as a whole, are indicative of an increase in stream power and one of the structures of the transitional regime. Two of these palaeosurfaces over which flow was rapid can be clearly seen, and are marked, in Figure 20. This last mentioned type of trough cross-bedding would thus represent the flashiest conditions of flow and have a very low preservation potential.

(ii) Planar cross-bedding

Planar cross-bedding is regarded as the avalanche front-type cross-stratification of which laboratory deltas (Jopling, 1965, pp. 55 - 65) are constructed. In natural streams this is the cross-bedding of transverse bars (Smith, 1972, p. 625), linguoid bars (Williams, 1971, p. 26) and sand waves (Harms et al., 1975, p. 48). The first two are essentially the same bedforms which rarely exceed 1 m in height (Smith, 1972, p. 625), but sand waves are very large features having WH = 8 - 16 m chords (WL) = 200 - 1 000 m (Coleman, 1969, p. 190).

Transverse bars evidently increase in abundance towards the more distal reaches of braided systems (Smith, 1970, p. 2993). The fractionation of bedforms down palaeoslopes of the Katberg Sandstone is not an obvious trend. Planar cross-bedding is fairly common in both the Katberg Sandstone and Burgersdorp Formations and rare in the Balfour Formation. This is rather a reflection of stream type than of actual flow regime, transverse bars being one of the dominant bar types of braided channels, and point bars of meandering streams. Because of its

association with the different bar types as outlined above, the hydrodynamic interpretation of planar cross-bedding must be done with the specific bedform in mind. Katberg and Burgersdorp planar cross-bedding (as described in Chapter II) appears to be most like the Platte River type and linguoid bar cross-bedding of Williams (1971, p. 27). Turner (1977, p. 243) designated similar cross-bedding planar A-type. Harms and Fahnestock (1965, p. 105) report that tabular cross-bedded sets form on avalanche faces which build out at deep water, low velocity sites in the channel. Williams and Rust (1969, p. 660) state that transverse bars only appear at low discharges. Williams (1971, p. 29) mentions that linguoid bars are generated by waning and low stage flow in the Central Australian streams. Harms et al. (1975, p. 48) are of the popular belief that planar cross-bedding is formed by migrating sand waves. The flow variable field of sand waves is shown in Figure 17. They state that sand waves are formed at lower flow strengths (stream power) than dunes; this is based on recent flume evidence where experimental sand waves were generated and were found to be in many respects similar to those of natural rivers (Harms et al., 1975, p. 36). Coleman (1969, p. 190) used fathograms to show that sand waves develop most commonly at peak flood and falling stage. Boothroyd and Ashley (1975, p. 212) show that linguoid bars formed during a rising flood stage in the braided lower Scott outwash fan. An aerial view of this region of the stream taken during rising flood stage showed linguoid bars actively growing away from eroding remnants of diamond shaped longitudinal bars. According to these last two workers, linguoid bars continue to be active at lower flood stages.

Smith (1970, p. 2995) states factually that transverse bars represent a profile of equilibrium. When this situation changes, such as with an increase in water depth, the bar top serves as a flat base for deposition. Thus overlying structures such as ripple lamination, trough cross-bedding or flat beds can be interpreted in terms of nett water depth and stream velocities above the layer of planar sets.

In conclusion therefore, transverse bars and thus planar cross-bedding represents the positions of depressions in the stream bed where avalanching foresets aggraded to a position of equilibrium. They are evidently lower flow regime structures classified approximately with

sand waves. The lower Scott fan braided channels investigated by Boothroyd and Ashley (1975, p. 197) in which active linguoid bars were seen forming, yield Froude numbers of mostly Fr = 0,25 - 0,5. An attempt was made to calculate Froude numbers for Katberg palaeochannels based on empirical measurements. This proved to be impossible since channel widths at the time of bar occupation could not be estimated even with reasonable accuracy. For example, where the method was tested Fr = 0,4 - 2,2 were obtained. Channel migration and subsequent transverse bar occupation (see Fig. 20) have created the illusion of very wide palaeochannels and thus calcualted flow velocity and Fr were anomolously high.

(iii) Ripple cross-bedding

Where sets are seen superimposed without drift these are interpreted as aggradational ripple bedforms generated under low velocity flow with a high suspended load content. Ripple drift lamination, according to Reineck and Singh (1975, p. 96), occurs basically by two mechanisms.

Type 1

With a high suspension/bedload ratio both stoss and lee sides of individual ripples are preserved. (Type C of Jopling and Walker, 1968).

Type 2

With a decrease in the suspension/bedload ratio removal of stoss side laminae takes place and only the lee sides of ripples are preserved. (Type A of Jopling and Walker, 1968).

Climbing ripples, referred to as micro cross-bedding of the kappa and lamda sorts earlier on, are small scale analogues of stacked dunes. All these abovementioned types are common in the dark siltstones and sandstones of the Balfour Formation but less so in the mudstones and siltstones of the Burgersdorp Formation. Ripple development, as mentioned earlier, is virtually absent in the Katberg Sandstone where it occurs mainly in fine grained mud drape deposits at high topographic levels of the palaeochannels.

Ripples occur in virtually all sedimentary environments from deserts to ocean bed (Selley, 1976, p. 223). Environment therefore cannot be easily inferred from ripple structures themselves. Blatt et al. (1972,

p. 132) state that ripples respond only slightly, if at all, to changes in flow depth. Harms et al. (1975, pp. 54 - 55) illustrate clearly the origins of the various types of ripple cross-bedding, through a range of flow conditions, grain size and aggradation rate. Briefly these are as follows :

Bedform and conditions	Cross-bedding
Current ripples on sand bed near equilibrium, linguoid, lunate and cuspate forms.	In plan view small scale troughs, rib and furrow. In section, nu-cosets.
Current ripples on silt, low velocity.	Same as above.
Current ripples on silt, high velocity.	Low angle forset dips, tangential lower bounding surfaces.
Combined flow and wave ripples, crests longer and more sinuous.	Slight downcurrent inclination, tangential bed not distinctly trough shaped.
Wave ripples, long symmetrical ripple crests.	Small scale troughs but symmetrical dips preserved.
Climbing ripples, low aggradation. Sinuous ripple crests.	Ripple drift cross-lamination with lenticular stacked sets.
Climbing ripples, high aggradation. Sinuous ripple crests.	Ripple drift cross-lamination with wavy cross-section.

4. Antidune structures

Antidunes are trains of ripple-like bedforms produced by flow in or near the supercritical state. They are bedforms which are in phase with the water surface and they are produced under rapid flow conditions

in the upper part of the upper flow regime. (Reineck and Singh, 1975, p. 39).

In the eastern parts of the present study area vague symmetrical bedded structures were noted in apparently massive sandstone lithosomes. The above writers state that antidunes vary in height from 1 mm to 45 cm, with wavelengths of 1 cm to 6 m. Some of the symmetrical waves seen had heights of almost 80 cms. In other cases 'ripped up' shale flakes, indicative of very high current velocities, were seen suspended in almost structureless sandstone. In one example (Fig. 21) the dispersal pattern of shale flakes in the sandstone is shown. Low angle cross-bedding was visible in one part of the unit and was seen to dip up current. Selley (1976, p. 128) illustrates a similar situation from an active alluvial channel fill sequence.

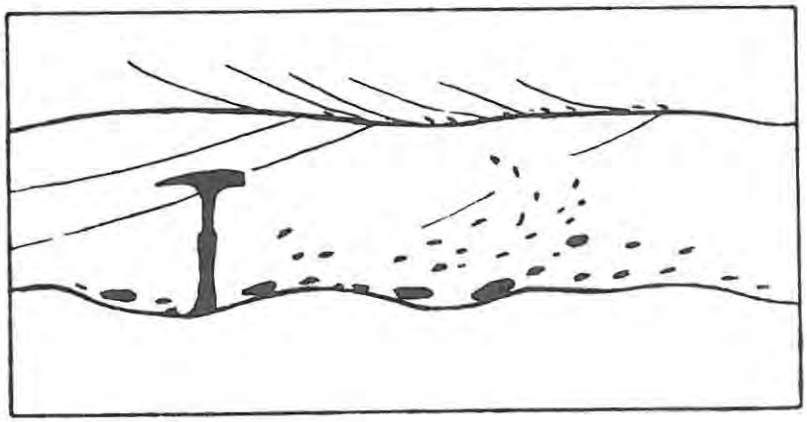

Fig. 21 Camera lucida drawing of antidune structure. Note shale flake dispersal pattern in sandstone host, palaeoflow from left to right. Loc., Cathcart, Katberg Sandstone (slide from C J Gunter).

Where antidune structures were seen these were always associated with UFB lamination. Such structures were observed in sandstones of the Katberg Sandstone and Burgersdorp Formations only. The sections of

Vaalkraans (11), Hobb's Hill (10) and Windvoelberg (9) show their stratigraphic positions. It is possible that many of the wavy scour surfaces present in other parts of the area may represent modified antidune bedforms. Hand et al. (1969, p. 1310), who specifically studied antidunes in conglomeratic sandstone, state that antidune structures may be far more abundant in the geological record than has been assumed. These workers suggest that the antidune trains they studied developed beneath a sheet of water only 1 or 2 cm deep, moving with a velocity of roughly 100 cm/sec down a palaeoslope of 2,7° or more. Calculations made for the present study and based on empirical data similar to those of Hand et al. (1969, p. 1313) yield current velocities of over 100 cm/sec in some cases. Palaeoslope calculations for the same streams, however, yielded gradients of less than 0,5° in all cases. Flow depths based on grain size and bottom shear stress (Allen, 1966, p. 430) were calculated to have been approximately 2 cm in some Katberg and Burgersdorp streams, and Froude numbers were more than 1 in all cases.

It is suggested here that at least some of the antidune structures of the Katberg Sandstone and Burgersdorp Formations originated in high velocity, shallow channels flowing down moderate slopes. At the stage of antidune formation the streams were in the upper regime of flow.

C. STREAM HYDRAULIC THEORY

To sedimentologists, velocity, V, is probably the most important flow variable (Harms et al., 1975, p. 12). Velocity in natural channels is primarily influenced by the slope, S, of the channel, but also depends on water depth, D as was shown by the Manning equation. Hydraulic radius, R, is sometimes used to express depth. The two are approximately equal in wide channels such as those found in nature (Middleton, 1965, p. 249). Velocity also increases with mean annual discharge, Q_m, in a downstream direction. This indicates that the increase in depth overcompensates for the decreasing river slope (Leopold and Maddock, 1953, p. 16). Lane (1955, pp. 745 and 746) suggested that grain size of sediment, d, and discharge, Q_w, are the

main variables influencing the shape and size of natural channels. He combined these variables in the equation :

$$Q_s \, d \sim Q_w \, S \qquad (1)$$

Schumm (1971, pp. 4 - 14) states that the greater the quantity of water that moves through a channel, the larger its cross-sectional area will be. He also demonstrates how the width/depth ratio, F, for stable channels could be related to the percentage of silt-clay in the channel, M, by the following equation :

$$F = 225 \, M^{-1,08} \qquad (2)$$

Schumm (1972, pp. 98 - 107) has further demonstrated how meander wavelength, L, gradient (slope), S, mean annual flood, Q_{ma}, and mean annual discharge, Q_m, of modern and palaeochannels can be impressively compared. The equations obtained for the various palaeochannel parameters are as follows :

Meander wavelength

$$L = 18 \, (F^{0,53} \, W^{0,69}) \qquad (3)$$

Slope

$$S = 30 \, \frac{F^{0,95}}{W^{0,98}} \qquad (4)$$

It can be seen from equations (2), (3) and (4) that an increase in width/depth ratio, F, would indicate a greater sediment bedload, larger meander wavelength and steeper gradient. Schumm (1972, p. 102) found the values for calculated mean annual flood, Q_{ma}, which he considers to be approximately equal to bankfull discharge, Q_b, to be particularly close to actual measured values for comparable channel sizes. The channel forming discharge is usually the bankfull discharge, therefore mean annual flood is closely related to channel shape and size. Thus :

$$Q_b \simeq Q_{ma} = 16 \, \frac{W^{1,56}}{F^{0,66}} \qquad (5)$$

A good estimate of velocity, V, can be obtained using palaeochannel hydraulics, by dividing channel area, A, into Q_{ma}.

$$V = \frac{Q_{ma}}{A} \qquad (6)$$

Discussion

Most of Schumm's equations are based on recognition and accurate measurement of palaeochannel dimensions. He has demonstrated that once these dimensions are known, calculations of reasonable accuracy can be made. However, the problem is to recognise the true limits of a palaeochannel. There are no set criteria whereby this can be done. Clues must be sought in the field, where the final assessment of what represents a palaeochannel must be made and dimensions recorded.

For example, superposition of channel fill deposits may result in a very thick valley fill deposit which might be mistaken for a deep palaeochannel. Channel migration combined with valley fill will yield enormous palaeochannel dimensions. On the other hand, scour by continually switching channels will be reflected in considerably reduced palaeochannel depths, and thus cross-sectional area. The effect that misrepresented dimensions might have on the dependent variables of the various equations can be such as to render the results totally meaningless. Walker (1975, p. 77) states that Schumm's method of palaeochannel analysis allows interpretation of aspects of the fluvial system that cannot be done otherwise. Schumm himself is of the opinion that the equations should be used to estimate palaeochannel discharge, slope, water velocity, etc., but if these estimates conflict with other geological evidence then they should be regarded with reservation.

D. PALAEOCHANNEL ANALYSIS

1. Introduction

In any study of this kind it is essential that palaeochannel dimensions can be observed and measured. Even when this is possible the orientation of the section has to be considered and palaeochannel depth can prove

to be elusive as mentioned earlier. Cotter (1971, p. 132) applied Schumm's equations, from earlier published work, to palaeochannel dimensions obtained from Upper Cretaceous sandstones. From these he estimated meander wavelength, discharges, sinuosities, channel slope and water velocity. Cotter applied alternative methods, e.g., using the Manning equation for calculating stream velocity and a modification of the same formula using shear stress to derive channel slope. The values he obtained supported those derived from Schumm's multiple regression equations.

During the present study thirty-four palaeochannels were measured from fresh exposures of Balfour, Katberg and Burgersdorp rocks. In addition to the flow variables calculated by Cotter and those derived by Schumm (1972), Manning n, channel pattern, Froude number and thus flow regime were obtained for consideration.

2. Method

Palaeochannel exposures were sought in the field and dimensions measured. All channels measured had some lag material along their basal surface. This was usually in the form of a shale pellet layer overlying a scour surface. Channel depth was obtained in a number of ways. Turner (1977, p. 244) states that epsilon cross-bedded sets represent the channel depth over point bars at bankfull stage. Cotter (1971, p. 130) reports that Allen (1965) and Moody-Stuart (1966) used the same method to estimate stream depth. Solitary large scale epsilon sets were not observed within typical point bar sequences, but Sp-epsilon sets ere were found within palaeochannel boundaries. Selley (1976, p. 218) writes that for aqueous dune structures water depth cannot have been less than preserved set height. This method was used with some success where structures such as ripples or other sets were seen to overlie sigmoidal heterogeneous foresets resting on the scoured channel base.

Perhaps the most successful and certainly the most reliable method used in this study was where a full fining upward sequence could be observed within a channel sandstone which had scoured into other underlying strata. This was more difficult in the case of the Katberg Sandstone because palaeostreams apparently contained mostly bedload material of uniform grain size. However, very fine heavy mineral

particles with grain diameters of 0,06 mm often segregate as dark bands on what appears to be the top of channel filled UFB laminated sandstone. The critical bottom shear stress required to move such particles was calculated to be 1,5 - 3,0 dynes cm^{-2} (see section on heavy mineral bands and palaeohydraulics) and the corresponding value for the host sand slightly less. It is possible that these dense, very fine grained particles were only set in motion as traction layers relatively late in the channel fill cycle, when the value of Manning n dropped sufficiently with the formation of flat beds. At places in the Katberg Sandstone silt drapes are common and usually overlie channel fill sequences of flat beds and cross-strata. However, it is rare to find a fully preserved sequence of this kind and usually thicknesses were estimated from channel edge projections. True fining upward cycles were observed at places, especially in the Balfour Formation where point bar type sequences of stacked sedimentary structures were sometimes fully preserved. Blatt et al. (1972, p. 136) state that migration of a bar produces a sequence of sedimentary structures whose total thickness is equivalent to the maximum depth of the palaeochannel.

Calculation of water depth from the equation combining shear stress, stream power and flow velocity (Allen, 1967, p. 430) yielded extremely small values; 1 - 2 cm in most cases. This may have been the case during the deposition of a single set of flat beds at some stage of channel fill. Similar shallow depths were obtained using the modified Darcy-Weisbach equation (Hand et al., 1969, p. 1313) :

$$S = f \frac{V^2}{8gD} \qquad (7)$$

In this formula, f is the combined effect of grain and bed roughness which is equivalent to the Von Karman constant. A value of 0,4 was used which refers to the field between dunes and UFB. For the final calculated palaeochannel attributes only those depths obtained from in-channel bar sequences were considered.

Once channel depth was obtained, apparent channel width was measured along the exposed section, and the angle between this section and the palaeoslope azimuth was recorded. The latter was obtained from primary current lineations on UFB sets. The resultant angle α and apparent

channel width x were then used to calculate true palaeochannel width W (see Fig. 22). Very oblique sections were avoided.

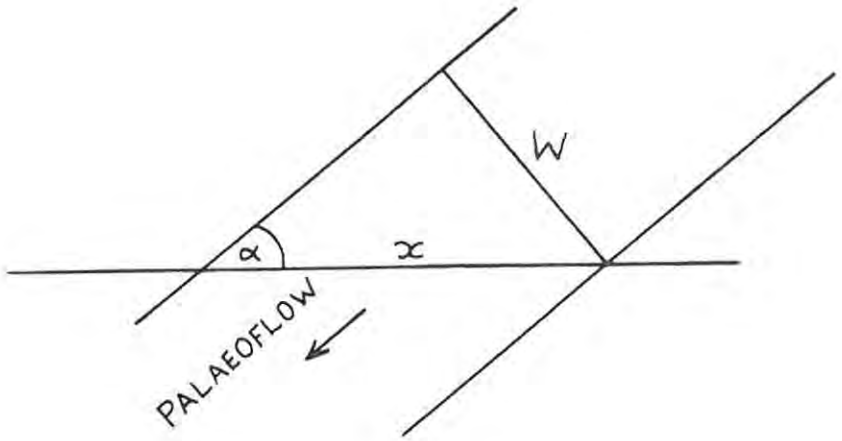

Fig. 22 Method of calculating true channel width in field outcrop. $W = x \sin \alpha$. (x = exposed channel width as seen in section, α = angle between section and palaeoslope.)

3. Data processing

A FORTRAN computer program was written enabling rapid calculation of data. This method is strongly advised because individual parameters are in different units and intermediate conversion calculations have to be made. A single line of palaeochannel data takes approximately one hour to calculate manually.

Table 1 contains the calculated palaeochannel attributes for the 34 Beaufort Group streams considered. A palaeochannel from Upper Witwatersrand Group quartzites has been included for comparison. Meander wavelength, slope, sinuosity, mean annual flood and velocity have all been calculated from Schumm's (1972) equations, and metricated. Manning n values were calculated from the Manning equation for which imperial units must be used. This was done to check the accuracy of the raw field data. In most cases, calculated Manning n could be reconciled with the observed channel bedform. Froude numbers were calculated to establish the likely regimes of flow for the individual palaeochannels. The character strings 'Braided' and 'Meander' under flow type are derived

TABLE 1

Calculated palaeochannel attributes and flow dynamics via multiple regression equations and empirical formulae. Formation and locality shown.

OBSERVATION **********	L * MEANDER WAVELENGTH M	S * SLOPE	P * SINUOSITY RATIO	Q *** BANKFULL DISCHARGE CU.M/SEC	V * CURRENT VELOCITY CM/SEC	N * MANNING ROUGHNESS	F * FROUDE NO	FLOW TYPE *********	FORMATION AND LOCALITY **********	
1	776.8175	0.0008	1.5588	126.3337	59.2785	0.0235	0.4403	LOWER FLOW REGIME MEANDER	WITS	
Station 1 from Upper Witwatersrand Group, for comparison)										
2	992.6816	0.0026	1.2546	39.8192	73.9535	0.0151	1.0015	UPPER FLOW REGIME BRAIDED	KAT	(3)
3	1134.6113	0.0018	1.2689	72.1813	57.8468	0.0207	0.6405	LOWER FLOW REGIME MEANDER	BALF	SEYMOUR
4	698.0275	0.0008	1.5961	116.7496	43.0965	0.0324	0.3200	LOWER FLOW REGIME MEANDER	BALF	SEYMOUR
5	372.1559	0.0004	2.0393	152.1003	40.2988	0.0397	0.2116	LOWER FLOW REGIME MEANDER	BALF	SEYMOUR
6	743.6386	0.0002	1.9450	525.1577	39.8508	0.0453	0.1480	LOWER FLOW REGIME MEANDER	BALF	SEYMOUR
7	512.7284	0.0002	2.1118	399.1304	49.1190	0.0369	0.1824	LOWER FLOW REGIME MEANDER	BALF	SEYMOUR
8	1200.4811	0.0002	1.7141	649.7989	38.1349	0.0459	0.1514	LOWER FLOW REGIME MEANDER	BALF	SEYMOUR
9	3138.0387	0.0009	1.1262	316.7586	53.6719	0.0251	0.4202	LOWER FLOW REGIME MEANDER	BALF	(3)
10	561.6985	0.0002	2.0096	426.9668	42.8363	0.0423	0.1591	LOWER FLOW REGIME MEANDER	BALF	(3)
11	846.4267	0.0002	1.9043	807.4635	37.3139	0.0512	0.1182	LOWER FLOW REGIME MEANDER	BALF	(3)
12	1256.1343	0.0022	1.1930	59.7467	90.4047	0.0126	1.1550	UPPER FLOW REGIME BRAIDED	KAT	(3)
13	491.3432	0.0011	1.6510	66.5972	74.7086	0.0178	0.6407	LOWER FLOW REGIME MEANDER	KAT	(3)
14	858.4450	0.0010	1.4073	114.6441	81.5315	0.0166	0.6369	LOWER FLOW REGIME MEANDER	KAT	(3)
15	972.2845	0.0011	1.4195	110.1859	61.8622	0.0213	0.5506	LOWER FLOW REGIME MEANDER	KAT	N of (3)
16	429.7539	0.0013	2.1516	304.5523	28.7124	0.0617	0.1141	LOWER FLOW REGIME MEANDER	BALF	S of (1)
17	151.3359	0.0094	2.4687	78.3155	49.4561	0.0327	1.2593	LOWER FLOW REGIME MEANDER	BALF	S of (1)
18	794.0901	0.0002	2.0369	637.7231	34.0475	0.0555	0.1131	LOWER FLOW REGIME MEANDER	BALF	S of (1)

19	437.8797	0.0008	1.7697	82.7673	38.8343	0.0362	1.2884	LOWER FLOW REGIME MEANDER	BURGOP	(6)
20	2375.7772	0.0008	1.2172	288.1839	48.8297	0.0292	0.3627	LOWER FLOW REGIME MEANDER	BURGOP	(6)
21	1901.0519	0.0013	1.1828	142.9161	68.0727	0.0134	1.6527	LOWER FLOW REGIME MEANDER	KAT	(6)
22	574.4469	0.0032	1.3485	23.5545	119.2206	0.0091	1.7710	UPPER FLOW REGIME MEANDER	KAT	(6)
23	704.8226	0.0026	1.3252	33.1759	71.9272	0.0155	0.9754	TRANSITION MEANDER	KAT	(6)
24	189.1634	0.0040	1.6846	7.9200	92.9012	0.0114	1.5429	UPPER FLOW REGIME MEANDER	KAT	(6)
25	198.6444	0.0040	1.6486	8.5115	83.7377	0.0126	1.3907	UPPER FLOW REGIME MEANDER	KAT	(6)
26	144.2333	0.0041	1.7697	6.7215	102.4943	0.0103	1.7022	UPPER FLOW REGIME MEANDER	KAT	(6)
27	253.2557	0.0053	1.4952	7.5252	117.6925	0.0085	2.2579	UPPER FLOW REGIME MEANDER	KAT	(6)
28	481.5825	0.0016	1.5587	42.8507	81.6766	0.0151	0.8579	TRANSITION MEANDER	KAT	(6)
29	4223.8209	0.0010	1.0256	325.6184	54.8450	0.0236	0.4704	LOWER FLOW REGIME BRAIDED	KAT	(8)
30	2009.6247	0.0009	1.2321	214.7145	84.4426	0.0158	0.6803	LOWER FLOW REGIME MEANDER	KAT	(8)
31	1398.3780	0.0013	1.2659	113.9463	79.4817	0.0159	0.7021	LOWER FLOW REGIME MEANDER	KAT	(8)
32	3768.1535	0.0016	0.9887	195.4640	59.9149	0.0201	0.6293	LOWER FLOW REGIME BRAIDED	KAT	(9)
33	1249.4157	0.0022	1.1953	59.5103	88.7606	0.0129	1.1143	UPPER FLOW REGIME BRAIDED	BURGOP	(10)
34	544.9063	0.0010	1.5845	92.8361	61.6872	0.0220	0.4979	LOWER FLOW REGIME MEANDER	KAT	(12)
35	3531.6398	0.0008	1.1115	390.1041	49.5747	0.0276	0.3682	LOWER FLOW REGIME MEANDER	KAT	(1)

****

BEDFORM TYPES
****

LOWER FLOW REGIME: LOWER FLAT BED (NO GRAIN MOVEMENT) RIPPLES, T-BARS, SANDWAVES, DUNES

TRANSITION : WASHED OUT DUNES (FULL IN SCOUP)

UPPER FLOW REGIME: UPPER FLATBED (SHOOTING FLOW) STANDING WAVES, ANTIDUNES, (ALL SHOW CONTINUOUS PARTICLE MOVEMENT), VIOLENT ANTIDUNES

from Leopold and Wolman's (1957, p. 60) equation :

$$S = 0{,}013\ Q_b^{-0{,}44} \text{ (metric)} \qquad (8)$$

For a given discharge, braided streams occur on higher slopes than those given by the equation, and meandering streams occur on lesser slopes.

Before any of the calculations are started, true channel width, W, and cross-sectional area, A, are calculated by the program. The latter is assumed to have the shape of an inverted trapezium.

4. Interpretation

If meander wavelength and mean annual flood are considered together a good idea of stream size can be obtained. Large streams will have large L and Q_{ma} values. It follows that such streams should have lower velocities except where steeper slopes are indicated. Sinuosity, which is the ratio of stream length to axial length (the straight down valley length of the stream), can be checked against stream type. Meandering streams are considered by some workers to have sinuosities of more than 1,5 and braided streams less than this (Dury, 1969, p. 179). See Figure 23 overleaf.

This is probably a better criterion to use than equation (8) since no area between braided and meandering habit is defined by this latter method. Sinuosity gives an idea of the degree of braiding or meandering achieved by the stream.

Velocity considered together with discharge will give an indication of the competency and capacity of the streams. A rivulet can have the same velocity as a large river but certainly not the same competency or capacity. Velocity and Manning n should reflect the flow regime. Since this is obtained from the Froude number, Fr can be compared with these. Once the flow regime is known, the origins of observed sedimentary structures can be deduced from the predicted bedforms of the various regimes. Size of palaeostreams can be compared to modern rivers and thus an idea of source area, climate and environment of deposition can be obtained.

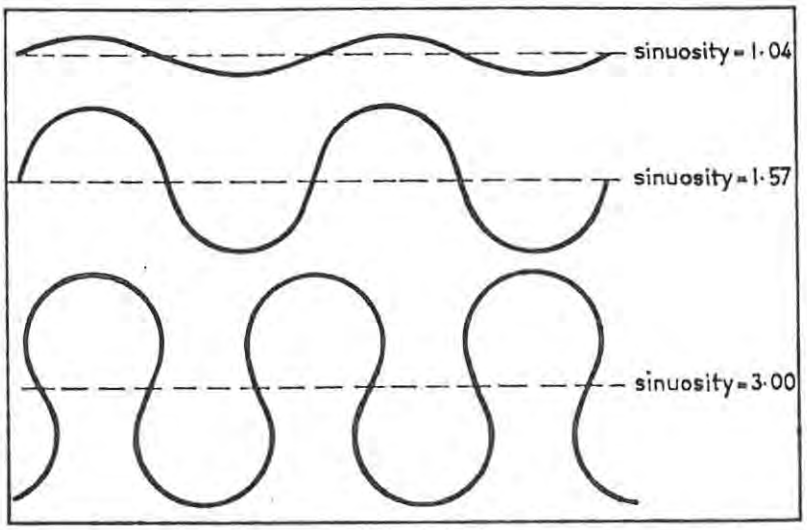

Fig. 23 Relative stream sinuosities. See text p. 52 for significance (after Dury, 1969).

Although there is much criticism about mathematical manipulation of such data, much can be said in defence of the method. Relatively few attempts have been made to analyse sedimentary processes in terms of palaeohydraulics (Blatt et al., 1972, p. 192). This method enables better interpretation of other environmental analyses in that it offers a check against other methods. In certain cases it may be the cause of careless speculation, but in spite of the uncertainties involved in the calculations, it offers a valuable source of information where channeling was obviously a principal process.

Schumm (1972, p. 105) states that it is unlikely that many palaeochannels would have equalled the discharges of rivers like the Amazon and the Mississippi. Even palaeovalley dimensions listed by Schumm (1972, Table 2) are less than the channel dimensions of these two modern rivers. These facts conform with the observations made during the present study, and calculated discharges for some Beaufort palaeochannels are compared with those of other ancient deposits and of modern rivers in Table 2.

TABLE 2 : Discharge data from some ancient and modern rivers

Modern :

River	Qmax m^3/sec	Climate	Reference
Nile	9 680	Temp. highland/arid	Kalinin (1968)
Red	476	Semi-arid	Kalinin (1968)
Mississippi	14 200	Temperate	Kalinin (1968)
Colorado	1 520	Arid	Kalinin (1968)
Rio Grande	156	Arid	Kalinin (1968)
Brahmaputra	140 000	Sub-tropical	Coleman (1969)
Donjek	1 400	Glacial	Rust (1972)
Platte	2 124	Semi-arid	Smith (1970)
Yana	125	Glacial/humid	Boothroyd (1975)

Ancient :

Palaeochannels	Qmax m^3/sec(ave)	Climate	References
Katberg (Trias)	390 (105)	Arid ?	This study
Burgersdorp (Trias)	304 (143)	Semi-arid ?	This study
Balfour (Permo-Trias)	807 (315)	Humid ?	This study
Witwatersrand (pE)	126		Minter (1978)
Ferron (Cret)	566	Humid	Cotter (1971)

According to Minter (1978), Donjek type (Miall, 1977, p. 46) braided streams prevailed where the above Witwatersrand palaeochannel was observed, and the measured discharge might only represent the thalweg of a larger channel. A further analysis of the Beaufort palaeochannels will be made in the next section.

E. BEDFORM STATISTICS

1. Method

Well exposed sections were sampled for sedimentary structures at 1 m intervals. Since beds in the area examined normally consist of cosets ranging in thickness between 0,3 and 2,0 m, this sampling method will be similar to a kind of first-order Markovian chain analysis. At that stage the Markov chain depends only on single steps, i.e., the relationship between a given bed and the bed immediately succeeding it (Miall, 1973, p. 348). Structures were recorded at the sampling interval under the categories, LFB, ripples, planar cross-bedding, trough cross-bedding, UFB and antidunes. Under LFB facies Fm and Fl which did not show ripple lamination were also included, and all symmetrical cross-bedding and undulatory surfaced massive units were recorded as antidunes. Cross-stratification was considered in terms of Allen's (1963) classification and interpreted as explained earlier. Where longitudinal sections of trough and planar crossbeds were visible, foreset azimuths were measured directly where rock fracture permitted a three dimensional view of the individual foreset laminae. A device, best described as a self levelling rotatable protracter when used in conjunction with a Brunton compass, was employed for the purpose. Foreset strike, and thus azimuth, and dip can be measured as shown in Figure 24. The device was designed by Dr W E L Minter of the Anglo American Corp. Sedimentology Research Unit in Welkom, O.F.S. The advantage in using a device of this sort is that variation in foreset dips and azimuths can be accurately measured and thus the changes in palaeoflow over what would have been transverse or linguoid bars can be appreciated.

Column totals, as listed in Table 3, were obtained from the various bedform structure categories. Histograms showing the relative abundance of the different sedimentary structures and their corresponding regimes of flow were also constructed. These together with analysed minor sequences, typical of that part of the formation being examined, appear in the conceptual scheme (Fig. 25A - L), below.

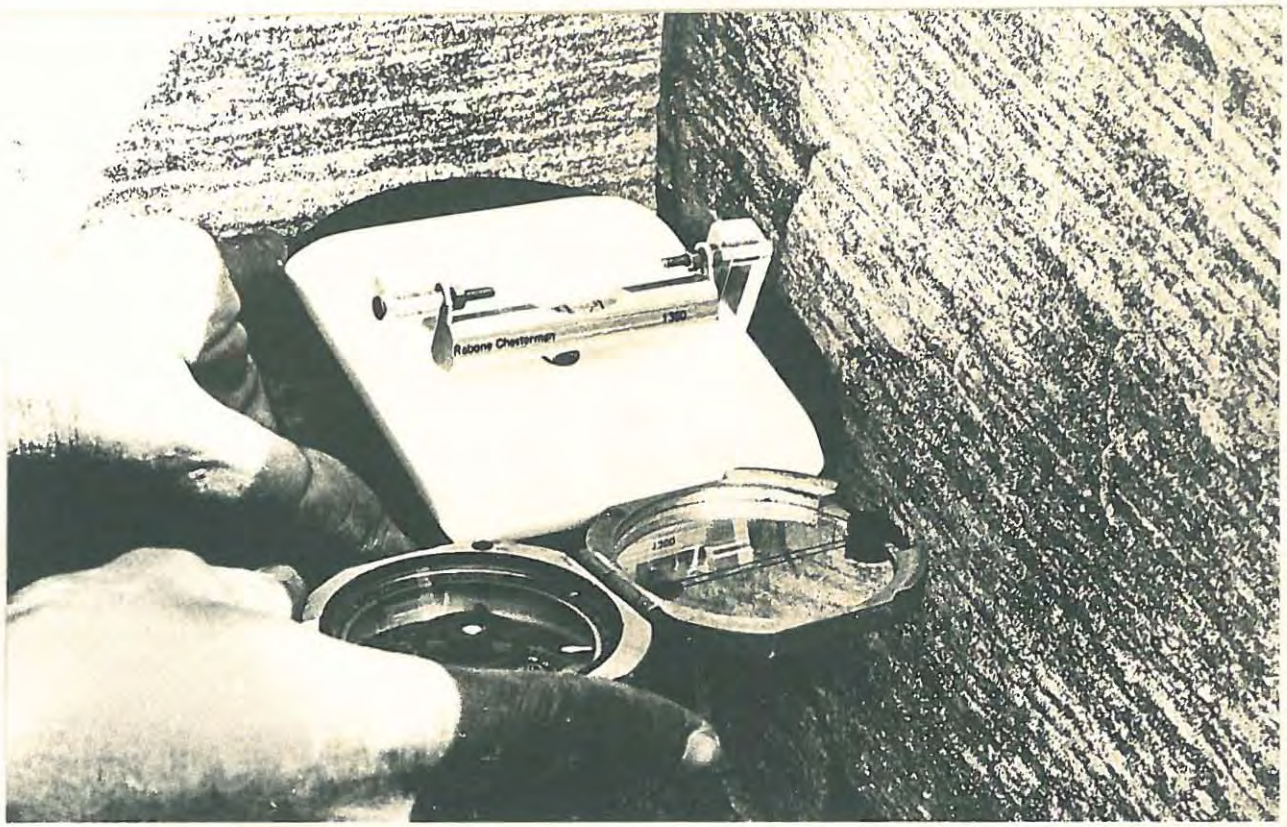

Fig. 24 Device used for accurate measurement of true dip and azimuth of cross-bedding foresets. Base of protractor (black plate) positioned on same foreset, spirit level part (white plate) rotated until bubble is level; dip and strike (thus azimuth) then measured directly as shown.

TABLE 3 : Relative abundances of bedform structures in the Katberg Sandstone, Balfour and Burgersdorp Formations.

Formation	Percent of total structures						Number of
section no. & posn.	LFB	Sr	Sp	St	UFB	Sm 2,3	readings
Balfour - Seymour area	8	34	6	40	11	-	348
Katberg - (3) lower	-	-	20	10	67	3	116
Katberg - (3) upper	3	1	16	29	44	4	194
Burgersdorp - (6) lower	7	31	3	21	38	-	58
Katberg - (6) upper	1	3	9	33	54	-	182
Katberg - (8)	1	-	2	33	63	1	390
Katberg - (9)	1	-	2	29	65	3	312
Katberg - (10)	3	-	10	37	43	7	60
Burgersdorp - (10) lower	28	-	1	36	36	-	156
Katberg - (12)	17	4	21	13	45	-	144
Katberg - (1) (2) lower	2	-	11	17	70	-	242
Katberg - (1) (2) upper	-	-	7	54	39	-	316

Fig. 25 A - L Conceptual scheme showing main sedimentological attributes of typical sequences, and their interpretation, from the Katberg Sandstone, Balfour and Burgersdorp Formations.

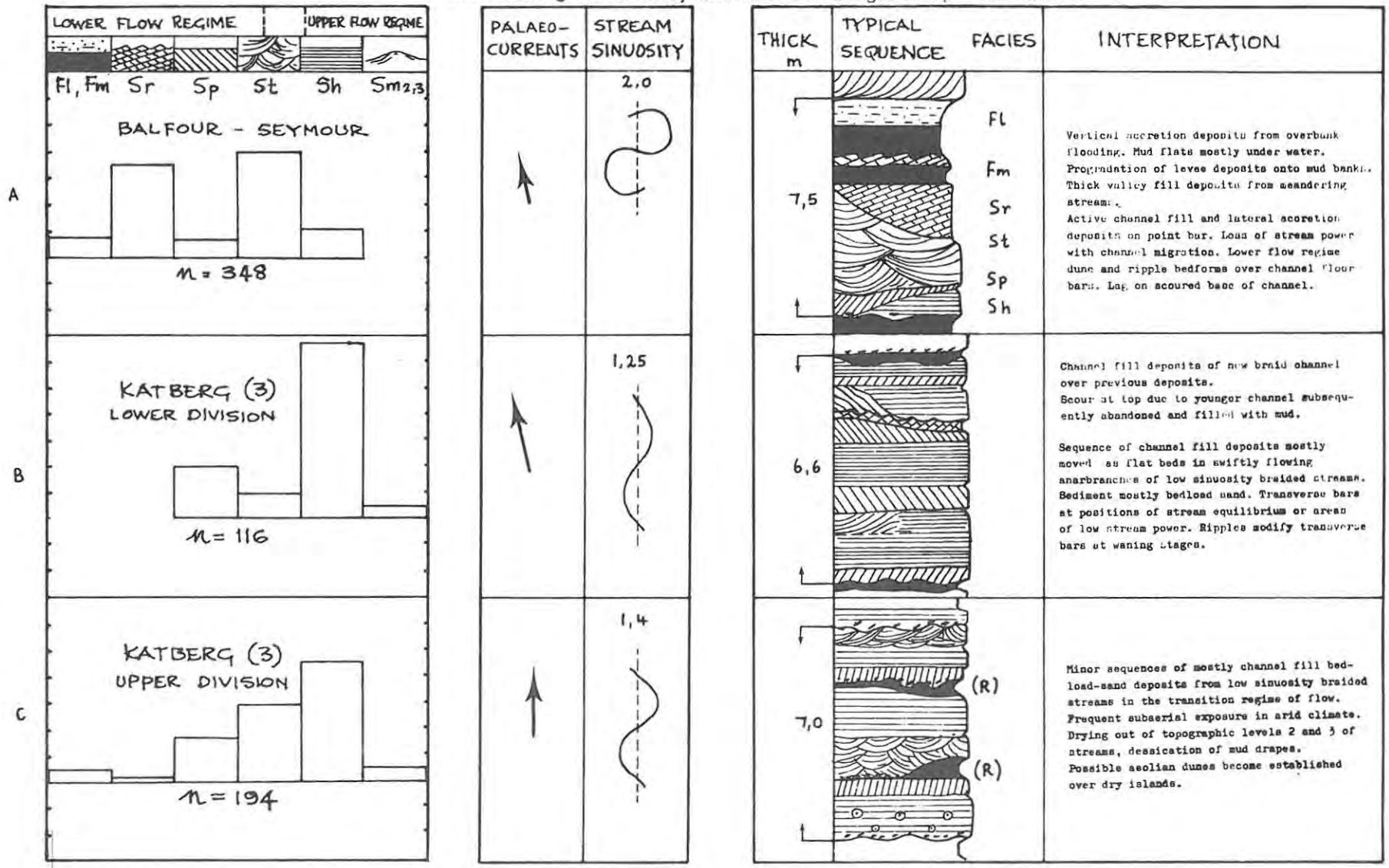

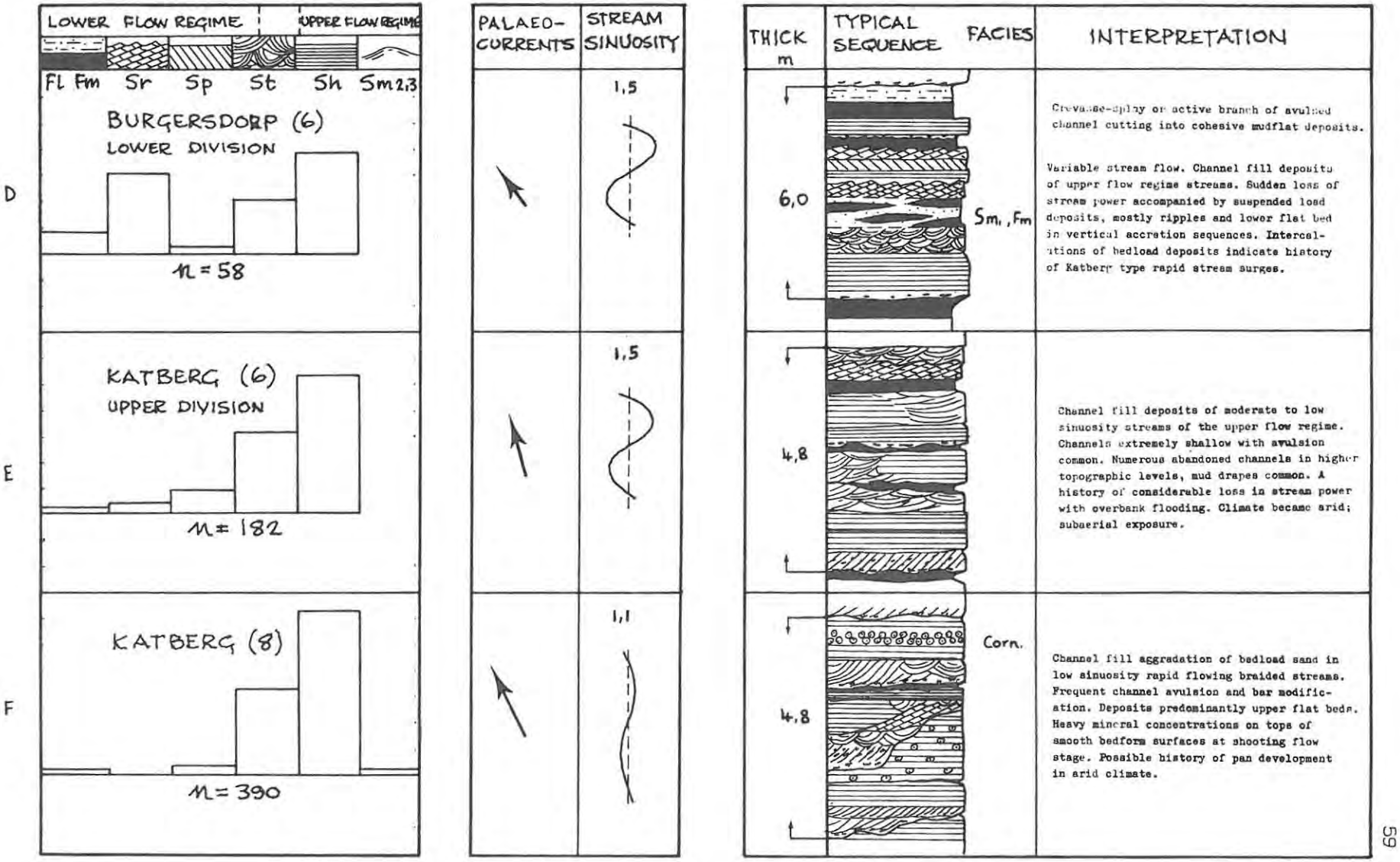
LOWER FLOW REGIME
UPPER FLOW REGIME
Fl Fm Sr Sp St Sh Sm2,3
PALAEO-CURRENTS
STREAM SINUOSITY
THICK m
TYPICAL SEQUENCE
FACIES
INTERPRETATION
D
BURGERSDORP (6)
LOWER DIVISION
n = 58
1,5
6,0
Sm1, Fm
Crevasse-splay or active branch of avulsed channel cutting into cohesive mudflat deposits.
Variable stream flow. Channel fill deposits of upper flow regime streams. Sudden loss of stream power accompanied by suspended load deposits, mostly ripples and lower flat bed in vertical accretion sequences. Intercalations of bedload deposits indicate history of Katberg type rapid stream surges.
E
KATBERG (6)
UPPER DIVISION
n = 182
1,5
4,8
Channel fill deposits of moderate to low sinuosity streams of the upper flow regime. Channels extremely shallow with avulsion common. Numerous abandoned channels in higher topographic levels, mud drapes common. A history of considerable loss in stream power with overbank flooding. Climate became arid; subaerial exposure.
F
KATBERG (8)
n = 390
1,1
4,8
Corn.
Channel fill aggradation of bedload sand in low sinuosity rapid flowing braided streams. Frequent channel avulsion and bar modification. Deposits predominantly upper flat beds. Heavy mineral concentrations on tops of smooth bedform surfaces at shooting flow stage. Possible history of pan development in arid climate.

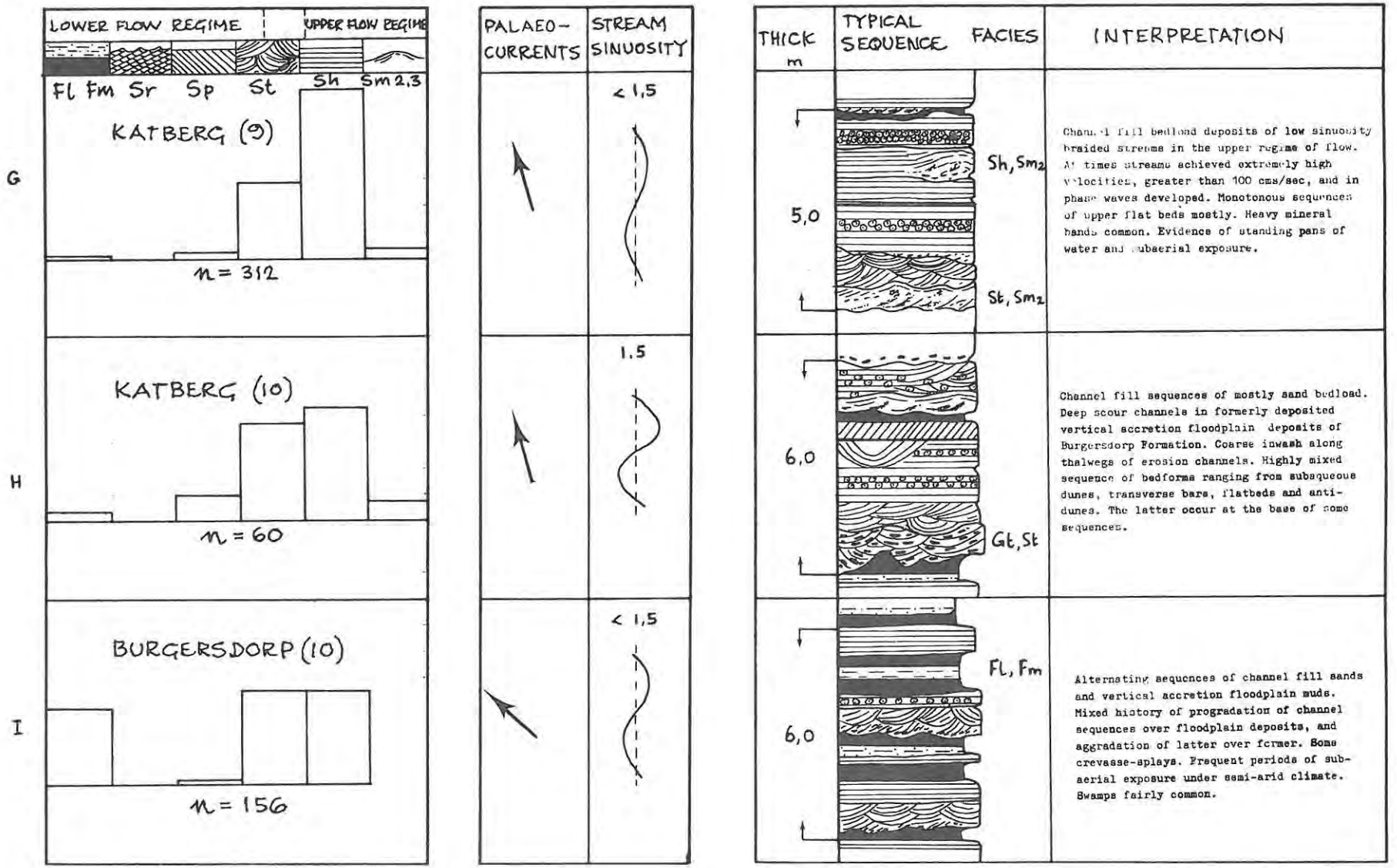
LOWER FLOW REGIME
UPPER FLOW REGIME
Fl Fm Sr Sp St Sh Sm 2,3
KATBERG (9)
n = 312
KATBERG (10)
n = 60
BURGERSDORP (10)
n = 156
G
H
I
PALAEO-CURRENTS
STREAM SINUOSITY
< 1,5
1.5
< 1,5
THICK m
TYPICAL SEQUENCE
FACIES
INTERPRETATION
5,0
Sh, Sm2
St, Sm2
Channel fill bedload deposits of low sinuosity braided streams in the upper regime of flow. At times streams achieved extremely high velocities, greater than 100 cms/sec, and in phase waves developed. Monotonous sequences of upper flat beds mostly. Heavy mineral bands common. Evidence of standing pans of water and subaerial exposure.
6,0
Gt, St
Channel fill sequences of mostly sand bedload. Deep scour channels in formerly deposited vertical accretion floodplain deposits of Burgersdorp Formation. Coarse inwash along thalwegs of erosion channels. Highly mixed sequence of bedforms ranging from subaqueous dunes, transverse bars, flatbeds and anti-dunes. The latter occur at the base of some sequences.
6,0
Fl, Fm
Alternating sequences of channel fill sands and vertical accretion floodplain muds. Mixed history of progradation of channel sequences over floodplain deposits, and aggradation of latter over former. Some crevasse-splays. Frequent periods of sub-aerial exposure under semi-arid climate. Swamps fairly common.

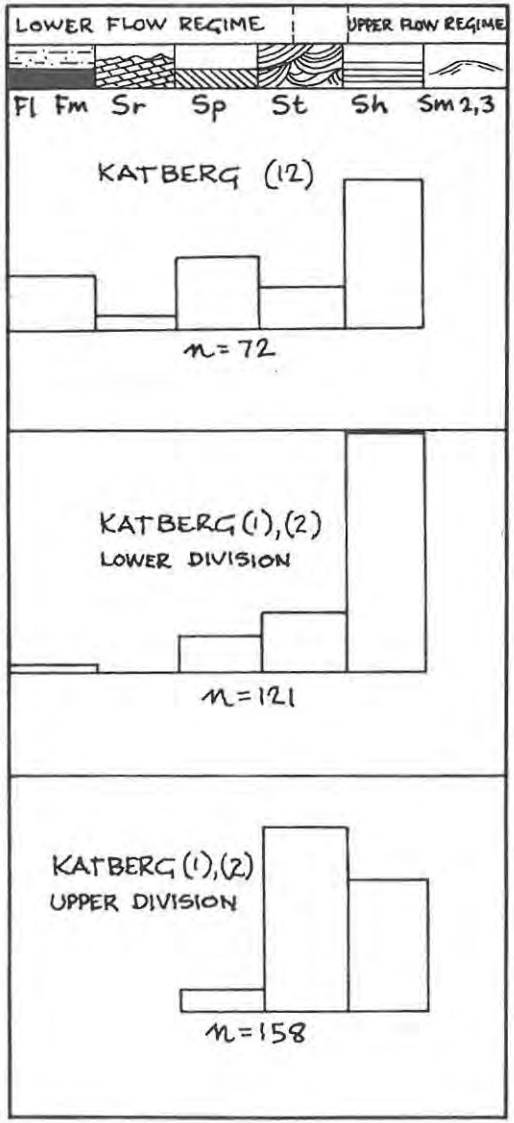
LOWER FLOW REGIME
UPPER FLOW REGIME
Fl Fm Sr Sp St Sh Sm 2,3
KATBERG (12)
J
n=72
KATBERG (1),(2)
LOWER DIVISION
K
n=121
KATBERG (1),(2)
UPPER DIVISION
L
n=158

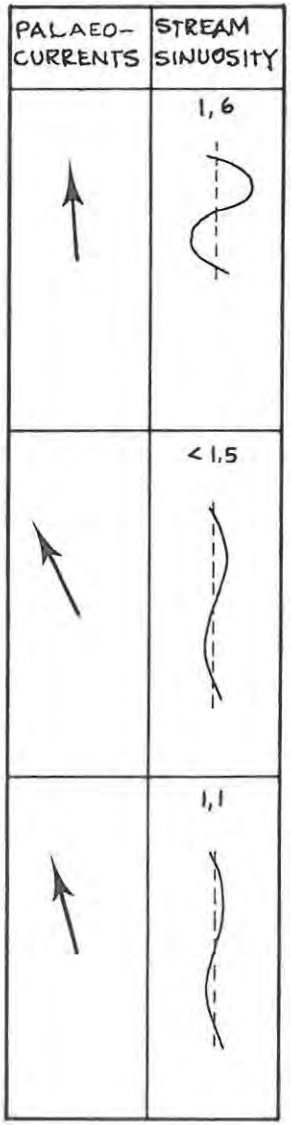
PALAEO-CURRENTS
STREAM SINUOSITY
1,6
< 1,5
1,1

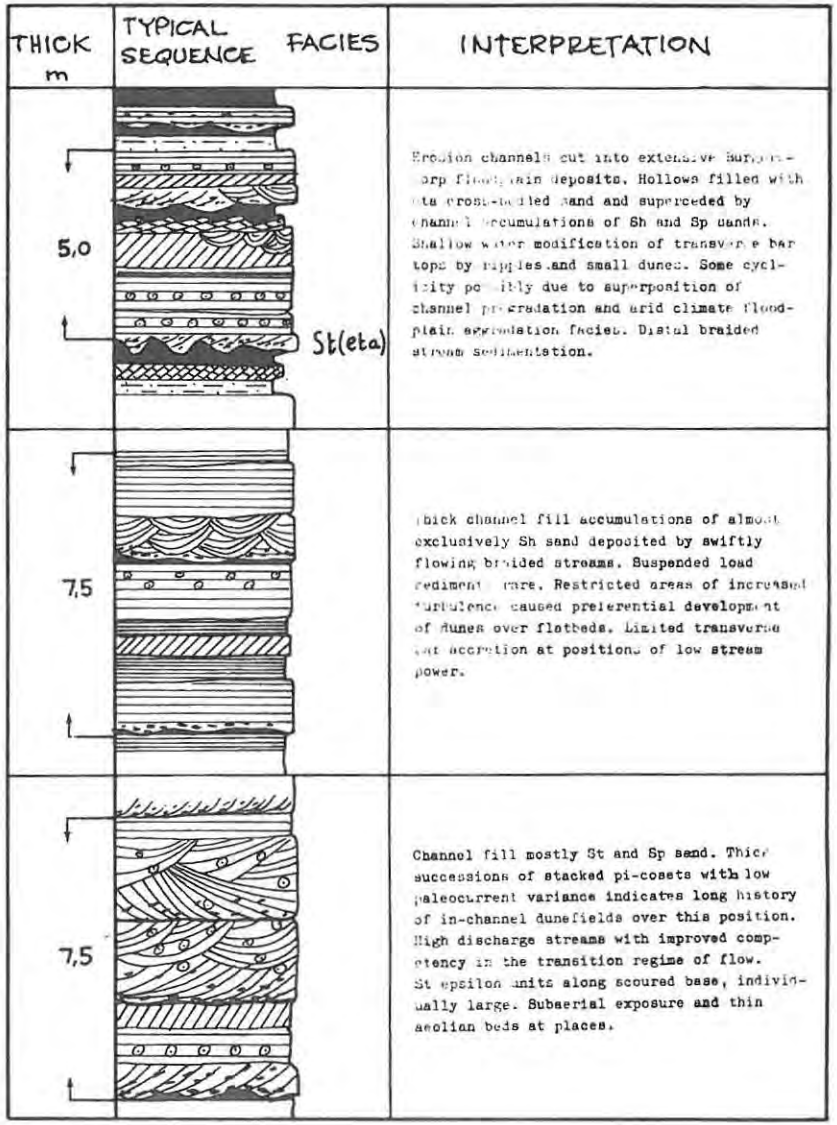
THICK m
TYPICAL SEQUENCE
FACIES
INTERPRETATION
5,0
St(eta)
Erosion channels cut into extensive subaerial floodplain deposits. Hollows filled with ripple cross-bedded sand and superceded by channel accumulations of Sh and Sp sands. Shallow water modification of transverse bar tops by ripples and small dunes. Some cyclicity possibly due to superposition of channel preservation and arid climate floodplain aggradation facies. Distal braided stream sedimentation.
7,5
Thick channel fill accumulations of almost exclusively Sh sand deposited by swiftly flowing braided streams. Suspended load sediment more. Restricted areas of increased turbulence caused preferential development of dunes over flatbeds. Limited transverse bar accretion at positions of low stream power.
7,5
Channel fill mostly St and Sp sand. Thick successions of stacked pi-cosets with low paleocurrent variance indicates long history of in-channel dunefields over this position. High discharge streams with improved competency in the transition regime of flow. St epsilon units along scoured base, individually large. Subaerial exposure and thin aeolian beds at places.

2. Facies relationship models (Matrix Analysis)

The conceptual scheme above is a distillation of the essence of Beaufort Group sedimentation in the area under study. A further refinement was carried out with the establishment of facies relationship models for the three formations. The method used was that of Walker (1975, p. 68), who applied it to the fluviatile Battery Point Formation of Quebec. In that case the facies used for the construction of the predicted matrix were obtained from observation of similar criteria directly from field outcrop. For the Battery Point sequence eight facies were used. Distinctions were made on cross-strata based on thicknesses of planar sets and types of trough sets and cosets. McDonnell (1978, p. 43) analysed fluvial sequences of the Triassic Gosford Formation of Australia. In that case a 5 x 5 matrix was constructed based on five generalised lithofacies obtained from vertical facies profiles.

For the present study five main facies were used in the analysis. They are as follows :

A : Scoured surface with or without shale pellet conglomerate.
B : Heterogeneous cross-bedding, epsilon and eta units, also structures of greatest stream power including Facies $Sm_{2\ 3}$.
C : Facies St, Sp, Sh (UFB).
D : Facies Sr, Sh (LFB).
E : Facies Fl, Fm, Sm_1.

The starting point for each analysis was the vertical stratigraphic column of each formation. Fifty to sixty facies from four stratigraphic columns were used in each example. In the case of the Balfour and Burgersdorp Formations all the available data was used, but for the Katberg Sandstone only stratigraphic columns (8) and (11) were used. The choice was arbitrary, but checks carried out on two other profiles yielded similar facies relationships. The Katberg model is therefore a very consistent one (but of weak memory).

Method :

The facies A to E are listed exactly in the sequence in which they occur

Matrix analysis of Balfour Formation lithofacies

E C D E D E / Ç E D E DE DE DE / A C E C E / A C D / C D
A C D E / B C D E / A D E / A B C D / C E / A C D E / A C

Tally Matrix

	A	B	C	D	E	
A		1	5	1		7
B			2			2
C				7	4	11
D	1		2		10	13
E	6	1	3	5		15
	7	2	12	12	14	

Secondary Matrix

	A	B	C	D	E	
A		·71	3·25			
B			1·5			
C				4·25	·79	
D					6·2	
E	3·8	·38		1·25		

Facies Relationship Model for Balfour Formation

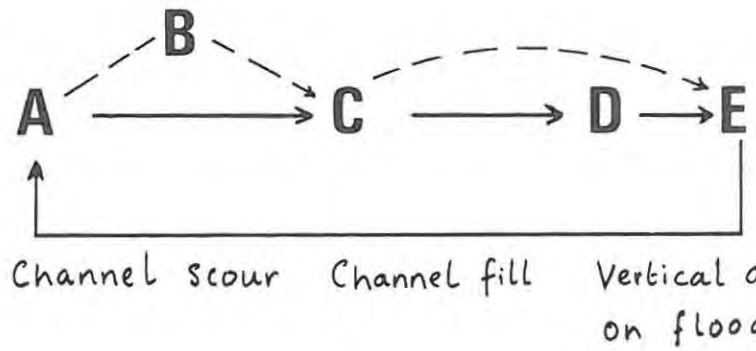

Matrix analysis of Katberg Sandstone lithofacies

ABCE/AC/AB/AC/CE/ABC/AC/ACE/ACE/ACE/ABC/ACB/
ABC/AC/ABCE/C/C/C/ABC/ABCE/ABC/AC/BC/ABC/ABC

Tally Matrix

	A	B	C	D	E	
A		11	9			20
B	2		11			13
C	11	2	3		7	23
D						
E	6		1			7
	19	13	24		7	

Secondary Matrix

	A	B	C	D	E	
A		6.9	.75			
B			6.0			
C	4.1				4.4	
D						
E	3.9					

Facies Relationship Model for Katberg Sandstone

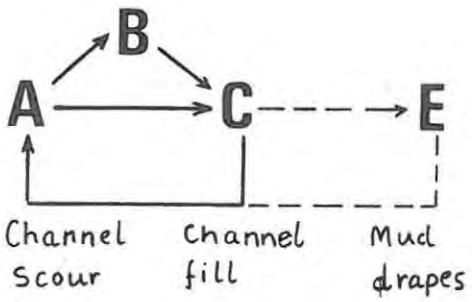

Matrix analysis of Burgersdorp Formation lithofacies

E/C/E/C/E/ABCD/ABCD/ABCDE/DEDEDE/ABCE/BCE/
ABCE/ACE/ABCE/ACE/CDDE/ADE/CE

Tally Matrix

	A	B	C	D	E	
A		6	2	1		9
B			7			7
C				4	9	13
D	2			1	6	9
E	7	1	4	3		15
	9	7	13	9	15	

Secondary Matrix

	A	B	C	D	E	
A		4.8				
B			5.3			
C				1.8	6.5	
D	0.5				3.5	
E	4.5		0.3	0.5		

Facies Relationship Model for Burgersdorp Formation

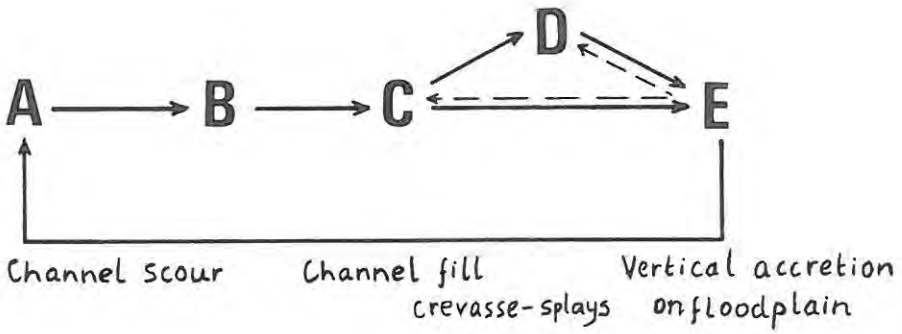

please append to pp. 63-65

KATBERG SANDSTONE

TALLY MATRIX

	A	B	C	D	E	ROW SUM
A		11	9			20
B	2		11			13
C	11	2	3		7	23
D						
E	6		1			7

PROBABILITY MATRIX

	A	B	C	D	E	ROW SUM
A		.55	.45			1.0
B	.15		.85			1.0
C	.48	.09	.13		.30	1.0
D						0.0
E	.86		.14			1.0

No. of Transitions, 63

from which,

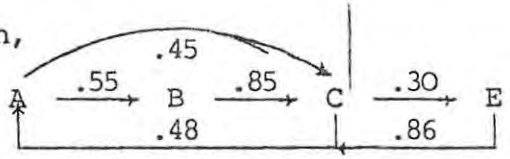

This diagram is essentially similar to the one given, but statistically based.

The probability matrix is calculated simply by dividing each item in the row by the rowsum. This produces a probability matrix of the type shown. Each element is a conditional probability. i.e. the probability that state A will follow state E is .86, providing that state E occurs in the stratigraphic sequence. Larger sample numbers are desirable. Similarly probability matrices for the Burgersdorp and Balfour Formations are given below.

BALFOUR FM. Probability Matrix

Burgersdorp Fm. Probability Matrix

in the vertical profile being analysed. Scoured contacts are indicated with a slash between transitions. From this facies sequence a transition frequency matrix (McDonnell, 1978, p. 44) or tally matrix (Walker, 1975, p. 71) is constructed. The tally matrix shows the frequency with which the facies listed on the left hand side are followed by those listed across the top.

From the tally matrix the ~~predicted or probability~~ facies relationship matrix is constructed in the following way. Row and column totals of the tally matrix are cross multiplied, the product is divided by the total number of recorded transitions. The quotient obtained thereby is subtracted from the observed number of transitions in each unit of the tally matrix (Walker, 1975, p. 70). Thus the transitions that occur more commonly can be singled out for treatment and the final facies relationship model is a combination of statistical and subjective consideration. The matrix/transition analyses for the Balfour, Katberg Sandstone and Burgersdorp Formations respectively appear ~~overleaf~~ above.

3. Bed relief index

A measure of the topographic relief across Katberg palaeochannels was made using the method devised by Smith (1970, p. 2998) for the braided Platte River. Bedforms of the Katberg Sandstone, as deduced from primary sedimentary structures, appear to be similar in many respects to those of the present day Platte River. Bed relief index (BRI) was measured at five localities in the central part of the study area, for two reasons. Firstly to ascertain how proximal or distal the palaeostreams under study were, and secondly to predict the distance away of the Lower Triassic Beaufort Group source area which lay somewhere to the south of the present day coastline. Although only five BRI calculations were made, they are typical of the Katberg Sandstone.

Method :

Channel profiles with flat topped bedding planes were singled out and all the elevation changes along their widths were recorded. Equal numbers of high and low points must be considered. Figure 26 shows a typical Katberg palaeochannel profile. All the high points are added

together and the total is subtracted from the sum of all the low points. The result is doubled and the two elevations at the edge of the traverse are either added or subtracted depending on whether they lie adjacent to a high or low point. The final figure of the top line is then divided by 1 000. For convenience the quotient is multiplied by 100 so that most BRI's have values greater than 1 (Smith, 1970, p. 3011). An example of a BRI calculation from the Katberg Sandstone is shown below.

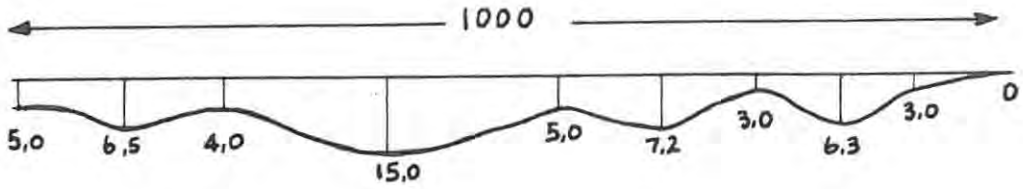

Fig. 26 Typical palaeochannel profile, and bed relief index calculation from Katberg Sandstone (units decimeters).

Example of calculation of B.R.I from Katberg Sst. loc.(8)

$$\frac{2\left[(6,5 + 15,0 + 7,2 + 6,3) - (4,0 + 5,0 + 3,0 + 3,0)\right] - 5}{1000} \times 100$$

B.R.I. = 3,5

F. HEAVY MINERAL BANDS AND PALAEOHYDRAULICS

Minter (pers. comm., 1978) believes that the heavy mineral layers of the Katberg Sandstone, like the pyrite lags of the upper Witwatersrand Group, represent a horizontal mosaic of coarse and dense scour material left behind by advancing ripple trains over flat beds. Smith (1972, p. 625) suggests a similar mechanism for alternating coarse and fine laminations

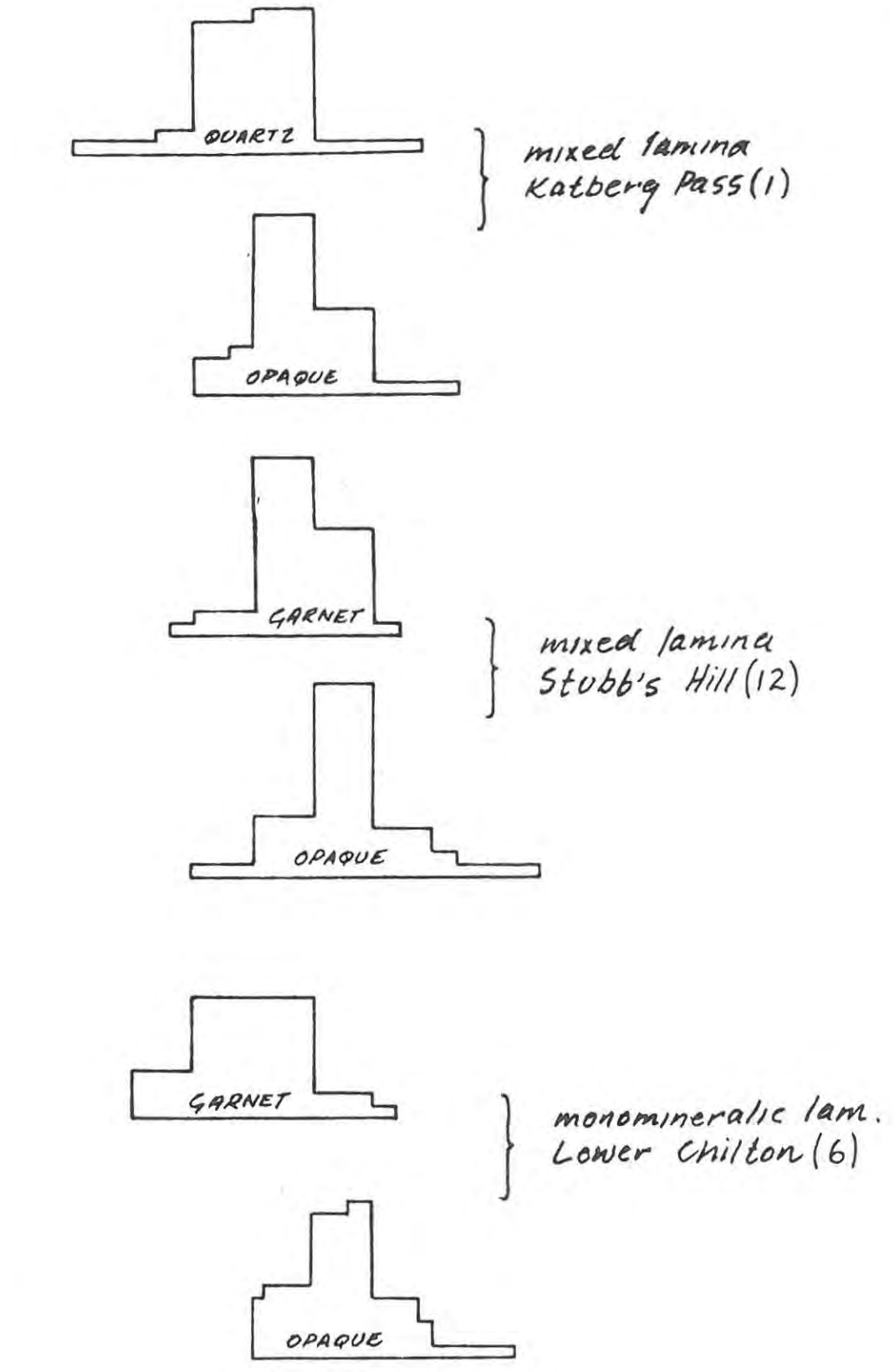

Fig. 27 Grain size histograms of various associates from individual heavy mineral laminae of the Katberg Sandstone.

Fig. 28 SEM micrograph of detrital titanomagnetite grain, notice euhedral shape and pitted surfaces (magnification 1 000 x).

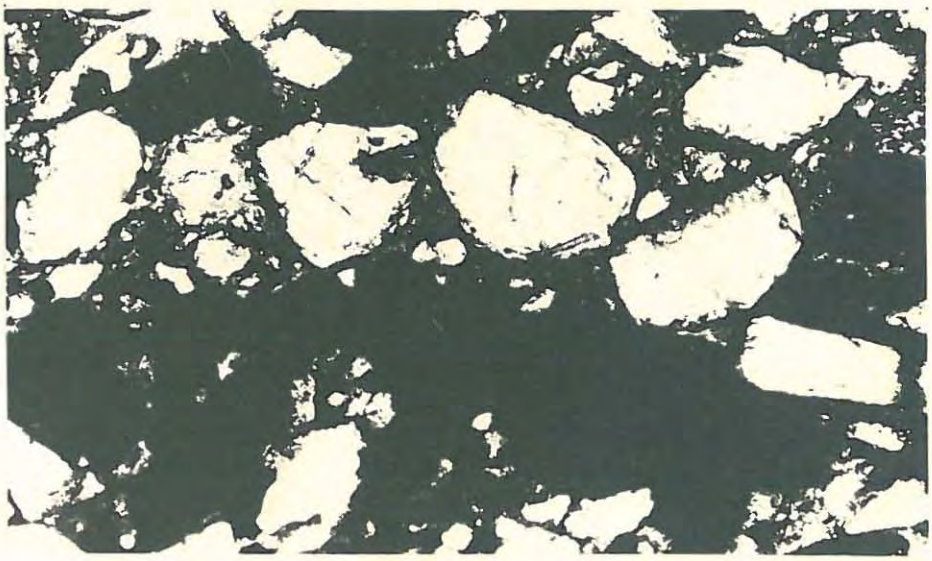

Fig. 29 Segregations of opaque minerals and garnet into monomineralic laminae (long axes of garnets 200 micron).

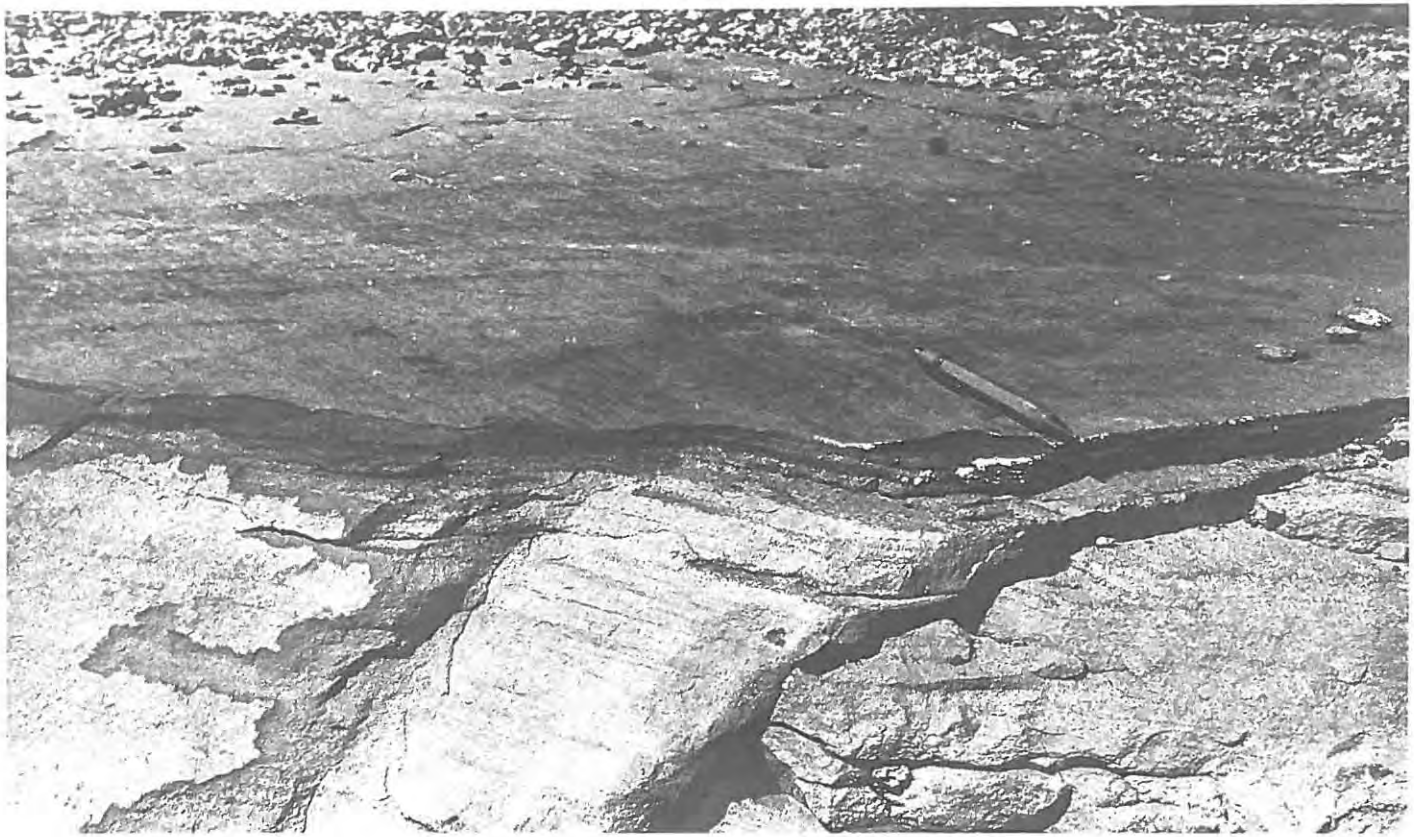

Fig. 30 Heavy mineral layers in UFB-sandstone. Shooting flow surfaces evident. Loc., Fairford (8), Katberg Sandstone.

in transverse bars of the Platte River. He found that scour pockets formed by leeside eddies in front of migrating ripples and dunes. The mechanisms of Smith and Minter are unlikely in the case of the Katberg bands, since no coarse material, cross-lamination or ripple activity has been noticed associated with them. The heavy mineral grain size is of the order 2 - 4ϕ, depending on the type (see Fig. 27).

May (1973, p. 203) showed experimentally how heavy minerals could be selectively transported by shoaling waves on beaches. He found that under certain wave conditions the heavy mineral fraction moved shoreward faster than did the lighter minerals. Once deposited, these heavy minerals were not easily removed by opposite flow. May's wave tank experiments assume water depths and kinematic forces well in excess of those derived for Katberg streams (Table 1).

SEM micrographs show that most of the grains making up the bands display rounding and pitting indicating a primary source (Fig. 28). Heavy minerals from the host rocks and surrounding Katberg sandstones have similar microprobe count rates and are in most respects identical.

These dispersed grains may have been temporarily stored in proximal gravel bars or other more distal bedforms such as dunes (trough cross-bedding) and even as lag material between ripples (ripple drift cross-lamination), however with increasing current velocities possibly brought about by decreased water depth or increased gradient or both, lower flow regime and transitional bedforms were washed out and upper flow regime horizontal lamination predominated.

The bands cannot be simply explained in terms of relative settling velocities. Individual laminae are often monomineralic in the sense that an opaque ore layer will be followed by a garnet layer as evidenced in Figure 29.

Diffusion and mixing are also common, but this may reflect local turbulence since juxtaposed quartz and magnetite, which is the main opaque component, are not in hydraulic equilibrium.

Deposition of bedload material depends among other factors on bottom shear stress (Briggs and Middleton, 1965, p. 15). Differences in flow

related to stream velocity and water depth will sort and deposit the various traction populations. Not all the grains being moved by a particular mechanism will necessarily be deposited, however (Blatt et al., 1972, p. 103). In the case under examination, individual laminae commonly change in gross composition from predominantly very fine grained (ϕ = 3,75) opaque oxides, to non-opaque clusters mainly of garnet (ϕ = 3,0). These two discreet fractions are very seldom mixed. Transitions do occur and seem to coincide with delicate bifurcations of the laminae, possibly initiated by concommitant minor changes in bed roughness.

Turning to a possible concentrating mechanism; dispersed heavy mineral grains would have been washed out from temporary storage, and moved along as part of the traction carpet. At certain velocities, critically related to the ease of sliding or rolling of the grains, most other available traction material was winnowed out, either by differential sliding or by increased saltation, leaving behind a select component. Small differences in bottom shear stress may have been ultimately responsible for the very select fractionation. Individual laminae are themselves parting lineation surfaces (Fig. 30).

Self-explanatory histograms were compiled based on several hundred grain measurements made on laminae from thin and polished sections. Initial grain dimensions were converted to corresponding sieve ϕ sizes using the Friedman (1958) correction scale. Employing median grain diameters from two monomineralic laminae, one for magnetite and the other for garnet, relative shear strengths required to move these two populations were calculated according to the line

$$\frac{d_s}{\nu} \quad 0,1 \left(\frac{\gamma_s}{\gamma_f} - 1 \right) g\, d_s$$

The value once calculated is projected onto the Shields' curve (Briggs and Middleton, 1965, p. 11) and the value β derived. From the equation

$$\beta = \frac{\tau_o}{(\gamma_s - \gamma_f)\, d}$$

β is a constant for turbulent flow $\sim$ 0,06. Thus for large grain

diameters corresponding to high Reynolds number (> 600) recourse to the Shields' diagram is not necessary. The values calculated for this study are based on the assumption that Katberg streams were fairly clear, i.e., that they carried very little dissolved and suspended material, and that water temperatures were not abnormal, thus a kinematic viscosity of 10^{-2} cm^2/sec could be used. High sand/shale ratios typical of most Katberg sequences and probable ephemeral palaeoflow do not render this assumption unlikely.

Shear stresses of 1,4 dynes cm^{-2} and
3,1 dynes cm^{-2}

were obtained for opaque and garnet layers respectively. A point to note here is that lower than normal shear velocities would be required to move sediment in this case because of the extreme shallowness of Katberg palaeostreams. The author has found that palaeochannel depth of less than 1 metre are the rule.

The heavy mineral laminae are part of a sequence of bed phases ranging from dunes, through upper flat bed, the latter being by far the more prevalent. This is probably due to the fine grain size (0,08 - 0,25 mm) of the host sandstones where laminae occur. Symmetrical cross-lamination, indicating the presence of standing waves or antidunes, was recorded from associated sandstones. The presence of in-phase waves in this grain size and mean water depth range would reflect very high current velocities (Fig. 17).

G. PALAEOCURRENT ANALYSIS

A total of 19 nearly evenly spaced localities were sampled along a 20 km front, normal to indicated palaeoslope. The general direction of the latter was obtained from Theron (1973, p. 63) and J C Theron (pers. comm., 1978). Palaeocurrent direction indicators were measured wherever they were observed at the various localities. No attempt was made to sample select stratigraphic levels except where different formations were involved within a given measured section. Alternatively, where a definite change in flow regime accompanied by modifications in bedform structures was noticed, the different units were measured separately. For example low angle trough cross-bedding and UFB lamination

would indicate Froude numbers of 0,6 - 1,0 but a sudden abundance of planar cross-stratification implies a loss of stream power, and high directional variance can be expected. Thus planar foresets were considered independently otherwise overall vector strength was reduced substantially.

The observation points of Deep River (4) and (4) S, have high variances (500 - 900) and relatively low vector strengths. Vector mean diverges somewhat from the general flow pattern. The presence of a proximal wedge of Burgersdorp sediments (see Fig. 2) and relative abundance of nu-cross-stratification are thought to have influenced the calculations. The latter is the bedform structure of large scale highly sinuous, lunate and caternary ripple trains. Some planar cross-bedding was seen in poor exposures here. It is highly likely that certain measured troughs were in fact curved front sections of small scale (10 - 30 cm) linguoid bars.. The resultant flow direction would not have had the unimodal character of true trough cross-bedding. Table 4 is a summary of collected and processed palaeocurrent data. Arrows indicating the vector mean for stations, and according to their lengths, the vector strength were plotted on the geological map overlay. It was deemed unnecessary to calculate the standard deviation and variance for each group. There is a direct relationship between these two parameters and vector strength. Theron (1970, p. 64) shows graphically the relationship between vector strength and standard deviation. Variance is the movement away from the central tendency, and is inversely proportional to vector strength. When the latter is considered together with the vector mean it is the best calculation procedure (Potter and Pettijohn,91963, p. 264). J C Theron (pers. comm., 1978) considers primary current lineations together with measured trough axes. The former are usually represented as symmetrically opposed directions on rose diagrams. The palaeoslope is well established in this area, therefore contradictory current lineation directions were rejected as improbable. During the present study, many trough sets were seen to contain this structure, thereby substantiating Theron's choice of method. The same procedure was followed here and in addition, related structures such as orientated concretions and flute casts were treated together.

Planar foreset azimuths were measured in road cuttings as described in section E of this chapter, and were calculated separately. The

vector mean and vector strengths of the various circular distributions of measurements were calculated according to the formulae of Reiche cited by Potter and Pettijohn (1963, p. 264).

TABLE 4 : Palaeocurrent data

Formation	Locality	Structure	n	$\bar{x}$	L	α
Katberg	(3)	tr. ax./p.c.l.	54	346	89	-
Katberg	(3)	pl. for.	8	25	99	38
Katberg	(3)	pl. for.	4	90	98	32
Katberg	(3)	pl. for.	12	38	99	28
Balfour	(3)	tr. ax./p.c.l.	18	357	98	-
Balfour	(3)	pl. for.	10	136	98	15
Balfour	SW of (3)	tr. ax./p.c.l.	28	317	90	-
Balfour	S of (1)	tr. ax./p.c.l.	34	344	61	-
Katberg	W of (3)	tr. ax./p.c.l.	10	347	99	-
Katberg	(1) (2)	tr. ax./p.c.l.	34	337	98	-
Katberg	(2)	concr.	6	332	99	-
Katberg	(1)	pl. for.	6	272	97	12
Katberg	(1)	pl. for.	3	304	99	16
Katberg	(1)	pl. for.	3	221	99	13
Katberg	(2)	tr. ax./p.c.l.	22	309	96	-
Katberg	(4)	tr. ax./p.c.l.	24	9	66	-
Katberg	S of (4)	tr. ax.	16	52	74	-
Katberg	N of (4)	tr. ax./p.c.l.	44	335	79	-
Katberg	(6)	tr. ax./p.c.l.	12	319	94	-
Katberg	(6)	pl. for.	3	83	99	5
Katberg	(6)	pl. for.	4	297	98	16
Katberg	(6)	pl. for.	5	336	99	-
Katberg	(6)	assym. ripp.	8	25	48	-
Katberg	N of (6)	tr. ax./p.c.l.	34	357	84	-
Katberg	(8)	tr. ax./p.c.l.	32	333	99	-
Katberg	(8)	pl. for.	14	252	98	17
Katberg	N of (8)	tr. ax./p.c.l.	30	332	60	-
Katberg	(9)	tr. ax./p.c.l.	18	345	85	-
Katberg	(9)	pl. for.	12	18	99	12

Formation	Locality	Structure	n	$\bar{x}$	L	α
Katberg / Burgersdorp	(10)	tr. ax./p.c.l.	48	311	85	-
Katberg	(10)	flutes	3	306	98	-
Burgersdorp	(11)	tr. ax./p.c.l.	24	286	58	-
Burgersdorp	(11)	rib and fur.	19	228	87	-
Katberg	(11)	tr. ax./p.c.l.	24	340	85	-
Katberg	(12)	tr. ax./p.c.l.	16	356	99	-
Katberg	(12)	pl. for.	5	24	95	10
Katberg	(12)	pl. for.	10	94	98	11
Katberg	(12)	pl. for.	6	18	99	14

(1) (3) etc.	Map reference of stratigraphic section
tr. ax.	Axes of trough cross-bedded units
p.c.l.	Primary current lineation
concr.	Orientated concretions
pl. for.	Foreset azimuths of planar cross-bedded units
rib and fur.	Rib and furrow
flutes	Flute casts
assym. ripp.	Assymetrical ripple marks
n	Number of readings
$\bar{x}$	Vector mean (degrees off TN)
L	Vector strength (percent)
α	Average dip of planar foresets

SYMBOLS

g	=	accel. of gravity
ρ	=	mass density
μ	=	dynamic viscosity
ν	=	μ/ρ = kinematic viscosity
γ	=	ρg = specific weight
γ_s	=	specific weight of particle
γ_f	=	specific weight of fluid
d_s	=	diameter of particle
β	=	Shield's beta (ratio obtained from Shield's graph)
d	=	grain size of sediment
D	=	stream depth
R	=	hydraulic radius (nearly equal to average stream depth)
W	=	channel width
A	=	channel cross-sectional area
F	=	W/D
P	=	sinuosity of stream
M	=	percent of silt and clay in channel
V, $\bar{U}$	=	average (stream) velocity
Re	=	Reynold's Number
Fr	=	Froude Number
S	=	slope or stream gradient
n	=	Manning's n (coefficient of bed roughness)
τ_o	=	shear stress
$\tau_o V$	=	stream power
k	=	Von Karmen's constant (total roughness of stream elements)
f	=	Darcy-Weisbach coefficient of friction
Q_s	=	sediment discharge
Q_w	=	water discharge
Q_m	=	mean annual discharge
Q_{ma}	=	mean annual flood
Q_b	=	bankfull discharge
L	=	stream meander wavelength

IV. PETROLOGY

A. APPROACH

Conventional transmitted and reflected light microscopy, later backed up by electron microscopy, techniques were used. During the preliminary thin section examinations it became immediately apparent that diagenetic silicification was a dominant process in the lithification of Beaufort Group sandstones. Scanning electron microscopy confirmed this. Hundreds of grains from 22 Beaufort sandstones taken from the study area were examined with the TV-Scan Accessory of the SEM. All observed quartz grains displayed secondary overgrowths. This phenomenon was strongly pronounced in those samples from the Katberg Sandstone. In many cases grains were estimated to have been enlarged by more than 50%. Figure 31 shows different phases of secondary silica overgrowth. Substantial enlargement of detrital quartz can be seen in figure 32 a. In some cases solution and secondary replacement dominate. Considering such diagenetic effects, the validity of conventional microscopic modal and grain size analyses is seriously questioned. Selley (1976, p. 98) states that extensive secondary quartz cementation effectively invalidates all modal analyses of sandstone composition.

An attempt was made to examine and evaluate grain surface textures with the SEM. Grains from known environments were placed on a stub grid and relocated on the TV-Scan Accessory. Figure 32b shows a rounded quartz grain from aeolian sandstone of the Clarens Formation (Cave Sandstone), and figure 32d is a photomicrograph of a quartz grain from bedload sand of the present day Fish River.

Figure 32 c shows well rounded quartz grains from suspected aeolian sandstone layers situated in the upper parts of the Katberg Sandstone at localities (1), (2) and (3) on the geological map. Original surface textures were found to be obliterated by diagenetic effects, but this secondary replacement often merely encases the original grain (Fig. 31b) and is sometimes indicative of former grain morphology.

The Scanning Electron Microscope used on loose grains extracted from some bands, is a Jeol model JSM -U3 with TV scan accessory, enabling rapid examination of many grains. Grains were mounted on a stub

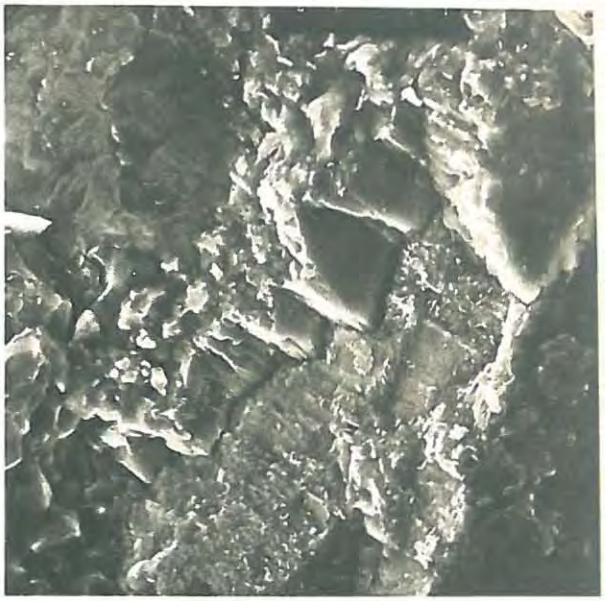

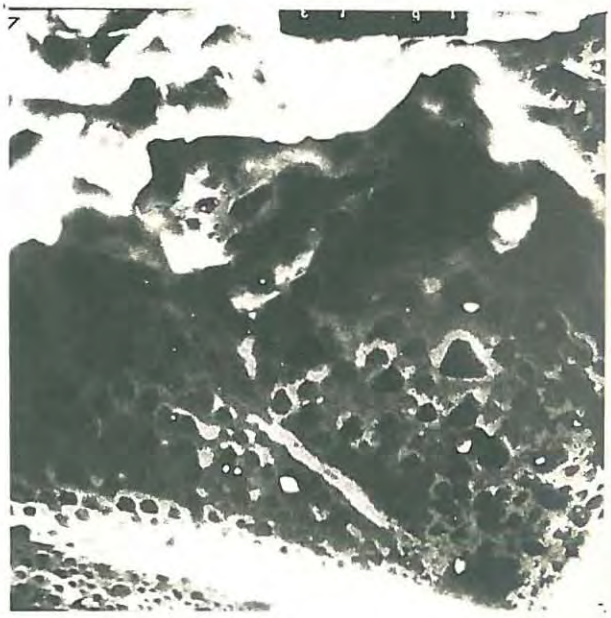

Fig. 31 a - d SEM micrographs showing diagenetic effects on quartz grains. Figs. a - c display substantial secondary silica growth, notice heavy silica plastering in c. Quartz cleavage pits (a solution effect) can be seen in d. (Magnifications a : 1 000 x, b and c : 2 000 x, d : 3 000 x)

32 a Secondary silica overgrowth, notice pyrimidal faces of new quartz growth (Magnification 300 x).

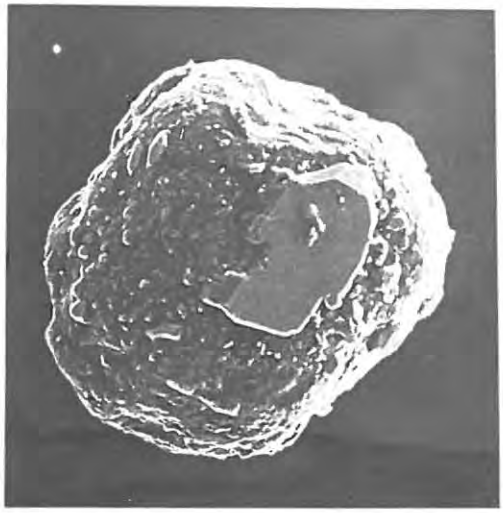

32 b Well rounded quartz grain from aeolian sandstone of Clarens Formation, notice euhedral secondary quartz appendages. (Magnification 400 x)

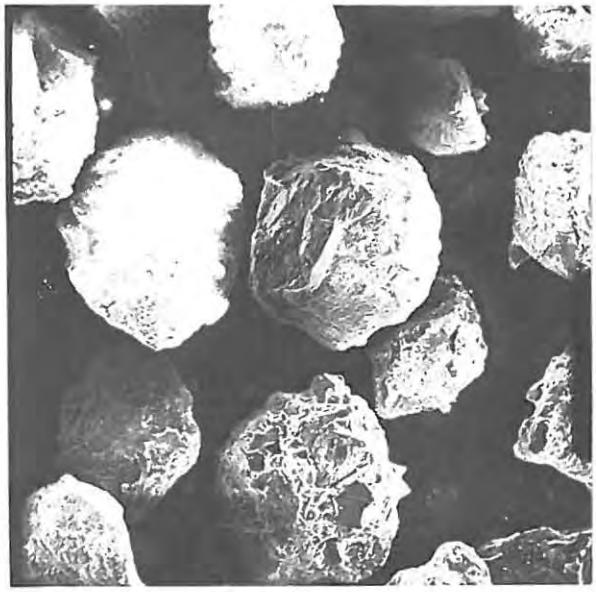

32 c

Similar to b, from suspected aeolian layers of the Katberg Sandstone at Katberg Pass (1), (2). (Magnification 150 x)

32 d

Mechanical rills of dynamic fluvial environment on quartz grain from bed of Fish River. (Magnification 3 000 x)

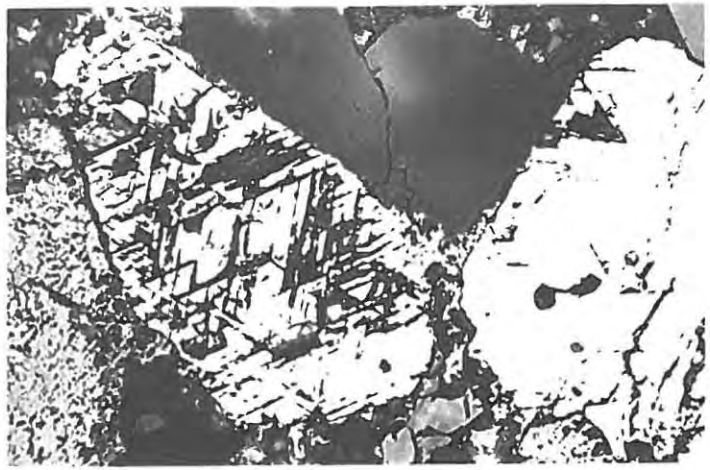

Fig. 33 a Widmanstatten texture in Katberg Sandstone titanomagnetites, grain at right almost completely martitized. Porous grain at top centre is ilmenite shrouded by cloud of leucoxene. Reflected light micrograph, magnetite grains approx. 100 microns in diametre.

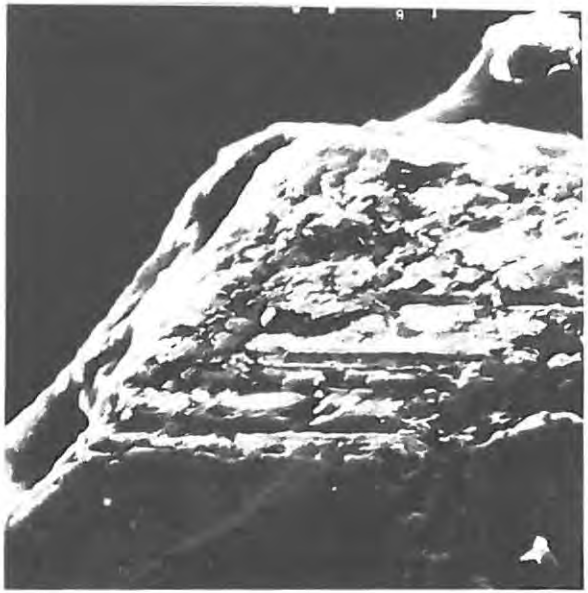

Fig. 33 b SEM micrograph of detrital titanomagnetite grain showing (111) alteration. (Magnification 4 000 x)

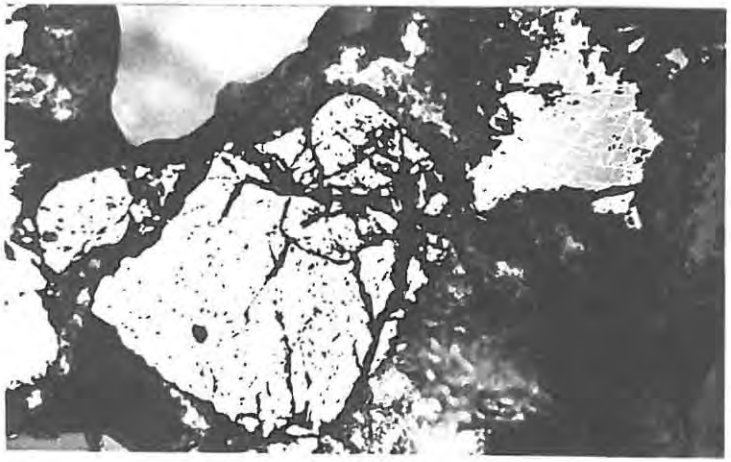

Fig. 33 c Reflected light micrograph of maghemite grain (higher reflectivity) alongside unaltered magnetite grain. Maghemite grain 100 microns in diameter.

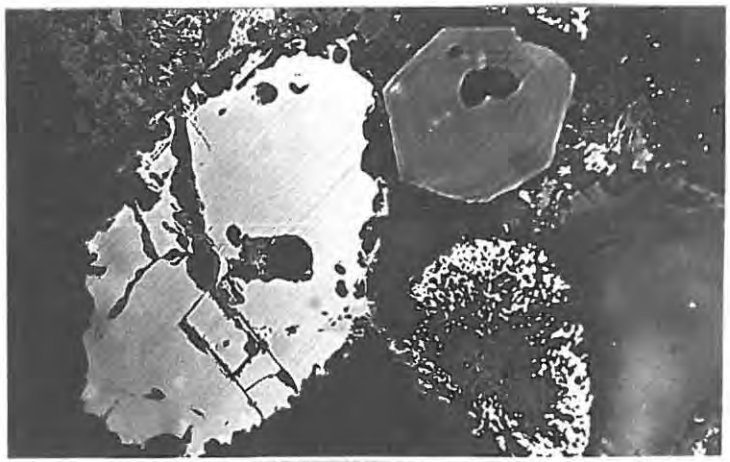

Fig. 33 d Reflected light micrograph of possible primary goethite grain (large metallic grain). Notice secondary quartz, euhedral grain at top right. Goethite grain 150 microns long.

containing cellotape adhesive and coated with gold, then sprayed with conducting film aerosol to eliminate charging (a type of fluorescence). This machine is housed at the Electron Microscopy Unit at Rhodes University.

Grains from the dark heavy mineral bands of the Katberg Sandstone were examined in thin section and polished mounts with conventional reflected light microscopy, and then with the Electron Microprobe. In the last case partial chemical analyses were carried out on the opaque phases so that thermometric predictions could be made on provenance rocks using Fe/Ti ratios of titanomagnetites.

B. ORE MICROSCOPY

Reference data for this section was obtained from Uytenbogaardt and Burke (1971) and Prof. H V Eales (pers. comm., 1978). The section deals mainly with the opaque phases from the heavy mineral bands and although most of the preliminary identifications were done by this most satisfying method, descriptions and plates will be kept to a minimum. The main phases within the opaque bands in order of abundance are magnetite, goethite and its polymorph lepidocrocite, maghemite, hematite, ilmenite and rutile. Rutile is included in this group because it seems to be associated with magnetite.

Many criteria were considered in the identification of the above phases, however, reflectivity was found to be the most reliable for less altered grains. Measurements were made using monochromatic (sodium) light. This was done to avoid the inconsistencies obtained using white light.

The most striking observation was the paucity of ilmenite as this is usually a fairly robust species. In addition, reflectivity values very close to that for pure magnetite (21% at 589 nm) were obtained on the Katberg magnetites. An average R value of 20,4% at 589 nm was obtained on over 50 typical grains. Drift off this value was ±1%. Higher values were noted in some cases (but less than for hematite), due to the presence of fine martite lamellae, but these were not considered.

In the light of these reflectivity values it may be assumed that the magnetites are lean in titanium and indeed quite pure. Virtually all observed magnetite grains display a prominant Widmanstatten Texture (triangular crosshatch pattern), see figures 33a, 33b, and this is due to martitization along (111) cleavages with subsequent alteration. It is possible that at least some of this (111) martitization may be a eutectic feature producing the (111) lamellae in the first place. Martitization (alteration of magnetite to hematite) is widespread and it is rare to find a magnetite grain not containing this species. In many cases complete martitization of magnetite has taken place. (Fig. 33a)

Maghemite (isometric magnetic Fe_2O_3), which has a relatively high (26%) reflectivity and is distinguished by its bluish white colour and isotropic character, was noticed occasionally. (Fig. 33c)

Goethite and lepidocrocite are present mostly as crypto-crystalline masses, as groundmass cement and in partly recrystallised clusters. Blotches containing a core of goethite surrounded by a colloform rim of lepidocrocite and manganese rich minerals were also noticed. There iron hydroxides display a variety of internal reflection colours. Occasionally brighter (R = 20%) uniform grains with a bluish tint, and an even tan brown internal reflection were seen (Fig. 33d). These may represent primary goethite.

Ilmenite, as mentioned earlier, is relatively scarce. Where it does occur, it is usually as a porous centre surrounded by a diffused cloud of, presumably, leucoxene (Fig. 33a). Rutile occurs as small euhedral crystals displaying strong nicotine coloured internal reflection. This mineral was seen mainly in the magnetite rich bands and is presumably secondary in origin and possibly formed as a paramorph of anatase from the breakdown of ilmenite.

C. MICROPROBE STUDY

1. Introduction and specifications

Although many of the observations of the preceeding study were substantiated with this method, it does not mean that where microprobe

analyses are possible, conventional ore microscopy is unnecessary.

This sort of study would not have been possible without prior microscopic examination. For example, martitized magnetite grains would have been indistinguishable from their relatively unaltered counterparts once the specimen was carbon coated. Another example is the case of goethite and lepidocrocite; the microprobe does not distinguish between polymorphs. The microprobe deals with element distribution and concentration, but yields little information on structure, Eales (pers. comm., 1978). The method used for the microprobe analyses was as follows.

The specimens containing typical heavy mineral bands were polished with the usual diamond grades, viz., 6, 3 and 1 micron, and finally with gamma alumina.

After a thorough investigation using conventional ore microscopy techniques, during which the main opaque phases were identified, low power photomicrographs were made of selected areas. Certain grains were also microindented with a Vickers diamond. This, together with the micrographs, facilitated relocation of these key areas in the optics of the microprobe. Grains with predetermined reflectivity which was found to be consistent for a particular phase were then marked on the photographs. The individual grains of known reflectivity were then analysed for iron and titanium. With the electron beam very slightly defocused to 5 microns, counts were carried out over 10 second intervals. As soon as consistent count rates were established for the various phases of known reflectivity, one hundred opaque mineral grains representing the main phases were probed and analysed for Fe and Ti.

The microprobe on which the analyses were done is a Cambridge Mark V Electron Probe Micro-analyser belonging to the Geology Department at Rhodes University, Grahamstown. The machine was operated at 20 kV accelerating voltage and the specimen current was 30×10^{-9} amps. All specimens, polished thin sections and polished circular mounts were carbon coated.

2. Results

Since the main object of the exercise was to determine the titanium percentage of the magnetites, the probe was set up to analyse for iron and titanium. The standard used for iron was synthetic magnetite giving an average count rate of 67 400 over 10 seconds. That for titanium was a kimberlite ilmenite with a value of 28 000. While plotting the measured count rates of iron and titanium for each grain, it soon became evident that certain class intervals corresponding to the main ore phases would become apparent (Fig. 34). Typical count rates for magnetites were Fe : 60 000, Ti : 3 500. Class intervals for some of the other phases are marked on the diagram.

N.B. The Faraday cage was constantly returned to for beam optimization, thereby eliminating any errors or drift relating to the results.

3. Data processing

Raw count rates from the probe were refined using the Bence-Albee correction routine (1968), employing the α-factors of Albee and Ray (1970). The corrections were applied using the computer program HVE mk II in the Department of Geology at Rhodes University.

The program refines cation values using an optional step inserting oxygen into the equation for calculating α-factors, i.e., oxygen is considered an X-ray absorber in the case where Fe_2O_3 is known to be present, thereby introducing excess O_2 over the amount indicated by FeO. There is a subsidiary program that does redistribute Fe between FeO and Fe_2O_3 on the assumption that the formula is that of stoichiometric spinel. TiO_2 is assigned to ulvospinel. Totals here are expected to be less than 100% because no analyses were carried out for other important elements, notably Mg, Al, Cr, Ni, V and Mn. An example is given below of the initial percentages calculated by the program HVE mk II for a typical grain of Katberg magnetite, and after the secondary refinement where Fe is assigned to ferrous and ferric iron.

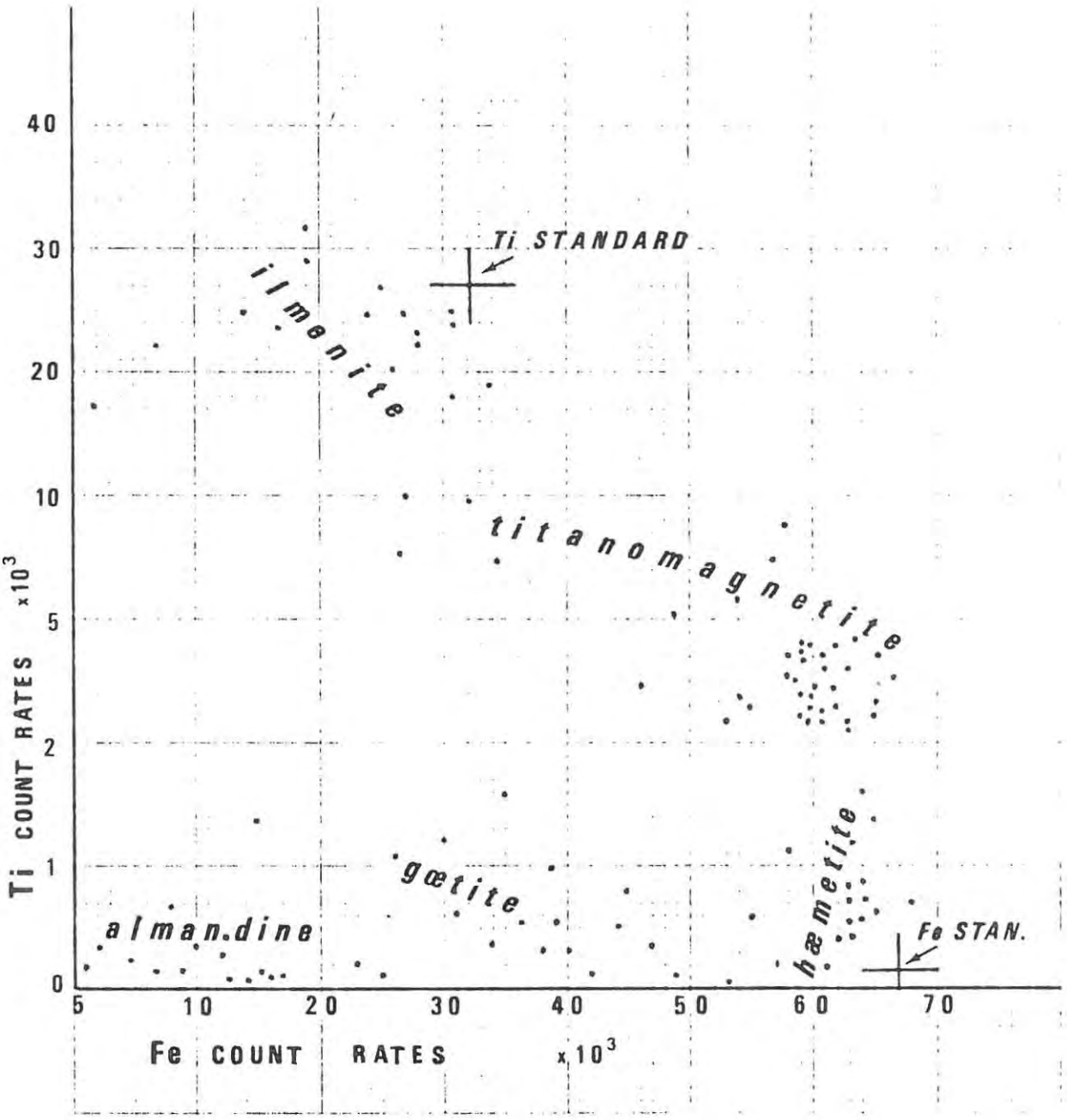

Fig. 34 Graph showing fields (count intervals) of main heavy mineral phases in Katberg laminae. Each point represents an integrated ten second microprobe count.

Sample KH 3 grain 13. Count rates Fe 61,192 : Ti 3,521

Provisional oxide %		Recalculated oxide %
TiO_2	5,98	6.07
FeO	83,24	35,32
Fe_2O_3	-	54,24
Total	89,21	95,63

D. SANDSTONE PETROGRAPHY

As stated previously, modal and grain size analyses are not regarded as being of much value in the present study, however for the purpose of comparison with other Beaufort Group workers, petrographic analyses of this kind were done.

1. Grain size analysis

The method used is quick and straightforward. The diameter of the microscope field is calibrated and the number of grains cut by the crosshairs are counted. The average grain diameter for each observation is obtained by dividing the total number of grains along the two traverses into twice the measured diameter of the field. Twenty observations were carried out on each slide, and overall averages per slide computed. Twenty-six slides were used from samples representing all three formations. This is virtually identical to the method outlined by Selley (1976, p. 13). Once averages were obtained, Friedman's (1958) thin section phi-correction routine was employed to convert to equivalent seive sizes. The results were plotted against the lithofacies whence the sample originated (Fig. 35). Closed circles are plots for Balfour sandstones, open circles for Katberg sandstones, and X's refer to Burgersdorp sandstones.

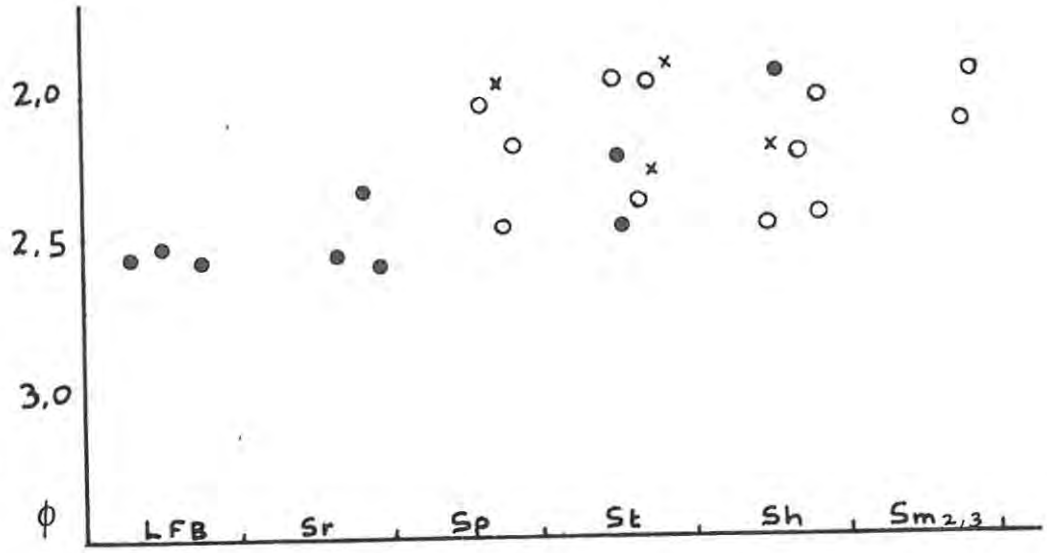

Fig. 35 Graph points of average grain diameters from sandstone thin sections (n = 400 points per slide). Open circles - Katberg sandstones, closed circles - Balfour sandstones, X's - Burgersdorp sandstones corresponding lithofacies shown at bottom.

2. Modal Analysis

The object of any modal analysis is to classify the rock primarily and thereby get an idea of its petrogenesis. Modal analyses carried out during this study are compared with those of other workers in Table 5 below.

TABLE 5 : Modal analyses of Beaufort Group sandstones

	Mineral percent of total rock					
Formation	Q	F	M	RF	n	Source
Katberg	35,5	16,1	11,5	36,9	18	Johnson (1976)
Katberg	32,7	17,1	44,8	5,3	12	Gunter (pers. comm.)
Katberg	32,4	23,6	32,3	11,7	14	This study
Burgersdorp	41,8	8,8	15,7	33,8	10	Johnson (1976)
Burgersdorp	43,5	12,7	38,5	5,3	6	This study
Balfour	18,6	28,5	13,4	39,5	23	Johnson (1976)
Balfour	24,5	23,7	43,1	8,7	8	This study

Q	quartz		
F	feldspar		
M	detrital matrix		
RF	rock fragments		
n	number of slides	Johnson	200 - 300 points/slide
		Gunter	± 1 000 points/slide
		This study	±1 000 points/slide

3. Plagioclase determinations

In addition to modal analyses, determinations of anorthite content of plagioclase feldspars were made. The following techniques were used.

(i) Universal stage method

Only normal twins which appeared to be reasonably unaltered were used, and only seven determinations from three Katberg sandstones were carried out. Normal twins are recognised when both twin sub-members show equivalent extinction when their mutual composition plane is vertical and rotated about the E - W axis (A4) of the stage. The indicatrix axes X, Y and Z are plotted on a stereogram together with the twin axis (pole of (010) plane). The stereogram is then rotated so that Y is at the centre. The twin axis plot is then located on the migration curve (Burri et al., 1967, Plate X) and anorthite content is read directly off it. The method was not very satisfactory as stereographic overlay plots did not always correspond with the anorthite curve. Plagioclase compositions ranging from An_7 to An_{52} were obtained.

(ii) Refractive indices

RI measurements were done on a number of grains from six crushed and sieved samples from the Katberg Sandstone. This method is accurate and no values exceeding An_{50} were obtained. The RI curves used were those of Chayes cited by Kerr (1959, p. 272).

(iii) Michel-Levy method

This method is illustrated and appears together with the plagioclase determination curve in Kerr (1959, p. 258). Left and right hand

rotations to extinction of alternate twin sets about the (010) composition plane are performed. The average extinction angles are referred to the Michel-Levy graph and anorthite content is read off directly.

Most of the data appearing in table 6 below were obtained by this method. Ten to fifteen grains per slide from twenty-eight Beaufort sandstones were measured.

TABLE 6 : Plagioclase compositions of Beaufort sandstones

Anorthite range	Katberg n = 14	Burgersdorp n = 6	Balfour n = 8
Albite	24%	10%	4%
Oligoclase	34%	48%	88%
Andesine	41%	42%	18%
Labradorite	1%	-	-

4. General petrographic descriptions

As mentioned earlier, the detrital character of quartz grains has been destroyed in most cases by diagenetically generated quartz overgrowths. These are apparently in optical continuity with original grains. This feature is developed in the Katberg Sandstone to the extent that some sections show completely sutured grain contacts over large areas. More commonly though, there is an approximately even spread of long and sutured grain contacts. Concavo-convex contacts of quartz grains are more common in Balfour sandstones. Virtually all quartz seen had undulose extinction. Commonly secondary quartz masses poikilitically enclose other minerals. In a few cases, only seen in Burgersdorp samples from Hobb's Hill (10), quartz grains appeared reasonably free of secondary overgrowth. In these slides grains appeared to be fairly well rounded and contacts mostly concavo-convex to long. However, secondary microcrystalline chert was well represented. Generally for all samples studied, polycrystalline quartz was common and needle-like inclusions ever present.

Feldspar of Balfour sandstones and siltstones appeared mostly to be in an advanced state of alteration. Frequently vague grain outlines could be drawn around totally kaolinised masses or cryptocrystalline clayey aggregates. Katberg and Burgersdorp feldspars, although largely altered, can be clearly distinguished from the matrix. All creamy to pinkish sandstones have reddish stained feldspars and a high percentage of opaque ore minerals and garnet. The opposite is true for greenish-grey varieties commonly associated with upper flat bed lamination. In samples with yellow and pinkish oxidized colours, massive goethite stain and oxidation halos around opaque mineral nuclei were observed. On the other hand, in grey and greenish sandstones, authigenic chloroitization was a common feature. Mottling seen in some Katberg and Balfour sandstones may be due to the presence of prehnite as is the case with some Ecca Group sandstones investigated by A A Mitchell (pers. comm., 1978). This could not be confirmed in the present study.

Symplectitic textures and irregular quartz/feldspar intergrowths (myrmekite) appeared to be common in some Katberg sandstones especially those from the cream and pinkish coloured St-sandstones of Katberg Pass (1) and (2), upper division. These are interpreted as either originating from primary gneissic and pegmatitic source rocks, or of being a diagenetic effect due to burial metamorphism, where silica is released at the expense of orthoclase at a Ca/K-feldspar boundary (Spry, 1969, p. 104). Evidence of burial metamorphism in the Katberg Sandstone is testified to by the presence of a high percentage of plagioclase in the An_{0-10} range. C J Gunter (pers. comm., 1978) confirmed that with grains from several samples he investigated from the Katberg Sandstone he obtained albitic types to the virtual exclusion of other feldspar.

Rock fragments did not appear to be as commonly present as suggested by the modal analyses of Johnson (1976). This observation is supported by that of Gunter for the case of the Katberg Sandstone. Perthite, microperthite and peristerite (indistinctly unmixed antiperthite to mesoperthite) feldspars were identified from a range of Katberg sandstones. Two Burgersdorp samples contained abundant microperthite. Gunter (pers. comm., 1978) has identified perthite from sandstones of the Katberg Pass (1) and Devil's Bellow Nek (2) area.

The only rock fragments that could be clearly distinguished as such were small clusters of muscovite or biotite and quartz or grains with symplectitic textures, especially where they had sutured boundaries on quartz grains. Pure polycrystalline quartz was not used as a criterion except where mica was associated.

V. SEDIMENTATION AND TECTONISM - CONCLUSIONS

A. GENERAL

This final chapter is modelled on the scheme of Folk (1974, p. 122) who devised a genetic code for sandstones, developed on the work of Stille, Knopf, Kay, Krynine, Krumbein and Sloss and others (Folk, 1974, p. 113). By this scheme five main points are considered in deciphering the genesis of sandstones. Within each category conclusions are based on the relevant findings during the present study.

B. FOLK'S (1974) GENETIC CODE FOR SANDSTONES

1. Tectonics of the source area, which controls erosion rate, geomorphology, etc.

2. Palaeogeology of the source terrain, which controls mineralogy.

3. Tectonics of the depositional site which controls thickness patterns, etc.

4. Depositional environment, which controls texture, sedimentary structures, etc.

5. The effects of climate and the degree of weathering in the basin and at the source.

C. TECTONIC INFLUENCES

The tectonic influences of the code fall mainly under categories 1 and 3. Tectonism in the source area and subsidence in the basin are the main considerations.

During Katberg time (L. Trias.) the tectonics of the source area were highly variable including folding, faulting and epeirogenic uplift on a regional scale. In the western part of South Africa, Lower Beaufort Group sediments are folded in perfect rhythm with Cape Supergroup sediments. In the eastern part of the country the folded

Cape Supergroup does not extend further than 27° east where it is truncated by the coastline. At that position the tectonic axis of the fold belt is roughly ESE, and when projected out to sea, would run through the old source area position of the eastern Beaufort Group. It roughly corresponds to the position of Du Toit's (1937, p. 80) Samfrau Geosyncline. Theron (1973, p. 70) is of the opinion that the Samfrau Geosyncline may not have existed that far east. The position of Karoo Supergroup source areas (a position to the south of East London for the eastern Karoo sequence), and extensions of the Cape Fold Belt are areas of great uncertainty.

Some of the formations underlying the Katberg Sandstone display the effects of folding as far north as Fort Beaufort, where they are clearly evident in road cuttings. This folding, albeit gentle, is 50 km away from the Cape Fold Belt in the south. Figure 2 of this study shows gentle synclinal to monoclinal flexing of the Katberg Sandstone along a N - S section. The dips shown in the section are regional and therefore unlikely to have been caused by dolerite intrusion. This warping is interpreted as distal effects of Cape folding which continued right through Katberg sedimentation and indeed through sediment consolidation.

Vertical epeirogenic movements in the source area with resultant block faulting of the horst and graben type may have been responsible for the generation of coarse grained arenaceous deposits along the coast around East London. These fault-bounded, pebbly sandstones have been correlated with the Katberg Sandstone (Johnson (1966), Mountain, (1974) p. 13). The latter writer reports (p. 22) that dating of these coastal faults is not all that clear, but that post Karoo-dolerite age is suggested. A minimum throw of more than 1 km is implied based on present topographic positions. This figure becomes much greater when adjustment is made for palaeoslope especially in proximal areas. It is suggested here that these faults partly delineated narrow rapidly subsiding foredeep areas during Katberg time, which filled rapidly from ephemeral stream sedimentation. A recent survey of those pebbly sandstones by Dr N Hiller of Rhodes University and the present writer showed that they were mostly upper flat-bedded and trough cross-bedded

sandstones, pebbly in places with individual lithosomes separated by pebble covered scour surfaces. The foredeep faults mentioned earlier may have remained active in post-Katberg times.

The position of the source area was said to be quite uncertain. J C Theron (pers. comm., 1978) suggested to the writer that the apex of his (1973) palaeocurrent dispersal pattern (since refined further) would be located roughly 100 km off the present southeast coast at approximately 28°E 34°S. Bed relief indicies computed for Katberg Sandstone palaeostreams of the present study area suggest a distance of 250 - 350 km from the source (Fig. 36). Miall (1977, p. 48) however, states that there are no absolute indicators that can be used to estimate proximity to source in the braided-stream environment. This should be seen as a general statement. In the special case of the Katberg Sandstone, the large clast diameter of pebbles present in the coastal fragment and their rapid size diminution 100 km inland, when considered together with the work of Theron corroborates the BRI derived figure of the present study.

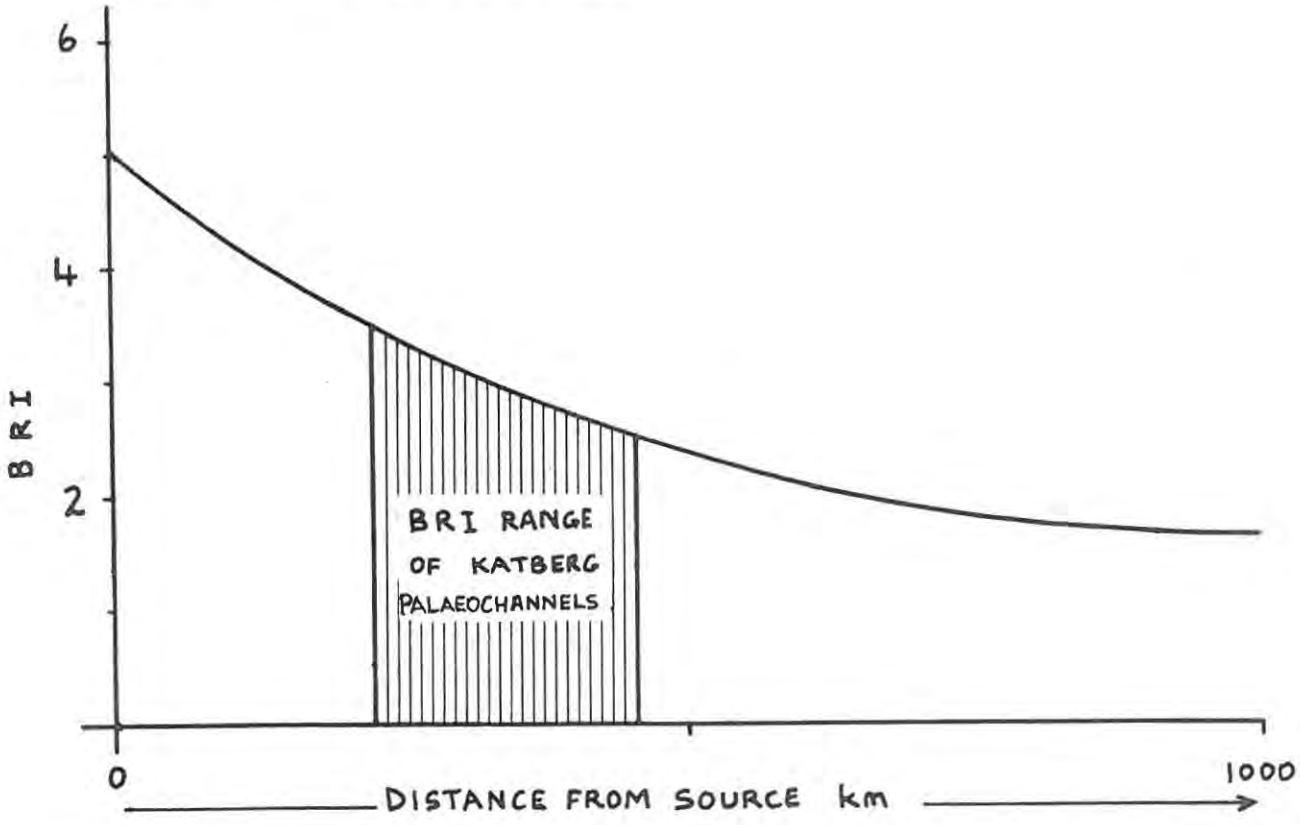

Fig. 36 Range of bed relief indicies calculated for the Katberg Sandstone. Curve adapted from data of Smith (1970) for Platte River.

That would pinpoint the source at roughly the same position as suggested by Theron or possibly a little further away from the present coastline.

Source area tectonism is reflected by the sedimentary sequences of the depositional site. Tectonic uplift of the source area will tend to raise the equilibrium profile at that end, and channel or valley fill sequences will accumulate to the new equilibrium profile (Matthews, 1974, p. 161). During Balfour sedimentation the equilibrium base was being raised very slowly and complete fluvial sequences were being deposited on a slowly subsiding plain. During Katberg time and the distally equivalent Burgersdorp Formation, source area tectonism was pronounced but interrupted. This is reflected in the numerous erosional scour surfaces interrupting sequences. An attempt was made during the present study to measure the amount of subsidence during Katberg sedimentation by measuring and totalling (sometimes extrapolating) the thicknesses of complete sequences between diastems. The figure of 1 200 metres was arrived at for the central study area (3). It is certainly not the final word on the subject as the difference between a diastem surface and one resulting from topographic differentiation in the palaeostreams could often not be spotted with certainty. Both W E L Minter and B R Turner (pers. comm., 1978) are of the opinion that the numerous erosional breaks within the Katberg sequences they examined have resulted from in channel processes rather than basin tectonics. H Geldsetzer (pers. comm., 1975), reflecting the ideas of Wheeler (1964, p. 599), suggested that the characteristic imcomplete Katberg sequences were generated by a megacycle of strong subsidence, frequently interrupted by minor uplifting pulses. This is certainly suggested by the 'weak memory' probability matrix (section E, of Chapter III) of the Katberg model.

Schwarzacher (1975, p. 57) discusses the probelm of just how reliable a record of tectonism can be produced by sedimentation. He states that not many sedimentologists would accept that an rise in water level by say 2 - 3 cm would lead to a clear cut change from non-deposition to deposition. In the case of the Katberg, diastems were considered the more regular and persistent erosional breaks. Although, the two are difficult to distinguish, a count was made along section (6) where diastems were found to be outnumbered by river differentiation breaks by a figure of at least 4 : 1.

The tectonic framework of the Katberg-Burgersdorp depositional site is inferred to have been as follows :

A prograding sheet-wedge of sand was deposited as upper flow regime, channel fill, mostly bedload sand which, depending on source area tectonism, wedges out into vertical accretion floodplain aggradation deposits along its distal margins. The (Katberg) sandstone wedge is presently three dimensional, thickest at localities (3), (4) and (5) and wedging out to the north and east at Whittlesea and Cathcart and to a lesser extent at Katberg Pass (1). Floodplain aggradation (Burgersdorp) deposits were more extensive at times of decreased source uplift. These positions in space and time are indicated by the southward penetrating thin red shale wedges (see Fig. 2) of Burgersdorp shale into Katberg sandstone. The classic concept of transgression and regression has been avoided as the terms carry no connotation concerning the tectonic nature of the dynamic event (Matthews, 1974, p. 71). The geological map (at the back) shows the areas of furthest progradation of Katberg sandstone and most widespread aggradation of Burgersdorp shale. Within the two main cycles of progradation of Katberg sandstone and aggradation of Burgersdorp shale, small scale opposite events occur (see Figs. 2 and 4). These are represented by upper flow regime channel fill sands and crevasse-splays of the Burgersdorp in the eastern study area, and ripple cross-laminated siltstones and Fl or Fm deposits of Lower Chilton (6) and elsewhere in the Katberg Sandstone.

D. SOURCE PETROLOGY

The sandstones of the Beaufort Group in the study area can be classified as arkosic wackes according to the scheme of Dott (1964, p. 629). They are generally feldspathic sandstones in more common language. (pettijohn, 1975, p. 214). Deformation of quartz grains seen as undulose extinction and some polycrystalline aggregates showing cataclastic effects, indicate a metaquartzite, quartz-schist or granite-gneiss parentage. The peristerites and mesoperthitic to antiperthitic feldspars seen in Katberg sandstones indicate a granulitic/charnockitic source (Spry, 1969, p. 182). Pittman (1970, p. 595) states that mesoperthite is known to occur only in granulite. This granatoid type was therefore probably represented in the provenance area. Fe/Ti ratios obtained from the microprobe study of

Katberg titanomagnetites indicate temperatures of formation in the region of 560 - 650°C. This figure is based on those obtained by Buddington and Lindsley (1964, p. 333) for granitic and pegmatitic rocks with similar titanomagnetite compositions. Katberg titanomagnetites are lean in TiO_2 which is presumably present as ulvospinel (Fe_2TiO_4), considering the relative paucity of ilmenite in the heavy mineral bands. The thermometric predictions made on Katberg source rocks, based on the weight percentage of TiO_2 in the magnetites, accord with the other petrographic observations. According to Buddington and Lindsley's Fig. 7, titanomagnetites of this range (up to 6% TiO_2) originate in a range of rocks from granite pegmatite, through hornblendite, diorite, hornblende and biotite mesoperthitic granites and some granophyre.

The microcline and orthoclase (mostly as perthite) seen in some slides, and symplectitic textures of these and others, may owe their origin partly to this last rock type. C J Gunter (pers. comm., 1978) reports seeing anorthoclase in some Katberg sandstones. Only two feldspar grains with moderate 2V angles were seen during the present investigation. This species is either rare in Katberg rocks or has been kaolinized beyond positive identification. Anorthoclase is indicative of a high temperature alkaline volcanic parentage.

Pebbles retrieved from St-sandstones at Katberg Pass (1) and (2), are an assortment of red granite, felsite, granite prophyry, gneiss, pegmatite quartzite and possibly epidosite. It is not impossible that at least some of these, the larger ones perhaps, were derived from erosion of Dwyka Tillite. However, Mountain (pers. comm., 1978) regards the two sets of clasts to be of different assemblages; J C Theron (pers. comm., 1978) rejects the Dwyka source on the grounds that the tillite would almost certainly have been covered by a substantial thickness of younger sediments.

E. DEPOSITIONAL ENVIRONMENT AND CONCLUSIONS

Throughout Karoo sedimentation, Eastern Gondwanaland apparently remained intact. Africa's position in relation to Antarctica is still uncertain. Truswell (1977, p. 186) points out that any fits between Africa and Antarctica are essentially geometric. Numerous

workers including Mountain (1939, p. 168), Johnson (1966, 1976), J C Theron (1973, p. 61), I C Rust (1973, p. 547), Kingsley (1977, p. 243) and Turner (1978, p. 171) favour a south-easterly source for the Karoo sequences they have studied. Palaeocurrents of the present study indeed accord with their views.

The global position of Africa in Permo-Triassic times, and the elevation of this southern source area would both affect the palaeoclimate and thus the sedimentation during Beaufort time. Anderson and Schwyzer (1977, p. 233), place the southern part of Africa between 50°S and 60°S in their Gondwana reconstructions of the Permo-Triassic. Assuming the planetary climatic belts to have been roughly the same as today, (since the earth has remained in the same orbit around one sun), that would position the southern Beaufort source areas at a latitude similar to present day Tierra del Fuego. There mountain slopes commonly receive in excess of 5 000 mm of rain per year, and glaciers are common. Flint (1961, p. 151) states that evidence of palaeoaltitude is likely to be elusive. Turner (1978, p. 173) gives a possible altitude figure of 4 200 m for some provenance areas during Molteno (Upper Triassic) sedimentation. Notwithstanding violent uplift in the source terrain since Lower Triassic times, these high peaks must have existed at similar elevations during Katberg sedimentation. The resultant sequences, however, do not corroborate this hypothesis. B E Lock suggested to the present writer that the Beaufort sedimentation represents a molasse type sequence. Miall (1978, p. 1616) writes of molasse that the sedimentological characteristics are distinctive, but that such facies are not found exclusively in molasse sequences. This appears to be the case with the south-eastern Beaufort Group in general. Van Houten (1973, p. 1973) defined molasse as a thick detrital sequence that accumulated in a late orogenic foredeep on the flank of a craton, and was fed with debris eroded from an uplifted range and its associated thrust sheets. The only Beaufort sediments of this south-eastern part of the country fitting that definition, are those downfaulted alluvial fan deposits presently being studied by Hiller and Stavrakis (in preparation). Excluding these, the remaining Karoo sequences were accumulated on more regular extensive floodplains subsiding differentially in time and space. The undeniable fact that laterally juxtaposed Beaufort sequences cannot be stratigraphically correlated testifies to this.

During Balfour sedimentation the climate was probably temperate to humid. Source area slopes and proximal areas may have been wet, with a local base level already established. Petrographic evidence in the form of badly decomposed goethite stained feldspars and a high percentage of detrital matrix, indicates this. The colours of Balfour sediments are mostly those of a reducing environment. However, colour alone does not give a clear picture of climatic conditions at the time of deposition (Nairn, 1961, p. 4). Amphibia, reptilia, fishes, fresh water molluscs and abundant vegetal growth characterise the fauna and flora of that geological period. This abundance of life seems to preclude very harsh (very dry or cold) conditions.

The changeover from Balfour proper to Palingkloof and consequently to Katberg sedimentation took place under an arid climate which entrenched itself throughout Katberg times and extended regionally into the area of Burgersdorp sedimentation. The diminution to virtually nothing of fauna and flora in the area of Katberg sedimentation reflects an hostile, arid, climate with almost no source of standing fresh water. In the distal parts of the L. Triassic Beaufort basin, water was available where the ephemeral Katberg streams debouched into shallow lakes which frequently dried out. This latter view is supported by the presence of mud cracked surfaces in virtually every good exposure of red Burgersdorp shale seen. Calcareous duricrust layers are present within shale flaked (from dessication) beds of Burgersdorp sediments at Stubbs Hill (12), Whittlesea. These are interpreted as having the characteristics of ancient playa lake accumulations such as those described by Russell (1885, pp. 81 - 86). The brown and red colours of Burgersdorp shales, together with a lack of organic debris, points to subareally exposed flood-plain aggradation depostis in a dry climate (Allen, 1970, p. 143).

The intense development of calcareous concretions (cornstone) in parts of the Katberg Sandstone either indicate penecontemporaneous formation and circulation of brines in an arid climate (Allen, 1960, p. 97) or late diagenetic carbonatization due to pH fluctuation (Deegan, 1971, p. 357). The former mechanism is favoured here since carbonate matrix can be seen to represent most of the ground mass. There is no preferential replacement of other minerals by carbonate. Vague contortions are commonly present in the more mixed cornstone

varieties. These may be due to slumping within the original sandbody as a result of adjustment within possible thixotropic sand (quicksand) patches, such as those described by Williams and Rust (1969, p. 657). The more common sandstone concretions, often seen orientated, are most likely diagenetic and appear to be related to bedding planes in Sh-sandstone. Pettijohn et al. (1972, p. 49) confirm this observation.

A point worthy of note in any environmental analysis is the mode of origin and content of detrital magnetite and ilmenite of the sediments. Miller and Folk (1954, p. 338) showed that the formation of redbeds depends primarily on the presence of igneous or metamorphic source rocks within which magnetite and ilmenite are formed. They contend that under reducing conditions these two minerals readily disappear and cannot be reconstituted. Redbed sediments must have originated in oxidizing environments and since their character is dependant on the presence of magnetite and ilmenite, at no time during their depositional history could they have passed through a reducing environment.

The views of Miller and Folk are partly supported by petrographic and microprobe evidence of the present study. Opaque grains from oxidized Katberg feldspathic sandstones were probed and found to be mostly titanomagnetite, martite, maghemite, goethite and ilmenite. There is a distinct association of almandine (pink coloured) garnet with these opaque minerals. Virtually no opaques or pink garnet were seen in Balfour sandstones, interpreted as having formed under reducing conditions. Petrographic observations showed the trends very clearly : abundant opaques and almandine are associated with oxidized usually pinkish sandstones, very little of the above is associated with greenish-grey chlorite rich sandstone.

On the other hand, Lojoie and Chagnon (1973, p. 91) state that both red and green claystones studied contained $\pm$ 8% ferric oxide. They maintain that the green colour results from reducing conditions and the red from a paralic oxidizing environment. During the present study, thin sections of finely laminated (1 mm divisions) sandstone from the Katberg Sandstone (11) were scanned for iron with the electron microprobe. The beam was defocussed to 20 microns and traverses were carried out. A cyclicity was obtained on graph printout, but this

did not always coincide with the spacing of the laminae. Peaks were obtained more often (ratio of 2,5 : 1) within pink laminae. Prof. H V Eales (pers. comm., 1978) suggested to the writer that the colour may merely reflect the oxidation state of iron minerals, and that the peaks represent fairly regular distribution of opaque minerals in the sandstone as a whole. T R Walker (1967, p. 353) contests the theory that sedimentary redbeds testify to the presence of an arid climate. He states that climate might in fact be irrelevant since iron oxide does not need to migrate through pore waters, as it can be transferred from within the clay lattice to the exterior of the grain. He found that as little as 0,1% hematite was sufficient to render the sediments bright red. The red colour in Katberg and Burgersdorp sandstones comes mainly from detrital clay particles and weathered opaque minerals. All things considered, however, the evidence for an arid climate during Katberg/Burgersdorp times seems indisputable.

Considering the river systems which existed during Beaufort time, the palaeochannel analysis and detailed logging of short typical sequences give a good idea as to their type. Much can be read from the palaeocurrent analysis too. Miall (1974, Fig. 1; 1976, p. 463) discussed palaeocurrent variance and classified it according to magnitude and the principal processes which bring it about. The greatest variance is Rank 1 due to differences in orientation between entire river tracts, and the smallest is Rank 5 generated within bars. Katberg palaeocurrents are mostly Rank 4 and 5 types, indicating that streams had low sinuosities and unimodal bedforms such as the in-channel dunefields of Katberg Pass (1) and (2), Elandsberg (3) and Woodburn (4), and shooting flow stratification surfaces endemic to the Katberg Sandstone. Burgersdorp palaeocurrents are Rank 1 - 3 types mainly. This is due to directional changes in channels brought about by frequent crevasse-splay. Sh-sandstones with very abrupt basal contacts onto thick red shale are the rule with Burgersdorp sequences. These crevasse-splay deposits do not seem to be controlled by the main palaeochannel flow.

Balfour palaeostreams have high sinuosities (2 - 2,5) and palaeocurrent variance is mainly due to directional changes in channels and parts of channels. Large variances in primary current lineations may be due to the combined effects of bar head and bar platform currents (see

Bluck, 1971, p. 131). The sequence of bedform structures displayed by Balfour palaeostreams are typically those of meandering streams accreting thick valley fill sequences. Allen (1970, p. 142) states that within such deposits flat beds occur in any part of the point bar and frequently alternate with ripple cross-bedding. The interpretation of these structures appears in figure 25a.

Meandering streams have more cohesive bank material and channels become entrenched. Valley fill deposits generally have good preservation potential and full A - E sequences are preserved. The Burgersdorp and Balfour matrices are of the strong memory type (i.e., highest positive values of probability matrix clustered along principal diameter) and are interpreted (the latter especially) as being valley fill models.

The weak Markovian tendencies (weak memory) of the Katberg probability matrix (see Chapter III) are interpreted as rapid development and shift of bedforms (bars and flatbed channel sands) with numerous intervening erosional states. Consequently, large portions of sequences are not represented in the stratigraphic record. The strong memory of transition C - A bears witness to the frequent erosional breaks during channel fill or immediately succeeding drape development. This is typical of the flashy sedimentation of constantly avulsing braided streams. Within the braided regime the largest streams, that is those with greatest capacity, flowed at Katberg Pass (1) and (2), and although they flowed in the transitional regime of flow (Table 1) their apparent increased competency is attributed to their greater discharge coupled with fairly high velocities. In comparison, most other Katberg palaeostreams are indicated to have had wide shallow channels characterised by swift flow and mostly upper flow regime flatbed sedimentation. The palaeostreams of the Katberg Sandstone and their deposits resemble best the Platte River braided stream model established by Smith (1970) and compared with other classic types by Miall (1977, p. 47). The conceptual scheme showing typical Katberg sequences (Fig. 25) gives the interpretation of conditions of deposition. Katberg palaeostreams have without doubt the classic characteristics of modern braided streams. Constant channel switching (avulsion), transverse bar formation and dissection, deposition of bedload material, lack of ripple cross-lamination and deposition of mud drapes are amongst the main criteria. These abound in sequences of that arenaceous formation.

REFERENCES

A C S N (American Commission on Stratigraphic Nomenclature), 1961. Code of Stratigraphic Nomenclature. A.A.P.G. Bull., 45 : 645 - 660.

AGNEW, S., 1958. The landforms of the Hogsback area in the Amatola range. Fort Hare Papers, 2.

ALBEE, A.L. and RAY, L., 1970. Correction factors for electron probe microanalysis of silicates, oxides, carbonates, phosphates and sulphates. Analyt. Chem., 42 : 1408 - 1414.

ALLEN, J.R.L., 1960. Cornstone. Geol. Mag., 97 : 43 - 48.

ALLEN, J.R.L., 1963. The classification of cross-stratified units, with notes on their origin. Sedimentology, 2 : 93 - 114.

ALLEN, J.R.L., 1965 . The sedimentation and paleogeography of the Old Red Sandstone of Anglesea, North Wales. Yorkshire Geol. Soc. Proc., 35 : 139 - 185.

ALLEN, J.R.L., 1967. Depth indicators of clastic sequences. Marine Geol., 5 : 429 - 446.

ALLEN, J.R.L., 1968. Current Ripples. North-Holland, Amsterdam. 433 pp.

ALLEN, J.R.L., 1970. Physical Processes of Sedimentation. Allen and Unwin, London. 248 pp.

ANDERSON, J.M. and SCHWYZER, R.V., 1977. The biostratigraphy of the Permian and Triassic. Part 4 - Palaeomagnetic evidence for large scale intra-Gondwana plate movements during the Carboniferous to Jurassic. Trans. geol. Soc. S. Afr., 80 : 198 - 211.

BENCE, A.E. and Albee, A.L., 1968. Empirical correction factors for the electron micro-analysis of silicates and oxides. Jour. Geol., 76 : 382 - 403.

BLATT, H., MIDDLETON, G.V. and MURRAY, R., 1972. Origin of Sedimentary Rocks. 634 pp. Prentice-Hall, New Jersey.

BLUCK, B.J., 1971. Sedimentation in the meandering River Endrick. Scott. J. Geol., 7 : 93 - 138.

BOOTHROYD, J.C., 1976. Braided streams and alluvial fans. In : Hayes, M.O. and Kana, T.W. (Editors), Terrigenous Clastic Depositional Environments. A.A.P.G. Field Course. Technical Report No. 11 - CRD Coastal Research Division, Dept. of Geology, Univ. of South Carolina. pp. 17 - 26.

BOOTHROYD, J.C. and ASHLEY, G.M., 1975. Process, bar morphology, and sedimentary structures on braided outwash fans, northeastern Gulf of Alaska. In : Jopling A.V. and McDonnald, B.C. (Editors), Glacio-fluvial and Glaciolacustrine Sedimentation. SEPM Spec. Publ., 23 : 193 - 222.

BRIGGS, L.I. and MIDDLETON, G.V., 1965. Hydromechanical principles of sediment structure formation. In : Middleton, G.V. (Editor), Primary Sedimentary Structures and their Hydrodynamic Interpretation. SEPM Spec. Publ., 12 : 5 - 16.

BUDDINGTON, A.F. and LINDSLEY, D.H., 1964. Iron-titanium oxide minerals and synthetic equivalents. J. Pet. 5 : 310 - 357.

BURRI, C., PARKER, R.L. and WENK, E., 1967. Die Optische Orientierung der Plagioklase. Birkhauser verlag.

CLARK, J., 1962. Field interpretation of redbeds. Geol. Soc. Am. Bull., 73 : 423 - 428.

COLEMAN, J.M., 1969. Brahmaputra River : channel processes and sedimentation. Sediment. Geol., 3 : 129 - 239.

COTTER, E., 1971. Paleoflow characteristics of a Late Cretaceous River in Utah from analysis of sedimentary structures in the Ferron Sandstone. J. Sed. Pet., 41 : 129 - 138.

DEEGAN, C.E., 1971. The mode of origin of some late diagenetic concretions from the Scottish Carboniferous. Scott. J. Geol., 7 : 357 - 365.

DE RAAF, J.F.M. and BOERSMA, J.R., 1971. Tidal deposits and their sedimentary structures (seven examples from Western Europe) : Geol. en Mijnbouw, 50 : 479 - 504.

DE SWARDT, A.M.J: and BENNET, G., 1974. Structural and physiographic development of Natal since the Late Jurassic. Trans. Geol. Soc. S. Afr., 77 : 309 - 322.

DOTT, R.H., Jr., 1964. Wacke, Graywacke and matrix - what approach to immature sandstone classification? J. Sed. Pet., 34 : 625 - 632.

DURY, G.H., 1969. Hydraulic geometry pp. 146 - 156. In : Chorley, R.J. (Editor). Introduction to Fluvial Processes. 218 pp. Methuen and Co. Ltd.

DU TOIT, A.L., 1937. Our Wandering Continents. Oliver and Boyd Edinburgh.

FLINT, R.F., 1961. Geological evidence of cold climate, pp. 140 - 155. In : Nairn, A.E.M. (Editor). Descriptive Palaeoclimatology 380 pp. Interscience Publishers Ltd. New York.

FOLK, R.L., 1974. Petrology of Sedimentary Rocks. 182 pp. Hemphill Publishing Co. Austin. Texas.

FRIEDMAN, G.M., 1958. Determination of sieve size distribution from thin-section data for sedimentary petrological studies. J. Geol., 66 : 394 - 416.

HAMBLIN, W.K., 1970. X-Ray photography, pp. 251 - 284. In : Carver, R.E. (Editor). Procedures in Sedimentary Petrology, Wiley-Interscience. New York, 653 pp.

HARMS, J.C. and FAHNESTOCK, R.K., 1965. Stratification, bedforms, and flow phenomena (with an example from the Rio Grande). In : Middleton, G.V. (Editor). Primary Sedimentary Structures and their Hydrodynamic Interpretation. SEPM Spec. Publ. No. 12 : 84 - 115.

HAND, B.M., WESSEL, J.M. and HAYES, M.O., 1969. Antidunes in the Mount Toby Conglomerate (Triassic), Massachusetts. J. Sed. Pet. 39 : 1310 - 1316.

HARMS, J.C., SOUTHARD, J.B., SPEARING, D.R. and WALKER, R.G., 1975. Depositional environments as interpreted from primary sedimentary structures and stratification sequences. SEPM, Short Course No. 2, Dallas, 161 pp.

HATCH, F.H., RASTALL, R.H. and GREENSMITH, J.T., 1965. Petrology of the Sedimentary Rocks, 4th Edition. Thomas Murby and Co., London, 408 pp.

JACKSON, R.G., II, 1976. Deposition model of point bars in the lower Wabash River. J. Sed. Pet., 46 : 579 - 594.

JOHNSON, M.R., 1966. The Stratigraphy of the Cape and Karoo Systems in the Eastern Cape Province : Unpub. M.Sc. thesis, Rhodes Univ., Grahamstown.

JOHNSON, M.R., 1976. Stratigraphy and Sedimentology of the Cape and Karoo Sequences in the Eastern Cape Province. Unpub. Ph.D. thesis, Rhodes Univ. Grahamstown. 336 pp.

JOHNSON, M.R. and KEYSER, A.W., 1976. Explanatory Notes to Geological Map, 3226 King Williamstown Sheet, 1 : 250 000 Geological Series. Government Printer, Pretoria.

JOPLING, A.V., 1965. Laboratory study of the distribution of grain sizes in cross-bedded deposits. In : Middleton, G.V. (Editor). Primary Sedimentary Structures and their Hydrodynamic Interpretation. SEPM Spec. Publ., 12 : 53 - 65.

JOPLING, A.V., 1967. Origin of laminae deposited by the movement of ripples along a streambed : a laboratory study, J. Geol., 75 : 287 - 305.

JOPLING, A.V., and WALKER, R.G., 1968. Morphology and origin of ripple-drift cross lamination, with examples from the Pleistocene of Massachusetts. J. Sed. Pet., 38 : 971 - 984.

KALININ, G.P., 1968. Global Hydrology. Israel Program for Scientific Translations, Jerusalem, 310 pp.

KERR, P.F., 1959. Optical Mineralogy. McGraw-Hill, 442 pp.

KING, L.C., 1963. South African Scenery. 3rd Edition. Oliver and Boyd. Edinburgh, 308 pp.

KINGSLEY, C.S., 1977. Stratigraphy and Sedimentology of the Ecca Group in the Eastern Cape Province, South Africa. Unpub. Ph.D. thesis, University of Port Elizabeth.

KITCHING, J.W., 1977. The Distribution of the Karoo Vertebrate Fauna. Mem. No. 1, BPI for Palae. Res., University of the Witwatersrand, Johannesburg, 131 pp.

KOTTLOWSKI, F.E., 1965. Measuring Stratigraphic Sections. New York : Holt, Rinehart and Winston, Inc., 253 pp.

KRUMBEIN, W.C. and SLOSS, L.L., 1963. Stratigraphy and Sedimentation. Freeman, San Francisco, 637 pp.

LANE, E.W., 1955. The importance of fluvial morphology in hydraulic engineering. In : Schumm, S.A. (Editor), 1972. River Morphology. Benchmark Papers in Geology. Dowden, Hutchinson and Ross, Inc., Sroudsburg, Pennsylvania.

LEOPOLD, L.B. and MADDOCK, T., Jr., 1953. The hydraulic geometry of stream channels and some physiographic implications. U.S. Geol. Surv. Prof. Paper 252, 1 - 4 : 9 - 16.

LEOPOLD, L.B. and WOLMAN, M.G., 1957. River channel patterns : braided, meandering and straight. U.S. Geol. Surv. Prof. Paper 282 - B : 39 - 85.

MATTHEWS, R.K., 1974. Dynamic Stratigraphy : Prentice-Hall, New Jersey, 370 pp.

MAY, J.P., 1973. Selective transport of heavy minerals by shoaling waves. Sedimentology, 20 : 203 - 211.

McDONNELL, K.L., 1978. Transition matrices and depositional environment of a fluvial sequence. J. Sed. Pet., 48 : 43 - 48.

McKEE, E.D., 1965. Experiments on ripple lamination. In : Middleton, G.V. (Editor), Primary Sedimentary Structures and their Hydrodynamic Interpretation. SEPM, Spec. Publ. No. 12 : 66 - 83.

MIALL, A.D., 1973. Markow Chain analysis applied to an ancient alluvial plain succession. Sedimentology, 20 : 347 - 364.

MIALL, A.D., 1974. Paleocurrent analysis of alluvial sediments : a discussion of directional variance and vector magnitude. J. Sed. Pet., 44 : 1174 - 1185.

MIALL, A.D., 1976. Paleocurrent and paleohydrologic analysis of some vertical profiles through a Cretaceous braided stream deposit, Banks Island, Artic Canada. Sedimentology, 23 : 459 - 484.

MIALL, A.D., 1977. A review of the braided-river depositional environment. Earth-Science Reviews, 13 : 1 - 62.

MIALL, A.D., 1978. Tectonic setting and syndepositional deformation of molasse and other nonmarine paralic sedimentary basins. Can. J. Earth Sci., 15 : 1613 - 1632.

MIDDLETON, G.V., 1965. (Editor) Primary Sedimentary Structures and their Hydrodynamic Interpretation. SEPM, Spec. Publ. No. 12.

MILLER, D.N. and FOLK, R.L., 1954. Occurrence of detrital magnetite and ilmenite in red sediments : new approach to significance of redbeds. A.A.P.G. Bull., 39 : 338 - 345.

MINTER, W.E.L., 1978. Sedimentology of Witwatersrand Placers in the Welkom Goldfield (Resume). Unpub. handbook, Winter Field School No. 1, Welkom. Geol. Soc. S. Africa.

MOODY-STUART, M., 1966. High and low sinuosity stream deposits, with examples from the Devonian of Spitzbergen. J. Sed. Pet., 36 : 1102 - 1117.

MOUNTAIN, E.D., 1939. Pebble beds in the Lower Beaufort Series of the East London division. S. African J. Sci., XXXVI : 164 - 169.

MOUNTAIN, E.D., 1968. Geology of Southern Africa. Books of Africa, Johannesburg and Cape Town, 249 pp.

MOUNTAIN, E.D., 1974. The geology of the area around East London, Cape Province : an explanation of sheet map 3227 D (East London), 3228 C (Kei Mouth). Geological Surv. of S. Africa.

NAIRN, A.E.M., 1961. Descriptive Palaeoclimatology. Inter-science Publishers Ltd. New York. 380 pp.

O.P.E. 202, 1977. Grobbelaar, J.W. (Compiler), Simulation. Dept. of Stat. and Operations Research, Univ. of S. Africa.

PETTIJOHN, F.J., 1975. Sedimentary Rocks, 3rd Ed., Harper and Row. 628 pp.

PETTIJOHN, F.J., POTTER, P.E. and SIEVER, R., 1972. Sand and sandstone. Springer-Verlag, 618 pp.

PICARD, M.D. and HIGH, L.R., Jr., 1973. Sedimentary Structures of Ephemeral Streams. Developments in Sedimentology, 17. Elsevier, Amsterdam, 223 pp.

PITTMAN, E.D., 1970. Plagioclase feldspar as an indicator of provenance in sedimentary rocks. J. Sed. Pet., 40 : 591 - 589.

POTTER, P.E., and PETTIJOHN, F.J., 1963. Paleocurrents and Basin Analysis. Springer-Verlag. 296 pp.

REINECK, H.E. and SINGH, I.B., 1975. Depositional Sedimentary Environments. Springer-Verlag, New York, 439 pp.

RUSSELL, U.C., 1885. Playa lakes and playas. In : Neal, J.T. (Editor), Playas and Dried Lakes. Benchmark Papers in Geology, 20 : 81 - 86. Dowden, Hutchinson and Ross, Inc., Strousburg, Pennsylvania, 411 pp.

RUST, B.R., 1972. Structure and process in a braided river. Sedimentology, 18 : 221 - 246.

RUST, I.C., 1973. The sedimentary and tectonic framework of Gondwana basins in Southern Africa. In : Campbell,K.S.W. (Editor), Gondwana Geology, pp. 537 - 564. 3rd Int. Gondwana Symposium Canberra, 1973. Austr. Nat. Univ. Press, Canberra.

SCHUMM, S.A., 1971. Fluvial geomorphology. In : Shen, H.W. (Editor), Fluvial Geomorphology in River Mechanics. Water Resources Publication, 1971, Fort Collins, Colorado.

SCHUMM, S.A., 1972. Fluvial paleochannels. In : Rigby, J.K. and Hamblin, W.K. (Editors), Recognition of Ancient Sedimentary Environments. SEPM, Spec. Publ., 16 : 98 - 107.

SCHWARZACHER, W., 1975. Sedimentation Models and Quantitative Stratigraphy. Developments in Sedimentology 19, Elsevier, 382 pp.

SELLEY, R.C., 1970. Ancient Sedimentary Environments. Chapman and Hall, Ltd., London, 237 pp.

SELLEY, R.C., 1976. An Introduction to Sedimentology. Academic Press, London, 408 pp.

SIMONS, D.B., 1969. Open channel flow. pp. 124 - 145. In : Chorley, R.J. (Editor), Introduction to Fluvial Processes. Methuen and Co. Ltd., 218 pp.

SIMONS, D.B., RICHARDSON, E.V. and NORDIN, C.F., Jr., 1965. Sedimentary structures generated by flow in alluvial channels. In : Middleton, G.V. (Editor), Primary Sedimentary Structures and their Hydrodynamic Interpretation. SEPM, Spec. Publ., No. 12 : 34 - 52.

SMITH, N.D., 1970. The braided stream depositional environment : comparison of the Platte River with some Silurian clastic rocks, north-central Appalachians. Geol. Soc. Am. Bull., 81 : 2993 - 3014.

SMITH, N.D., 1972. Some sedimentological aspects of planar cross-stratification in a sandy braided river. J. Sed. Pet., 42 : 624 - 634.

SOUTHARD, J.B., 1975. Bed configurations. pp. 5 - 43. In : Depositional environments as interpreted from primary sedimentary structures and stratification sequences. SEPM Short Course No. 2. Dallas, 161 pp.

SPRY, A., 1969. Metamorphic Textures. Pergamon Press. 350 pp.

STRAVAKIS, N., (In prep.). Sedimentary opaque heavy minerals from the Katberg Sandstone, S. Africa.

THERON, J.C., 1970. Some Geological Aspects of the Beaufort Series in the Orange Free State : Ph.D. thesis. Univ. of the Orange Free State.

THERON, J.C., 1973. Sedimentological evidence for the extension of the African continent southwards during the Late Permain - Early Triassic times. pp. 61 - 71. In : Campbell, K.S.W., (Editor), Gondwana Geology. 3rd Int. Gondwana Symposium, Canberra, 1973. Austr. Nat. Univ. Press, Canberra.

TRUSWELL, J.F., 1977. The Geological Evolution of South Africa. Purnell, Cape Town.

TURNER, B.R., 1977. Fluviatile cross-bedding patterns in the Upper Triassic Molteno Formation of the Karoo (Gondwana) Supergroup in South Africa and Lesotho. Trans. geol. Soc. S. Afr., 80 : 241 - 252.

TURNER, B.R., 1978. Palaeohydraulics of clast transport during deposition of the Upper Triassic Molteno Formation in the main Karoo basin of South Africa. South African J. of Sci., 74 : 171 - 173.

UYTENBOGAARDT, W. and BURKE, E.A.J., 1971. Tables for Microscopic Identification of Ore Minerals. Elsevier, 429 pp.

VAN HOUTEN, F.B., 1973. Meaning of molasse. Geol. Soc. of America Bull., 84 : 1973 - 1976.

VISHER, G.S., 1965. Use of the vertical profile in environmental re-construction. A.A.P.G. Bull., 49 : 41 - 61.

VISHER, G.S., 1972. Physical characteristics of fluvial deposits. pp. 84 - 97. In : Rigby, J.L. and Hamblin, W.K., (Editors). The Recognition of Ancient Sedimentary Environments. SEPM Spec. Publ., No. 12.

WALKER, R.G., 1975. From sedimentary structures to facies models : example from fluvial environments. pp. 63 - 80. In : Depositional environments as interpreted from primary sedimentary structures and stratification sequences. SEPM Short Course No. 2. Dallas. 161 pp.

WALKER, T.R., 1967. Formation of redbeds in ancient and modern deserts. Geol. Soc. Amer. Bull., 78 : 353 - 368.

WHEELER, H.E., 1964. Baselevel lithosphere surface and time-stratigraphy. Geol. Soc. Amer. Bull., 75 : 599 - 610.

WILLIAMS, G.E., 1971. Flood deposits of the sand-bed ephemeral streams of central Australia. Sedimentology, 17 : 1 - 40.

WILLIAMS, P.F. and RUST, B.R., 1969. The sedimentology of a braided river. J. Sed. Pet., 39 : 649 - 679.

WINTER, H. de la R. and VENTER, J.J., 1970. Lithostratigraphic correlation of recent deep boreholes in the Karoo-Cape Sequence. pp. 395 - 408. Proc. and Pap. 2nd Gondwana Symp., CSIR, Pretoria.